Understanding and predicting disturbances on coral reefs at multiple spatial scales

Joseph Maina Mbui

Understanding and predicting disturbances on coral reefs at multiple spatial scales

by

JOSEPH MAINA MBUI, BSc. Hons, Msc.

PhD Thesis

Presented to the Faculty of Science of

Macquarie University

in Partial Fulfillment

of the Requirements

for the Degree of

Doctor of Philosophy, Biological Sciences

Macquarie University

March 2013

Statement of candidate

I certify that the work in this thesis entitled "*Understanding and predicting disturbances on coral reefs at multiple spatial scales*" has not previously been submitted for a degree nor has it been submitted as part or requirements for a degree to any other university or institution other than Macquarie University.

I also certify that the thesis is an original piece of research and it has been written by me. Any help and assistance that I have received in my research work and the preparation of the thesis itself have been appropriately acknowledged. In addition, I certify that all information sources and literature used are indicated in thesis.

Joseph Maina Mbui

Student Number: 41637526

PRINCIPAL SUPERVISOR: DR. JOSHUA MADIN

CO-SUPERVISOR: ASSOCIATE PROFESSOR. DR. IAN GOODWIN

ADJUNCT SUPERVISOR: DR. TIM MCCLANAHAN

TABLE OF CONTENTS

ABSTRACT

Understanding and predicting the vulnerability of coral reefs to disturbances that act at multiple scales is of paramount importance for guiding reef conservation initiatives. This thesis presents a series of studies that combined large environmental and ecological datasets with a broad range of quantitative tools in order to address questions about coral reef vulnerability around the world. First, I combined global spatial gradients of coral exposure to radiation stress factors (temperature, UV light and doldrums), stress-reinforcing factors (sedimentation and eutrophication), and stress-reducing factors (temperature variability and tidal amplitude) to produce a global map of coral exposure and identify areas where exposure depends on factors that can be locally managed. I show that exposure of coral reefs could be reduced by locally managing chronic human impacts (sedimentation and eutrophication) that exacerbate thermal stress. Using this first study as a roadmap, I then explore thermal stress adaptation and/or acclimation mechanisms in corals. Here, using environmental data and a biogeographic database of common *Symbiodinium* clades living in scleractinian corals, I establish the climatic gradients separating niches among these clades and developed geographical estimates of where corals are likely to acquire thermally compatible symbiont clades in order for them to compensate for increasing temperature. Finally, to explore sedimentation in greater detail, I model hydrological linkages among coastal watersheds and near shore reefs, and subsequently the relative affects of local land use manipulation versus global climate change on sediment dynamics. The results corroborate the hypothesis that there are strong linkages between watersheds' climate variability, hydrology, forest cover, population growth and the adjacent coral reefs. Moreover, the analyses suggest that regional land use management is far more important for influencing sedimentation rates in tropical reefs (such as Madagascar), than mediating climate change. All in all, I demonstrate a need and a framework for conservation science to focus research and management efforts on incorporating the factors that mitigate the effects of coral

stressors, and that enhance ecological resilience, until long-term carbon reductions are achieved through global negotiations.

I. INTRODUCTION

Anthropogenic climate change is exerting pressure on global biodiversity by altering the ecosystem equilibriums that have existed over millennia (Bernstein *et al.*, 2007). Meanwhile, human activities on land and sea continue to reinforce the pressure on biodiversity, most prominently by limiting the physiological and external response mechanisms for coral adaptation and resilience to extreme and variable physical conditions (Pimm & Raven, 2000). As it is unlikely that rising global average temperature will stabilize at 2°C above a pre-industrial level, considered a *'safe level'*, there is now a realization that unprecedented biodiversity loss is highly probable, especially if targeted local level actions aimed at reversing the trends are not decisively executed(Rau *et al.*, 2012). Therefore, the priority for the international community, conservation practitioners, biodiversity conservation NGO's, and other stakeholders, has been to encourage strategies aimed at mediating climate change at global and local levels in order to slow down or to prevent local extinctions (Bernstein *et al.*, 2007; Carpenter *et al.*, 2008).

Coral reefs are one of the most diverse and most threatened ecological systems. Loss of coral coverage of up to 80% has been reported in some reefs over the last 5 decades (e.g. (Gardner *et al.*, 2003; Wilkinson, 2004; De'ath *et al.*, 2012), with associated local species extinctions (Brainard *et al.*, 2011). These trends are thought to be a foretaste of the future outlook for coral reefs given the enormity of the pressures they face. These pressures include climate change induced ocean acidification (Kleypas *et al.*, 1999; Guinotte & Fabry, 2008; Helmle *et al.*, 2011), rising sea surface temperature (Hoegh-Guldberg *et al.*, 2007; Carpenter *et al.*, 2008), rising sea level and storm damage (Spencer, 1995; Madin *et al.*, 2012). Local pressures from human activities include overfishing, sedimentation and eutrophication from forest clearing and coastal development (Carpenter *et al.*, 2008; Wiedenmann *et al.*, 2013). Addressing the effects of these multiple

stressors is the present challenge for the conservation and scientific community.

Meanwhile, the adaptation and acclimation potential of coral reefs is uncertain(Rau *et al.*, 2012). The hypothesised mechanisms by which corals may persist through climate change induced pressures include: (i) symbiont shuffling (Buddemeier & Fautin, 1993; Baker, 2003), the ability of corals to switch their symbiotic composition to high thermal tolerance types, (ii) acclimation to thermal stress due to historical exposure to variable temperature (McClanahan & Maina, 2003); (iii) acclimation from increased reliance on heterotrophic feeding (Grottoli *et al.*, 2006) (iii) acclimation at the level of symbionts, e.g. via photo acclimatization, whereby thermal tolerance of photosystem II is increased following exposure to moderate thermal stress (Takahashi *et al.*, 2013). Despite lack of clear understanding of these adaptation and acclimation mechanisms, the management should explore the possibilities for incorporating the current knowledge, even as scientific research on the subject is gaining momentum.

Management strategies that help preserve adaptation and acclimation mechanisms through reduction of non-carbon dioxide threats have been proposed in numerous reports and policy documents (Rau *et al.*, 2012) e.g. ((Burke *et al.*, 2011; Waterhouse *et al.*, 2012). These include management of local threats, including fisheries management and integrated land-sea management. Conservation practitioners need to understand the nature of the pressures and potential threats different reefs face in order to tailor specific and effective conservation strategies. This understanding is a confluence of several disciplines, including oceanography, hydrology, climatology and biology. Therefore, to avoid catastrophic collapse in coral reef biodiversity, a greater integration of research and conservation is needed. Research should aim towards a holistic understanding of reef ecology with an end goal of implementable conservation strategies. From the other

perspective, conservation strategies need to draw from the cross-disciplinary research. My thesis is a major step in that direction; that is, bringing multidisciplinary research and conservation together.

I.I. CHAPTER OUTLINES

In this thesis, I present a series of multidisciplinary studies that aim to understand environmental disturbances and predict their consequences on coral reefs. In doing so, I specifically ask questions whose outputs are relevant for the conservation application, to help managers allocate conservation resources optimally and to make decisions that are scientifically motivated. This thesis demonstrates a need for multidisciplinary work in tackling several coral reef impacts that are relevant to coral reef managers. To do so, I explored new and topical aspects of coral reefs, including exposure and adaptation mechanisms, and the management decision support for implementation of a key coral reef management strategy involving integrated land-sea management. Further, these studies shed new light on, and evoke debate around, the key issues of adaptation, acclimation and conservation of coral reefs. The thesis is arranged in five data chapters, with each chapter prepared as a standalone publication. At the time of submission, three chapters have been published, one has been accepted for publication, and one is in review.

Chapter 1

Maina JM, McClanahan TR, Venus V, Ateweberhan M, and Madin J (2011) Global exposure of coral reefs to environmental stresses and the implications for local management. *PLoS ONE 6:e23064.* **Article citation metric on Google Scholar (August 2013): 30**

In the first Chapter, I investigate the exposure of coral reefs to multiple stressors on a global scale, and introduce the concept of using the

spatial variability of exposure to stressors to make decisions about spatial adaptive management. I use systems analysis and fuzzy logic approaches to represent synergistic and antagonistic interactions between stressors, and their possible influence on coral vulnerability. These are applied in a system's boundary (i.e. selected few stressors among multiple stressors) that comprises local (i.e., sedimentation and eutrophication) and global (i.e., sea surface temperature) pressures. By quantifying the relative exposure of reefs around the globe to different categories of stressors, I propose a management framework for evaluating the relative significance of stressors on reefs.

Chapter 2

McClanahan TR, Maina JM and Muthiga NA (2011) Associations between climate stress and coral reef diversity in the western Indian Ocean. *Global Change Biology* 17: 2023-2032. ***Article citation metric on Google Scholar (August 2013): 15***

In this Chapter, I collaborated with field biologists in this regional analysis of the relationship between the exposure metric developed in Chapter 1, and biodiversity. We examined the patterns of exposure and biodiversity in the western Indian Ocean region. I developed a spatial database and layers from fish and coral species richness field observations, and carried out geo-statistical analyses, aimed at identifying low stress-high biodiversity patterns, to help management decisions for prioritization of reefs in the region. Despite my authorship role being other than that of the lead author in this article, I incorporate this work as a chapter in my thesis because my contribution to the study is substantial (see table in I.I). Further, this article utilizes the coral exposure model I developed in Chapter 1, and therefore logically fits within the scope of my thesis, rather than as an appendix.

Chapter 3

Maina J, Franklin E, Venus V, McClanahan TR, Baker AC, Stat M, Putnam H, Pochon X, Gates R, Beaumont L, Madin JS. Environmental controls and global distribution patterns of hard coral endosymbionts. (In review, Global Change Biology, June 2013).

Having established the relative exposure and sensitivity of corals to the three categories of environmental stressors (i.e., radiative, reinforcing and reducing), two key components of vulnerability are established. The third component, the adaptation and acclimation potential of corals, is partly addressed in this chapter. Further, given the relative importance of thermal (radiative) stressors, in this chapter I investigate the potential for adaptation and/or acclimation to such stress globally. Specifically, I model the spatial distribution of the common *Symbiodinium* clades found in scleractinian corals, A-D, using environmental predictors. For these clades, I characterized the niches and identify factors that control their spatial arrangement. Conservation genetics has been promoted or hypothesised as one-way management may help in the adaptation of coral reefs. This chapter further develops these theories to provide an understanding of the spatial arrangements of the clades and their potential biogeographical ranges.

Chapter 4

Maina J, de Moel H, Vermaat JE, Bruggemann, JH, Guillaume, MMM, Grove CA, Madin JS, Mertz-Kraus R, Zinke J (2012) Linking coral river runoff proxies with climate variability, hydrology and land-use in Madagascar catchments. *Marine Pollution Bulletin*, 10: 2047–2059. ***Article citation metric on Google Scholar (August 2013): 8***

Sedimentation and eutrophication, destructive fishing and over exploitation are some of the local factors that have contributed to the decline of coral reefs through physical destruction and undermining of their resilience. Having examined thermal stress in the previous chapters, in Chapters 4 and 5 I look more closely at reinforcing stressors (i.e. sedimentation and eutrophication). In Chapter 4, I investigate for the physical and biological linkages between land-sea processes. In particular, near shore coral core derived sediment and river discharge signals (i.e. BaCa and G/B ratio) were used as response variables in multivariate analyses aimed at establishing the climatic and hydrological drivers drivers of near shore reef sedimentation. While land-sea linkages and interactions have been established in some regions (e.g., the Great Barrier Reef), this has not been established in the western Indian Ocean region, thus there is a need to carry out the same study in coral reef regions throughout the tropics to serve as scientific evidence and decision support for integrated land-sea management.

Chapter 5

Maina J, Moel HD, Zinke J, Madin J, McClanahan TR, Vermaat JE. (2013) Human deforestation outweighs future climate change impacts of sedimentation of coral reefs. *Nature Communications*, 4, 1986.

Having established the linkages between coastal processes and near-shore coral reefs, I developed a sorely needed framework for integrated land-sea management. Integrated land-sea management is a key management strategy for coral reef conservation. However, its implementation is hindered by lack of knowledge on specific afforestation targets affective for different watersheds. Furthermore, the effects of climate change need to be factored into the management framework. We carry out a scenario analysis with Madagascar as a case study. In these analyses, we establish empirical relationships

between forest cover and sediment supply to coral reefs, under different climate trajectories. The new framework takes into account the limitations of availability of hydrological data, and is applicable to tropical countries globally where coral reefs are found.

Synthesis

The Synthesis section summarizes the results in the context of lessons learned and the general contribution of this project to the field and future research areas.

Estimated proportion of contribution to articles

Co-authored published or submitted articles	Extent of the intellectual input by the candidate (%)				
	Study concept & design	Acquisition of data	Analysis & interpretation of data	Drafting of manuscript	Critical revision
Chapter 1: Global exposure of coral reefs to environmental stresses and the implications for local management	80	80	95	100	70
Chapter 2: Associations between climate stress and coral reef diversity in the western Indian Ocean	40	40	90	30	50
Chapter 3: Environmental controls and global distribution patterns of hard coral	75	50	75	100	75

endosymbionts					
Chapter 4: Linking coral river runoff proxies with climate variability, hydrology and land-use in Madagascar catchments	**50**	**50**	**95**	**100**	**70**
Chapter 5: Human deforestation outweighs future climate change impacts of sedimentation on coral reefs	**50**	**90**	**90**	**100**	**75**

Other relevant publications during candidature

McClanahan TR, Donner SD, Maynard JA, MacNeil MA, Graham NAJ, Maina J et al. (2012) Prioritizing Key Resilience Indicators to Support Coral Reef Management in a Changing Climate. PLoS ONE 7(8): e42884. doi:10.1371/journal.pone.0042884.

Grove CA, Zinke J, Scheufen T, Maina J, Epping E, Boer W, Randriamanantsoa B, Brummer G-J A (2012) Spatial linkages between coral proxies of terrestrial runoff across a large embayment in Madagascar. *Biogeosciences. 9: 3063–3081.*

Daw TM, Cinner JE, McClanahan TR, Brown KB, Stead SM, Graham NAJ, Maina JM (2012) To Fish or Not to Fish: Factors at Multiple Scales Affecting Artisanal Fishers' Readiness to Exit a Declining Fishery. *PLoS ONE,* 7: 2. 02.

Cinner JE, McClanahan TR, Graham NAJ, Daw TM, Maina JM, Stead SM, Wamukota A, Brown K , Bodin O (2012) Vulnerability of coastal communities to key impacts of climate change on coral reef fisheries. *Global Environmental Change*, 22: 12-20.

Research highlights/media

http://www.sciencedaily.com/releases/2013/06/130605071714.htm

Mapping reef stress (2011) Nature 476, 7361. doi:10.1038/476375d

http://www.nature.com/nature/journal/v476/n7361/full/476375d.html

http://news.sciencemag.org/sciencenow/2011/08/coral-reefs-winners-and-losers.html?ref=hp

http://www.itc.nl/Pub/News/in2011/Sept/Global-map-of-coral-exposure-to-stress.html

http://www.nature.com/news/2011/110419/full/news.2011.244.html

http://www.sciencedaily.com/releases/2012/08/120830105434.htm

References

Baker, A.C. (2003) Flexibility and specificity in coral-algal symbiosis: Diversity, ecology, and biogeography of Symbiodinium. *Annual Review of Ecology Evolution and Systematics*, **34**, 661-689.

Bernstein, L., Bosch, P., Canziani, O., Chen, Z., Christ, R., Davidson, O., Hare, W., Huq, S., Karoly, D. & Kattsov, V. (2007) IPCC, 2007: climate change 2007: synthesis report. Contribution of

working groups I. *II and III to the Fourth Assessment Report of the Intergovernmental Panel on Climate Change. Intergovernmental Panel on Climate Change, Geneva.<* http://www. *ipcc. ch/ipccreports/ar4-syr. htm*,

Brainard, R.E., Birkeland, C., Eakin, C.M., McElhany, P., Miller, M.W., Patterson, M. & Piniak, G.A. (2011) Status Review Report of 82 Candidate Coral Species Petitioned Under the U.S. Endangered Species Act. In: *NOAA technical memo*, p. 530. U.S. Department of Commerce

Buddemeier, R.W. & Fautin, D.G. (1993) Coral Bleaching as an Adaptive Mechanism - a Testable Hypothesis. *BioScience*, **43**, 320-326.

Burke, L., Reytar, K., Spalding, M. & Perry, A. (2011) Reefs at risk revisited. In. World Resources Institute

Carpenter, K.E., Abrar, M., Aeby, G., Aronson, R.B., Banks, S., Bruckner, A., Chiriboga, A., Cortes, J., Delbeek, J.C., DeVantier, L., Edgar, G.J., Edwards, A.J., Fenner, D., Guzman, H.M., Hoeksema, B.W., Hodgson, G., Johan, O., Licuanan, W.Y., Livingstone, S.R., Lovell, E.R., Moore, J.A., Obura, D.O., Ochavillo, D., Polidoro, B.A., Precht, W.F., Quibilan, M.C., Reboton, C., Richards, Z.T., Rogers, A.D., Sanciangco, J., Sheppard, A., Sheppard, C., Smith, J., Stuart, S., Turak, E., Veron, J.E.N., Wallace, C., Weil, E. & Wood, E. (2008) One-third of reef-building corals face elevated extinction risk from climate change and local impacts. *Science*, **321**, 560-563.

De'ath, G., Fabricius, K.E., Sweatman, H. & Puotinen, M. (2012) The 27–year decline of coral cover on the Great Barrier Reef and its causes. *Proceedings of the National Academy of Sciences*,

Gardner, T.A., Côté, I.M., Gill, J.A., Grant, A. & Watkinson, A.R. (2003) Long-term region-wide declines in Caribbean corals. *Science*, **301**, 958-960.

Grottoli, A.G., Rodrigues, L.J. & Palardy, J.E. (2006) Heterotrophic plasticity and resilience in bleached corals. *Nature*, **440**, 1186-1189.

Guinotte, J.M. & Fabry, V.J. (2008) Ocean acidification and its potential effects on marine ecosystems. *Year in Ecology and Conservation Biology 2008*, **1134**, 320-342.

Helmle, K.P., Dodge, R.E., Swart, P.K., Gledhill, D.K. & Eakin, C.M. (2011) Growth rates of Florida corals from 1937 to 1996 and their response to climate change. *Nature Communications*, **2**

Hoegh-Guldberg, O., Mumby, P.J., Hooten, A.J., Steneck, R.S., Greenfield, P., Gomez, E., Harvell, C.D., Sale, P.F., Edwards, A.J., Caldeira, K., Knowlton, N., Eakin, C.M., Iglesias-Prieto, R., Muthiga, N., Bradbury, R.H., Dubi, A. & Hatziolos, M.E. (2007) Coral reefs under rapid climate change and ocean acidification. *Science*, **318**, 1737-1742.

Kleypas, J.A., Buddemeier, R.W., Archer, D., Gattuso, J.P., Langdon, C. & Opdyke, B.N. (1999) Geochemical consequences of increased atmospheric carbon dioxide on coral reefs. *Science*, **284**, 118-120.

Madin, J.S., Hughes, T.P. & Connolly, S.R. (2012) Calcification, Storm Damage and Population Resilience of Tabular Corals under Climate Change. *PLoS ONE*, **7**

McClanahan, T.R. & Maina, J. (2003) Response of coral assemblages to the interaction between natural temperature variation and rare warm-water events. *Ecosystems*, **6**, 551-563.

Pimm, S.L. & Raven, P. (2000) Biodiversity: Extinction by numbers. *Nature*, **403**, 843-845.

Rau, G.H., McLeod, E.L. & Hoegh-Guldberg, O. (2012) The need for new ocean conservation strategies in a high-carbon dioxide world. *Nature Climate Change*, **2**, 720-724.

Spencer, T. (1995) Potentialities, Uncertainties and Complexities in the Response of Coral-Reefs to Future Sea-Level Rise. *Earth Surface Processes and Landforms*, **20**, 49-64.

Takahashi, S., Yoshioka-Nishimura, M., Nanba, D. & Badger, M.R. (2013) Thermal Acclimation of the Symbiotic Alga Symbiodinium spp. Alleviates Photobleaching under Heat Stress. *Plant Physiology*, **161**, 477-485.

Waterhouse, J., Brodie, J., Lewis, S. & Mitchell, A. (2012) Quantifying the sources of pollutants in the Great Barrier Reef catchments and the relative risk to reef ecosystems. *Marine Pollution Bulletin*, **65**, 394-406.

Wiedenmann, J., D/'Angelo, C., Smith, E.G., Hunt, A.N., Legiret, F.-E., Postle, A.D. & Achterberg, E.P. (2013) Nutrient enrichment can increase the susceptibility of reef corals to bleaching. *Nature Clim. Change*, **3**, 160-164.

Wilkinson, C.R. (2004) Status of the Coral Reefs of the World: 2004. In. Australian Institute of Marine Science, Townsville.

1. GLOBAL GRADIENTS OF CORAL EXPOSURE TO ENVIRONMENTAL STRESSES AND IMPLICATIONS FOR LOCAL MANAGEMENT

ABSTRACT

Background: The decline of coral reefs globally underscores the need for a spatial assessment of their exposure to multiple environmental stressors to estimate vulnerability and evaluate potential counter-measures.

Methodology/Principal findings: This study combined global spatial gradients of coral exposure to radiation stress factors (temperature, UV light and doldrums), stress-reinforcing factors (sedimentation and eutrophication), and stress-reducing factors (temperature variability and tidal amplitude) to produce a global map of coral exposure and identify areas where exposure depends on factors that can be locally managed. A systems analytical approach was used to define interactions between radiation stress variables, stress reinforcing variables and stress reducing variables. Fuzzy logic and spatial ordinations were employed to quantify coral exposure to these stressors. Globally, corals are exposed to radiation and reinforcing stress, albeit with high spatial variability within regions. Based on ordination of exposure grades, regions group into two clusters. The first cluster was composed of severely exposed regions with high radiation and low reducing stress scores (South East Asia, Micronesia, Eastern Pacific and the central Indian Ocean) or alternatively high reinforcing stress scores (the Middle East and the Western Australia). The second cluster was composed of moderately to highly exposed regions with moderate to high scores in both radiation and reducing factors (Caribbean, Great Barrier Reef (GBR), Central Pacific, Polynesia and the western Indian Ocean) where the GBR was strongly associated with reinforcing stress.

Conclusions/Significance: Despite radiation stress being the most dominant stressor, the exposure of coral reefs could be reduced by locally managing chronic human impacts that act to reinforce radiation stress. Future research and management efforts should focus on incorporating the factors that mitigate the effect of coral stressors until long-term carbon reductions are achieved through global negotiations.

1.1. INTRODUCTION

Corals globally are exposed to diverse and often interacting physico-chemical and biological disturbances (Hughes & Connell, 1999; Halpern *et al.*, 2008). The diversity, spatio-temporal heterogeneity, and interactions of these disturbances have complicated the understanding of the response of coral assemblages to multiple stressors (Hughes & Connell, 1999), and reduced the potential for spatially targeted coral reef management strategies. To counteract species extinctions predicted by many, e.g. (Sheppard, 2003; Carpenter *et al.*, 2008; Veron *et al.*, 2009), corals would have to adapt to temperatures of more than 2°C above normal thresholds by the turn of the century(Hoegh-Guldberg, 1999; Donner, 2009), in addition to coping with a suite of other stressors (McClanahan, 2002). For example, local stressors such as eutrophication from coastal watersheds exacerbate coral stress by changing the oligotrophic conditions where coral reefs function optimally (Hughes *et al.*, 2003; Knowlton & Jackson, 2008; Carilli *et al.*, 2009; Wooldridge, 2009), while overfishing and removal of grazers is accelerating a shift towards algal dominance (Hughes *et al.*, 2003; Bellwood *et al.*, 2004; Mumby *et al.*, 2007).

Given the bleak view of the status and prognosis for coral reefs globally, timely identification of spatial gradients of their exposure to global and local stressors is needed so that appropriate counter-measures can be formulated and implemented. The management strategies proposed include among others: (i) protecting coral reef locations with biological and environmental conditions that render them less exposed or vulnerable to stress (Game *et al.*, 2008; Maina *et al.*, 2008; McClanahan *et al.*, 2008; Baskett *et al.*, 2010); and (ii) reducing anthropogenic disturbances such as overfishing and pollution, which are likely to reduce the resistance and tolerance of corals to radiation (temperature and ultraviolet light) stress (Baker *et al.*, 2008; Bellwood & Fulton, 2008; Baskett *et al.*, 2009). Understanding of where, when and how global and local stressors affect corals can

strengthen the decision support needed for appropriate coral reef management (West & Salm, 2003; Crabbe, 2008; Donner, 2009; Houk *et al.*, 2010; Selig *et al.*, 2010). The two important considerations that have arisen from these multidisciplinary studies are: (i) assessment of the degree of exposure to multiple interacting stressors at different scales; and (ii) understanding how the environment interacts with the coral community structure and coral-algal symbiosis in influencing their sensitivity, vulnerability and adaptability to thermal, radiation and other physiological and biomechanical disturbances. The first of these two metrics are evaluated here as one of the important considerations that underpins the concepts of the resilience and vulnerability of coral reefs more generally (Hughes *et al.*, 2010).

Ecosystem vulnerability, although defined in different ways, is most often conceptualized as a function of the exposure, sensitivity and adaptive capacity of the perturbed organisms or ecosystems (Adger, 2006). Sensitivity is a property of a system that is difficult to estimate and is dependent on the interaction between the biological and ecological characteristics of a system as well as on the attributes of the environmental stimulus (Smit & Wandel, 2006). Unlike sensitivity and adaptive capacity, exposure is an attribute of the relationship between the system and perturbations, rather than of the system itself (Adger, 2006). These three metrics of vulnerability overlap and the environmental and biological processes that drive them are frequently interdependent (Smit & Wandel, 2006). For instance, many of the determinants of coral sensitivity (e.g. acclimatization) are similar to those that influence or constrain a system's adaptive capacity (e.g. genetic and species diversity, dispersal, and connectivity).

In this study, we derive a generic exposure metric and translate it into fuzzy logic mathematical expressions. The mmodelling of coral exposure, like many reef processes, is often hindered by poor knowledge of the physiology of corals complicated by contradicting

theories on coral-environment interactions (Baskett *et al.*, 2010), sparse data, and poor precision (Meesters *et al.*, 1998). Frequently, important observations are lacking and potentially valuable information may be non quantitative (Silvert, 1997), which may limit the usefulness of these models. For example, the ability of corals to adapt or acclimatize to abnormal conditions is not well understood (Baskett *et al.*, 2009). Fuzzy logic, first introduced by Zadeh (Zadeh, 1975), offers a methodology for dealing with these problems and provides an alternative approach to modelling complex systems. For example, translating data layers to fuzzy measures results in standardised measures of the possibility of belonging to a given set along a continuous scale from 0 to 1(Eastman, 2003). This approach is more realistic than a binary set membership rule as is used in Boolean analyses, especially when there is uncertainty inherent in the input data (Silvert, 1997).

1.1.1. Stressor interactions, coral response and environmental thresholds

In benthic aquatic habitats, the light and temperature environment is highly dynamic and is primarily a function of hydrodynamics (tidal regime, currents, and stratification), cloud cover, and turbidity among other factors (Mumby *et al.*, 2001; Anthony *et al.*, 2004; Anthony & Kerswell, 2007). For instance, extreme tides in turbid waters causes a much greater increase in benthic irradiance than in clear water (Dunne & Brown, 1996; Anthony *et al.*, 2004), which has been shown to cause significant coral mortality (Loya, 1976; Baird & Marshall, 2002; Brown *et al.*, 2002; Anthony *et al.*, 2004). Moreover, as wind speed falls, vertical-mixing decreases, resulting in decreased evaporative cooling and transfer of deeper cool water, which increases the likelihood of thermal stress on corals (Hoegh-Guldberg, 1999; Dunne & Brown, 2001b; Mumby *et al.*, 2001). Based on published hypotheses and conceptual deductions about the likely response of corals to a given stressor (Supplementary Information S2.1), we use a systems

analytical approach to idealize the coral-environment relationships. We considered a series of composite stressors derived from combinations of sea surface temperature (SST), UV irradiance, wind speed, tidal range, and chlorophyll a concentration data. SST, UV, wind magnitude and consistency (together referred here as radiation) are considered to be the primary climatic drivers of coral reef exposure. Tides and SST variability are considered to be stress antagonistic or reducing variables that mitigate the primary climatic stressors. Sedimentation and eutrophication are stress reinforcing or exacerbating interactive stressors because they can undermine the resilience of the coral reef ecosystem through either undermining physiological homeostasis or the recovery processes after disturbance (Fabricius, 2005; Wooldridge, 2009). Coral exposure is a function of derived stressors that interact with radiation having either reinforcing (additive or multiplicative) or reducing affects (antagonistic) (Darling & Côté, 2008; Halpern *et al.*, 2008; Dunne, 2010). It is this combination of reinforcing and reducing effects that causes the complex and sometimes surprising behaviour of composite coral-environmental systems that is not well predicted by simple models that consider one or few coral-environmental variables (McClanahan *et al.*, 2007c).

Most methods for estimating thresholds of environmental attributes, such as thermal and sediment levels, above which stress responses such as coral bleaching, diseases and mortality are likely to occur (Hoegh-Guldberg, 1999; Bruno *et al.*, 2007b; Williams *et al.*, 2010) mostly rely on availability of response observations [e.g. (Qian *et al.*, 2003)]. There are limited insights for identifying when thresholds may be crossed, in a setting with interactive, and cumulative impacts of multiple stressors, which often result in spurious and confounding effects (Halpern *et al.*, 2008; Houk *et al.*, 2010). In addition, a system's response to stressors can adopt various linear and non-linear complex behaviour patterns, which for modelling purposes can be represented in many forms of fuzzy logic membership functions

including trapezoidal, sinusoidal, logistic, Gaussian etc (Burrough & McDonnell, 1998; Halpern *et al.*, 2008).   In this study, we estimate environmental limits of corals (x_a and x_b) based on the distribution of global environmental data for locations where corals are found. We assume that geophysical variables in coral reef areas are distributed normally, where x_a and x_b are two standard deviations from the mean on the lower and upper tail. For simplicity, we assign a normal cumulative function (represented as logistic curve in fuzzy logic membership function) as the response of the interaction between coral and environment, where coral exposure is a function of the environmental variables considered, and initially increases or decreases exponentially along the environmental gradient respectively above or below the user defined minimum threshold (x_a), before levelling off at a user defined maximum threshold (x_b) (Halpern *et al.*, 2008)(Fig.1.1).
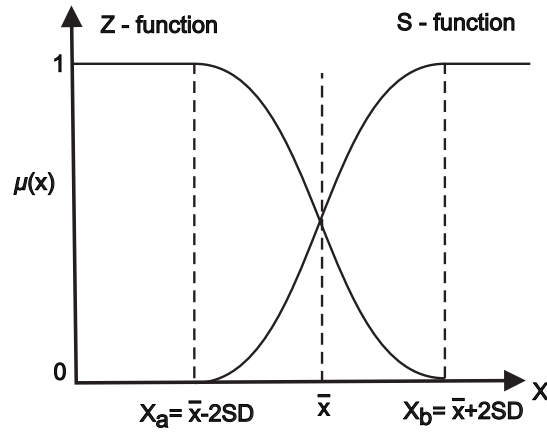

Figure 1.1: Increasing (S curve) and decreasing (Z curve) sigmoidal membership functions, which were used to standardize the environmental data. x_a and x_b are the control points for the lower and upper bounds along the stressor gradient; SD is the standard deviation, while x is the mean

Because coral bleaching and mortality is driven by factors such as temperature and their interactions with other stressors like pollution and sedimentation, it may be possible to prevent some damage by reducing the impact of stressors that are not related to climate change (Baker *et al.*, 2008; Baskett *et al.*, 2010). Additionally, fishing can influence grazers and algae and subsequently influence the overall recovery rates and resilience to climate disturbances (Hughes *et al.*, 2003). This study aims to identify the global spatial gradients of thermal and eutrophication stressors and of the key factors that reduce these stressors to develop a broad-scale metric of environmental exposure for coral reefs. In addition, we address the questions: (i) which of these stressors are corals most exposed to in their respective locations, (ii) which reef locations are least and most exposed to thermal and UV radiation and sedimentation stress, and (iii) how do these stress and reinforcing and reducing variables interact globally?

1.2. MATERIALS AND METHODS

We used environmental data from satellite observations and model outputs to derive variables that represent temperature and UV light (radiation), reinforcing and reducing stress.

1.2.1. Sea surface temperature

Sea surface temperature derived variables were obtained from the second version of the coral reef temperature anomaly database (CoRTAD) (Selig *et al.*, 2010). This database contains global SST and related thermal stress metrics at an approximately 4-km resolution weekly from 1982 through 2008, derived from measurements from the Advanced Very High Resolution Radiometer on-board NOAA suite of polar orbiting satellites. The global accuracy of the retrieval algorithm based on comparisons with in situ buoys indicates values of 0.02 - 0.5^{o}C (Kilpatrick *et al.*, 2001). When compared with in situ temperature from data loggers at shallow depth in the western Indian

Ocean, RMSE of 0.87^{o}C were reported (Maina *et al.*, 2008). The CoRTAD reanalysis database has also been evaluated using *in situ* observations from different coral reef locations globally and at depths ranging from 0-9m, which corresponds to depths of most coral reef habitats (Selig *et al.*, 2010). This evaluation reported RMSEs ranging from 0.49 - 0.81 ^{o}C, and a coefficient of determination (R^{2}) of 0.72 - 0.96 (Selig *et al.*, 2010). Overall, the performance of this data for global coastal applications is adequate, notwithstanding the fact that radiometers measure the temperature at the sea surface while most *in situ* measurements are based on bulk temperature at shallow depths.

We downloaded time series of weekly SST anomalies (WSSTAs), defined as the weekly averaged temperature in excess of 1°C or more above that week's long term average value; and thermal stress anomalies (TSAs), defined as the temperature excess of 1°C or more above the climatologically (long-term average) warmest week of the year (the warmest week of the 52 climatologically weeks averaged over 27 years) (Selig *et al.*, 2010), from the National Oceanographic Data Centre website (http://www.nodc.noaa.gov/sog/Cortad). Two different cumulative estimates of thermal stress were computed from each of these metrics: TSAs and WSSTAs were summed for each year and averaged over 27 years; and for each year, a maximum duration (in weeks) that WSSTA and TSA were greater than or equal to 1°C were computed and averaged over 27 years. These two metrics, the mean annual cumulative and mean yearly maximum duration, represent the characteristic magnitude and duration of the anomalies at a given location, which are important predictors of coral stress (Bruno *et al.*, 2007b; Selig *et al.*, 2010). Mean SST and the coefficient of variation for the 27-year monthly mean time series were also computed.

1.2.2. Chlorophyll and suspended solids

Oceanic satellite observations in the visible and near-infrared bands allow for the measurement of a variety of ocean color information including phytoplankton chlorophyll-*a,* total suspended matter (TSM), and colored dissolved organic matter (CDOM) (Wang *et al.*, 2010; Zhao *et al.*, 2010). For modeling purposes, ocean waters are commonly described as being of Case I or case II types (Morel & Prieur, 1977; Morel & Bélanger, 2006). The former type are those waters whose optical properties are determined primarily by phytoplankton and related colored dissolved organic matter (CDOM) and detritus degradation products; while the later represents the turbid coastal zones influenced by land drainage or sediment re-suspension, with optical properties mainly influenced by CDOM of terrestrial origin, mineral particles, various suspended sediments, urban discharges and industrial wastes (Morel & Prieur, 1977).

The application of ocean color data in coral reef areas is limited by the complexity of the water's optical properties in shallow coastal environments where they are found. The standard Case I algorithm for deriving chlorophyll concentration fail in turbid coastal waters resulting in over estimation of chlorophyll along most coastal areas (Morel & Bélanger, 2006), even if due to terrestrial influence considerable enhancements of the algal biomass in these shallow zones is expected. Further, the standard algorithms for both water types were developed on the assumption of optically deep waters. Therefore in clear shallow bottoms that are highly complex or reflective as with the case in coral reefs and atolls, bottom reflection can induce an increase in marine reflectance, which is wrongly interpreted as ocean color constituents (Boss & Zaneveld, 2003). Given these problems, until special algorithms that take into account the complexity in coral reef areas are developed and incorporated in the standard processing chains of the current ocean color satellites, the usefulness of ocean color data

for coral reef applications will remain limited (Boss & Zaneveld, 2003; Mumby *et al.*, 2004).

To derive chlorophyll estimates taking into account these problems we carried out a series of analyses with ocean color observations from the Sea-viewing Wide Field-of-view Sensor (SeaWiFS), Moderate Resolution Imaging Spectro-radiometer (MODIS), and Medium Resolution Imaging Spectrometer Instrument (MERIS) sensors (Supplementary Information S1.2). The GlobColour processor at the European Space Agency's GlobColour project (http://hermes.acri.fr/GlobColour) was used to process Level 2 data from the three sensors to derive monthly level-3 binned products, including case I and case II chlorophyll concentrations with their respective flags, at a resolution 4.63 km at the equator (http://www.GlobColour.info/products_description.html). Data from all the three sensors were merged to derive case I Chlorophyll, while MERIS Case II algorithm was used to retrieve case II chlorophyll (Schroeder *et al.*, 2007). These Level 3 outputs do not spatially differentiate the regions where each of the water types are relevant; therefore further analysis using turbidity flags is required to discern and merge regions with the different water types into a homogenous continuous layer (Morel & Bélanger, 2006). To achieve this, we used turbidity and depth flags (<30m) derived from the processing of level 2 products, in a logical expression designed to merge respective case I and case II regions in a given month, and further to exclude shallow water (<30m) pixels. Having masked shallower depths using the depth flags, we assumed similar water column properties in masked areas to those found in adjacent deeper (>30m) water pixels, and extrapolated the deeper water pixels to these areas. To achieve this for each layer, we applied 3x3 spatial interpolator, which calculates the median value of 8 pixels adjacent to the pixel being considered. In effect, pixels adjacent to the missing value maintained their original values while the missing pixel was assigned the resulting value from the interpolator

(Maina *et al.*, 2008). These monthly mean layers were then temporally aggregated for the long-term average.

1.2.3. Doldrums

Global sea surface wind speed (ms^{-1}) estimates for 10 m above sea level at a 28-km resolution are available from the National Climatic Data Center (NCDC, ftp://eclipse.ncdc.noaa.gov/raid1b/seawinds). NCDC wind data is based on the blended observations from multiple sensors, with reduced spatial and temporal gaps of individual satellite samplings, and reduced sub-sampling aliases and random errors (Zhang *et al.*, 2006). Despite the coastal application of this data by the Coral Reef Watch, inter-comparisons with other products have not been performed because sparse in-situ measurements over the vast ocean surface make errors difficult to quantify (Zhang *et al.*, 2006). Nonetheless, measurements from each sensor are passed through quality control prior to blending and gridding. Additionally, the blending of cross-calibrated multiple satellite observations is known to increase accuracy and resolution (Zhang *et al.*, 2006; Zhang *et al.*, 2009).

Daily averaged wind speeds (2000-2009) and the averaged 10-year mean monthly wind speeds (1995-2004) were downloaded. The National Oceanic and Atmospheric Administration (NOAA) coral reef watch defines doldrums as wind conditions with a daily mean of less than 3 m s^{-1}. To estimate the magnitude and consistency of wind regimes in a given location, a doldrums metric was computed by taking the annual average maximum number of days that wind speeds were greater than 3 m s^{-1} over 10 years (2000-2009) and multiplying this by the 10-year mean monthly average.

1.2.4. Tidal model

Over the last decade, the tidal research group of Le Provost and collaborators have produced a series of finite element solution (FES) tidal atlases; FES-2004 is the latest release. Data are computed from the tidal hydrodynamic equations and tide gauges and altimeter data assimilation (Le Provost *et al.*, 1998). When cross-validated with other tidal products, the FES-2004 atlas was found to be the most accurate, with improved performance in shelf and coastal areas and moderately deeper areas (Le Provost *et al.*, 1998; Lyard *et al.*, 2006). The accuracy of the 15 tidal components used in the model ranges from 2-12cm and varies by region (Lyard *et al.*, 2006). Therefore, local applications would require calibration with tidal observations at the same scale.

The digital FES-2004 tidal model and the associated extraction software were downloaded from the Laboratoire d'Etudes en Géophysique et Océanographie Spatiales website (http://www.legos.obs-mip.fr/en/soa) (Le Provost *et al.*, 1998; Lyard *et al.*, 2006). The software in C++ was modified to enable gridding of the tidal predictions for a user defined spatial and temporal extents. To minimize the computer processing time, the model's temporal resolution was degraded from hourly to 6-hr interval. These predictions were then aggregated for average, minimum, and maximum heights over seven day intervals and gridded at the model's spatial resolution of roughly 14-km. To capture the long-term conditions and variability, the model was run for 8 years from 1987 with a three-year interval, including 1987, 1990, 1993, 1996, 1999, 2002, 2005, and 2008. Tidal ranges were computed as the long term averaged difference between the weekly maximum and minimum simulated tidal heights.

1.2.5. Ultraviolet radiation

Daily global maps of UV-erythemal (biologically damaging) irradiance at the Earth's surface (for the spectral range 290 to 400 nm and in the units of milli-watts m-^{2}) in a 1 by 1.25 degree grid were retrieved for 1996 to 2001 from the NASA website (http://toms.gsfc.nasa.gov) (Herman *et al.*, 1999; Vasilkov *et al.*, 2001). This data is derived from the total ozone mapping spectrometer (TOMS) on-board Earth Probe-TOMS satellite. Erythemal radiation is a weighted average of UVA (315-400 nm) and UVB (280 to 315 nm) used as a measure of skin irritation caused by exposure sunlight(McKinlay & Diffey, 1987). Errors associated with this data have not been ascertained for many parts of the world, however evaluations in Canada using a ground-based spectrometer reported absolute accuracy of 6% under normal conditions and 12% under conditions of UV absorbing aerosol plumes (Herman *et al.*, 1999). These uncertainties are mostly influenced by the amount of ozone, clouds and aerosols, and terrain height. In the ocean, depth attenuation and the optical properties of the seawater influence the amount of radiation below water surface (Herman *et al.*, 1999; Dunne, 2008). Radiative transfer modeling that includes the ocean system has been performed to estimate in-water radiation field (Vasilkov *et al.*, 2005; Lyard *et al.*, 2006). Here we use Erythermal UV with no correction for the seawater optical properties. Previous reports have shown a good correlation of this data with coral bleaching where observations were made at varying depth (Maina *et al.*, 2008).

The current online values of UV irradiance and Erythemal exposure from EP-TOMS have errors after 2001, and therefore can not be used for UV changes as these are more prone to time-dependent errors from cloud cover and aerosols. The application of this data here is limited to global mean, where the overall error is expected to be relatively small, as the mainly negative cloud-height errors and other positive errors usually partly cancel, leading to an overall smaller error (Liu *et al.*,

2003). Consequently, UV average from 1997 to the end of 2001 was computed to represent local conditions in each grid square.

1.2.6. Coral exposure

Environmental variables were grouped into three categories based on the role that they play as coral stressors: (1) radiation variables, consisting of variables derived from temperature (mean SST, TSA and WSSTA magnitude and duration), UV-erythermal and wind speed data (doldrums index); (2) stress reinforcing variable (TSM and chlorophyll-*a*), representing sedimentation and eutrophication; and (3) stress reducing variables, consisting of SST variability and tidal range. Values of each variable that correspond with the approximately 4000 reef locations were extracted, and examined for normality and log10-transformations applied where necessary (Appendix S3). For each variable, a membership function with similar behavior pattern to a normal cumulative distribution function was used to characterize the relationship between coral exposure and a stress variable. Membership functions capture the degree to which the variable x is a member of a fuzzy set *A* using a suitably chosen function $\mu(x)$ (Burrough & McDonnell, 1998). Here we used spline-based logistic functions:

$$\mu_A(x) = \begin{cases} 0, & x \leq x_a \\ 2\left(\frac{x-x_a}{x_b-x_a}\right)^2, & x_a \leq x \leq \frac{x_a+x_b}{2} \\ 1 - 2\left(\frac{x-x_b}{x_b-x_a}\right)^2, & \frac{x_a+x_b}{2} \leq x \leq x_b \\ 1, & x \geq x_b \end{cases} \qquad \textit{(Equation 1.1)}$$

$$\mu_A(x) = \begin{cases} 1, & x \leq x_a \\ 1 - 2\left(\frac{x-x_b}{x_b-x_a}\right)^2, & x_a \leq x \leq \frac{x_a+x_b}{2} \\ 2\left(\frac{x-x_a}{b-x_a}\right)^2, & \frac{x_a+x_b}{2} \leq x \leq x_b \\ 0, & x \geq x_b \end{cases} \qquad \textbf{\textit{(Equation 1.2)}}$$

where x_a and x_b are control values and correspond to the lower and upper bound of a stressor values, respectively (Table 1.1). These were calculated for each variable as the mean value of minus or plus two standard deviations, respectively. Radiation and reinforcing variables were normalized using an increasing curve (Eq. 1.1) and stress reducing variables were normalized using a decreasing curve (Eq. 1.2) (Fig.1.1).

Spatial Principal Component Analyses (SPCA) was used to combine the standardized variables within each category. Principal Component Analysis transforms each variable into a linear combination of orthogonal common components (output layers), or latent variables with decreasing variation. The linear transformation assumes the components will explain all of the variance in each variable. Hence, for each output the latent component layer carries different information, which is uncorrelated with other components. This enables a reduction of output maps because the last transformed map(s) may be discarded as they have little or no variation left and may be virtually constant. The component weightings were calculated using coefficients of linear correlation to weigh the contribution of factors in spatial principal component analysis (Parinet *et al.*, 2004). SPCA was performed to synthesize the standardized variables within radiation, stress reducing, and stress reinforcing categories. A final composite map from each of these three groups was computed by summing PC's with contribution ratio >1, weighted by their respective contribution ratio (Eq. 1.3; (Li *et al.*, 2006; Maina *et al.*, 2008)).

$$E = \alpha_1\, Y_1 + \alpha_2\, Y_2 + \cdots + \alpha_m\, Y_m \qquad \textit{(Equation 1.3)}$$

where Y_i is the ith principal component, while α_i is its corresponding contribution ratio.

The output maps were standardized between zero and one, representing low and high exposure respectively. To combine the stress reducing and radiation variables, SPCA procedure described above was repeated with standardized radiation and reducing variables as the input variables. The output PC's were synthesized using a weighted sum equation (Eq. 2.3) to yield a layer with estimates of exposure to radiation taking into account the contribution from reducing variables. Fuzzy-integration-based approach was used to integrate the output from this procedure with the reinforcing variables into a single composite layer. (An *et al.*, 1991) lists five fuzzy operators that are most useful for combining fuzzy data (AND, OR, sum, product and gamma). Given two fuzzy sets (standardized layers) *A* and *B*, the fuzzy sum operator produces a layer whose values are equal to or greater than each of the input layers *A* and *B* and results in an increased effect (An *et al.*, 1991). We therefore used fuzzy sum operator to reflect the reinforcing behaviour of sediment and eutrophication to radiation stress:

$$\mu(x) = 1 - \prod_{i=1}^{n} 1 - \mu_i \qquad \textit{(Equation 1.4)}$$

where μ_i is the membership value for *i*-th map, and $i = A, B, n$ maps.

Coral reef location data was obtained from the Reef Base website (http://reefgis.reefbase.org/) and the Wildlife Conservation Society monitoring sites in the western Indian Ocean (Ateweberhan & McClanahan, 2010a). The location data were grouped into eleven

oceanic provinces (Fig.1.2). For the respective locations, exposure metrics as described above were extracted for the corresponding locations. Box plots of exposure metrics by stressors against the coral reef provinces were plotted.

1.2.7. Exposure gradation

Exposure gradation, also termed "defuzzification," is a process where fuzzy application outputs are converted into a crisp output to facilitate their interpretation (Burrough & McDonnell, 1998). We used an iso-cluster (clustering) approach to partition exposure membership grades map into 4 user-defined clusters of statistically homogenous classes (i.e. low, moderate, high and severe).

Table 1.1: Summary statistics for the variables used in the analyses based on (a) coral reef location points, and (b) all pixels within the image spatial boundaries (35N&S, 180E&W); (c) is control values x_a & x_b used in standardizing the variable layers

	Radiation							Reducing		Reinforcing	
	Mean SST	Mean sum SSTA	Mean sum TSA	Mean SSTA duration	Mean TSA duration	UV	Doldrum index	Tidal range	SST coeff. of var.	Chlorophyll	TSM
(a) Coral reef areas											
N	3822	3901	3901	3901	3901	3958	3963	3914	3822	3274	3325
Average	26.9	16	3.9	2	0.8	250	20.1	0.7	5.6	0.7	0.8
Std dev	1.3	1.2	1.4	1.4	1.6	22.9	1.5	2.3	1.6	1.2	1.5
Min	20.8	11	1	0.7	0.1	136.6	1	0.1	1.5	0	0.1
Max	29.6	52	24.3	10.6	5.7	322.4	111.5	3.3	21.9	13.8	44.9
(b) Global values											
Average	22.1	21	13.9	5.7	4	244.3	21.5	0.7	20.9	0.2	0.8

Std dev	4.4	1.5	2.6	2.6	2.6	45.6	1.7	2.2	2.2	0.6	0.8
Min	14.5	0.9	0	0	0	124.5	0	0	1.3	0	0.1
Max	29.7	90.3	84.7	16.5	12.9	419.6	134.8	4.9	51.8	27.2	45.2
(c) Control values										
X_a	24.3	10.8	1.9	1	0.3	204.2	9	0.1	2.2	0.1	0.2
X_b	29.6	23.7	8.2	4.1	2.1	295.8	45.1	3.6	14.4	2.4	2

Ocean provinces

Brazilian province, Caribbean, Central Indian Ocean, Central Pacific, Eastern Pacific, Great Barrier Reef, Micronesia, Middle East, Polynesia, South East Asia, Western Australia, Western Indian Ocean
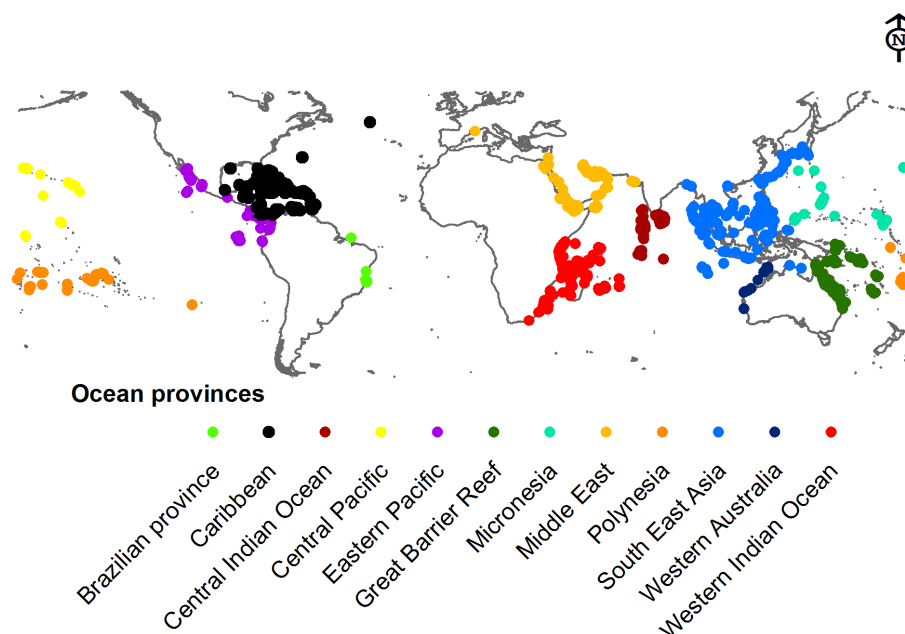
Figure 1.2: Coral reef locations grouped into eleven oceanic provinces after Donner (2009). Coral reef locations were obtained from Reefbase (http://reefgis.reefbase.org/), WCS coral monitoring sites in the western Indian Ocean, and from Ateweberhan & McClanahan (2010) doi:10.1371/journal.pone.0023064.g002

Data for the three stress categories and for the final model were extracted for the sample reef locations. Correspondence analyses

(Legendre & Legendre, 1998) were performed to detect the structural relationships among the oceanic provinces based on the three stress groups and on the exposure classes. The results of correspondence analysis were presented on a bi-plot that represents the configurations of points in projection planes formed by the first two principal axes(Legendre & Legendre, 1998). To determine the distribution of sampled locations by region on the basis of their respective partial exposure scores, exposure space bi-plots of reinforcing against radiation and reducing stresses were generated. Contours were also drawn on these exposure space bi-plots based on the break points of final model exposure classes.

1.3. RESULTS

1.3.1. Global patterns

Analyses of the partial and overall exposure from the three stress groups indicate that corals at locations in all the 12 oceanic provinces were evaluated as highly exposed to radiation and reinforcing stress, albeit with spatial variability within the regions (Fig.1.3, 1.4, 1.5). Ordination of the oceanic provinces by their respective exposure scores in each of the three stress groups in a correspondence analyses showed that 90% of the variation was captured by the first principal axis (c1) (Fig.1.3a). The marginal variances explained by the stress categories and their relative position on the correspondence bi-plot indicates that reinforcing variables were most influential (negative in c1), and in descending order radiation and reducing (lack of); radiation stress was neutral among all regions; and the reducing stress had the lowest influence on the first axis (Fig.1.3a).

When the regions were grouped based on their assigned exposure grades (Fig.1.3b), a pattern emerged where regions clustered around two exposure extremes as follows: South East Asia, Eastern Pacific, Micronesia, and the central Indian ocean grouped on the severe

exposure extreme, primarily due to low reducing (high reducing scores) and high radiation stress scores (Fig.1.3a, b), the Middle East and Western Australia were also in this group primarily due to high scores from reinforcing stress (Fig.1.3a). The second cluster of regions strongly associated with moderate-high exposure included the Caribbean, Great Barrier Reef (GBR), Central Pacific, Polynesia and the western Indian Ocean, all with moderate-high scores from radiation and GBR strongly associated with reinforcing stress; while the Brazilian province with low exposure did not conform well to any of these groups (Table 1.2, Fig.1.3a, b). Partial exposure scores from the three stress groups indicate that the Caribbean, GBR, South East Asia, and the western Indian Ocean were highly variable as depicted by the outliers in the lower and higher extremes of the whiskers (Figure 1.4) and by the distribution of sample points in the exposure space bi-plots (Fig.1.6b, f, j, l).

The GBR, Middle East and Western Australia were, in relative terms, exposed to high stress reducing effect (thus low exposure scores) from tidal movement and high temperature variability, while the central Indian Ocean, Central and Eastern Pacific, Polynesia, and South East Asia were relatively exposed to low reducing effect as shown by the high partial exposure scores attributed to low stress reducing conditions (Fig.1.4b). Western Indian Ocean and the Caribbean reefs were moderately exposed to reducing conditions with the later province being highly variable (Table 1.2, Fig.1.3a, 1.4). In the Middle East, high reinforcing stress was mainly in the Persian Gulf (Bahrain and Iran) and the Gulf of Oman, Southern Red Sea and Gulf of Aden, and Southern Asia on the Gulf of Kutch on the Northerly Gujarat coast among other locations.
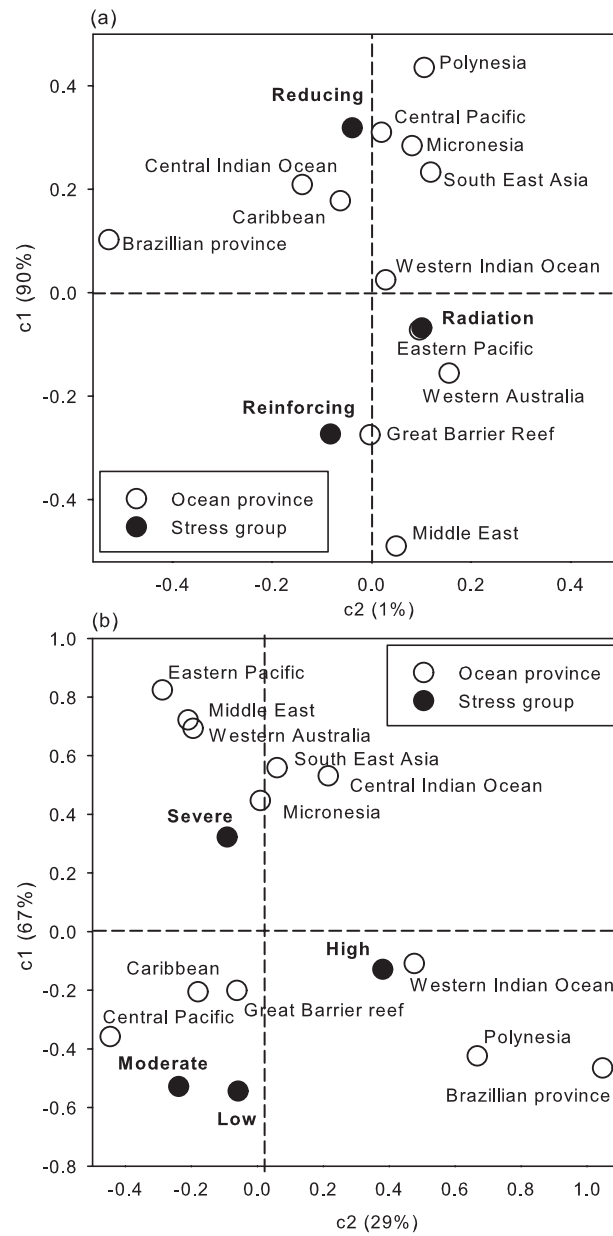
Figure 1.3: Correspondence bi-plots of the oceanic provinces based on the three stress groups (radiation, reducing, and

reinforcing) and based on exposure severity class (a & b respectively) doi:10.1371/journal.pone.0023064.g003

1.3.2. Regional patterns

The Central Pacific, Micronesia and Polynesia oceanic provinces were weakly exposed to reinforcing variables, and the overall exposure was largely due to high exposure to radiation stress (top and bottom right distribution of sample points in the exposure space bi-plots of Fig.1.6d,g,i). These regions were also exposed to relatively low stress-reducing effects alongside the central Indian Ocean and a more variable eastern pacific (Fig.1.4, 1.5, 1.6). In South East Asia, all locations with low to moderate overall exposure grades (on the bottom left of the exposure space bi-plots) were in the Far East in the coral reefs of Japan, while the rest of the region was mostly high to severely exposed primarily from radiation stress and a low stress reducing effect (Fig.1.6j). The reinforcing effect was generally low to moderate, but some locations were highly exposed to reinforcing effect including Kagoshima Bay and Western Shikoku in Japan, Polillo Islands and Bolinao in the Philippines, Pari Island, East Kalimantan, and Tanjong Berakit in Indonesia, and several locations in Thailand, Cambodia and Malaysia (Fig.1.7, See Supplementary Information S1.4). Reefs in South East Asia, including the Islands of Peghu, and Peru in Taiwan and Indonesia respectively, Honcau and Holong Bay in Vietnam, and Shikoku in Japan are overall severely exposed, although they have low to moderate exposure to radiation they have high to severe exposure to reinforcing stress (Table 1.2, Fig.1.7, and See Supplementary Information S1.4).

Western Australia is exposed to severe conditions due to reinforcing stress. Despite the high exposure to doldrums, the tidal variability was high and likely to mitigate radiation stress, for example in Tantabiddi, mangrove islands, and Onslow reef, all had low to moderate radiation stress. Ningaloo and Abrolhos Islands have low radiation but were

severely exposed to reinforcing stress alongside Dampier Archipelago, and in the South of Conzine and Withnell Bays. The reefs in the offshore islands off NW Australia in Seringapatam Reef, Hibernia, Timor Sea Reefs, Scott Reef, and Rowley Shoals were not exposed to high reinforcing stress, but were highly exposed to radiation stress due to high doldrums and low tide variability.

The Central Indian Ocean had many reefs with high exposure primarily due to radiation stress (Fig.1.6c). These reefs are generally exposed to relatively low reinforcing stress, with the exception of reefs in Sri Lanka and India (Fig.1.6c,1.7). The GBR was moderately exposed to radiation and highly exposed to reinforcing stress, and to relatively high stress reducing effects of winds and tides. However, reefs in Kimbe Bay in Papua New Guinea and Solomon Islands in South-west Pacific were highly exposed to radiation stress.

The western Indian Ocean reefs were mostly ranked high to severe in overall exposure, except for some reefs mainly in South Africa, Mauritius, Reunion, Rodrigues, and Torres Reef in Mozambique, which were least exposed (Fig.1.6l, see Supplementary Information S1.4). Although highly variable, the main stress contributor in this region was radiation and reinforcing stress. In most coral reef locations where exposure grade was severe, radiation and reinforcing stress were both high (Fig.1.6l). These reefs included Malindi and Kiunga in Kenya, reefs in southern Tanzania, most of western Madagascar, and Berreira and Vamizi reefs in Mozambique among others. Reefs at Grand River South East in Mauritius, Lagoa Pinnacle and Coral Gardens in Mozambique had low exposure to radiation stress but were severely exposed to reinforcing stress (Fig.1.6l, See Supplementary Information S1.4)
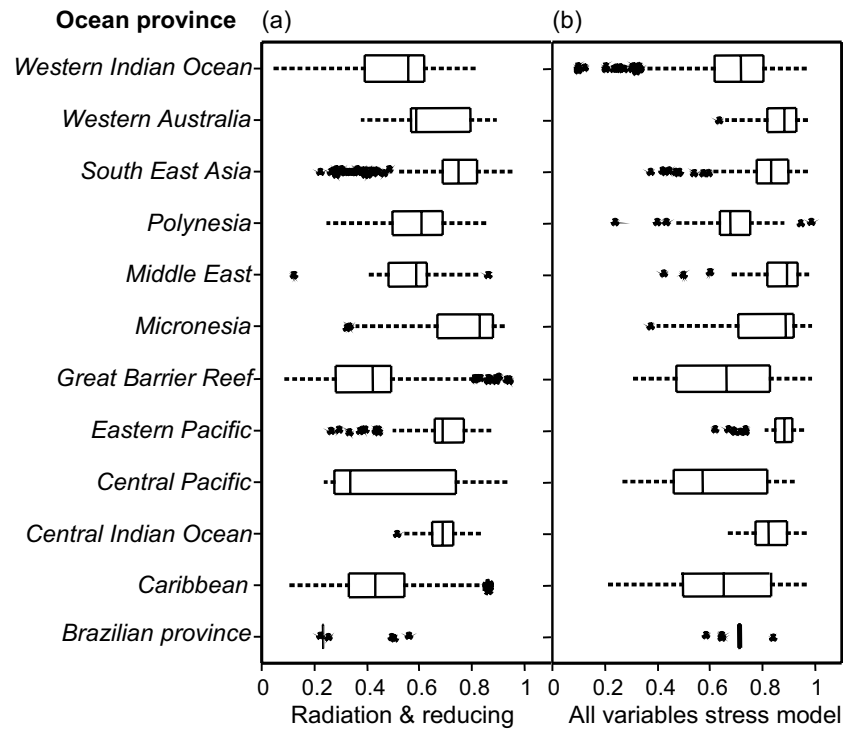
Figure 1.4: Box plots of distribution of, radiation, reducing, and reinforcing stress (a, b, & c respectively). doi:10.1371/journal.pone.0023064.g004
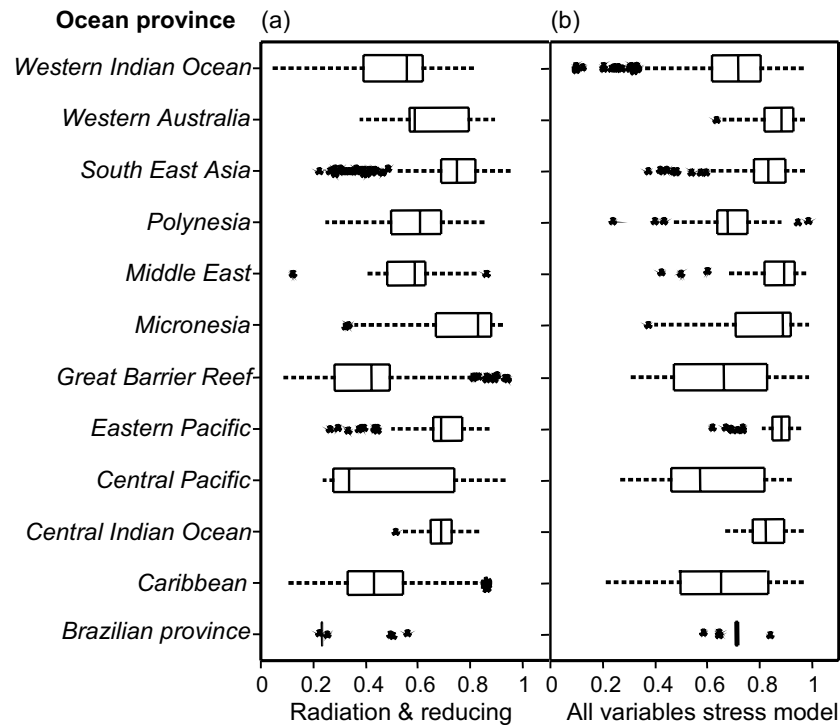
.

Figure 1.5: Box plots of distribution of combined radiation stress and stress reducing variables, and the overall exposure model (a & b respectively). doi:10.1371/journal.pone.0023064.g005

In the Eastern Pacific, reef locations in the south were mostly severely exposed to radiation stress and included Inguana, Saboga, Uraba, Taboga, Contadora Islands, and the Gulf of Chiriqui in Panama, several reefs in Gorgona Island in Colombia, Culera Bay in Costa Rica, and the Galapagos Archipelago in Ecuador (Fig.1.6e,1.7, and See Supplementary Information S1.4). The northern part of the Eastern Pacific, including along the Gulf of California, had high reducing and reinforcing effects.

Overall the Caribbean region was moderate to highly exposed but also with high spatial heterogeneity in the exposure variables (Fig.1.4, 1.5,

1.6, 1.7). The overall exposure of Caribbean reefs to radiation stress was moderate but several locations were outliers and highly exposed to radiation stress. Reef locations in high and severe exposure grades, with reinforcing as the major stress contributors, included reef locations in eastern Panama, Belize, the Bahamas, Cuba, eastern Mexico, and the Florida Keys (Fig.1.7; See Supplementary Information S1.4).

Table 1.2: Regional statistics for all three-stress groups, for radiation and reducing composite, and for the stress model

Ocean province	N	Radiation		Reducing		Reinforcing		Radiation & Reducing		Stress model	
		Mean	SE	Mean	SE	Mean	SE	Mean	SE	Mean	SE
Western Indian Ocean	407	0.5	0.0	0.5	0.0	0.4	0.0	0.5	0.0	0.7	0.0
Western Australia	26	0.7	0.0	0.4	0.0	0.6	0.1	0.7	0.0	0.9	0.0
South East Asia	412	0.7	0.0	0.8	0.0	0.4	0.0	0.7 f	0.0	0.8	0.0
Polynesia	123	0.5	0.0	0.8	0.0	0.3	0.0	0.6	0.0	0.7	0.0
Middle East	96	0.7	0.0	0.2	0.0	0.7	0.0	0.6	0.0	0.9	0.0
Micronesia	62	0.7	0.0	0.8	0.0	0.4	0.0	0.8	0.0	0.8	0.0
Great Barrier Reef	1530	0.5	0.0	0.3	0.0	0.5	0.0	0.4	0.0	0.7	0.0
Eastern Pacific	103	0.7	0.0	0.5	0.0	0.7	0.0	0.7	0.0	0.9	0.0
Central Pacific	17	0.5	0.1	0.7	0.1	0.3	0.0	0.5	0.1	0.6	0.1
Central Indian Ocean	169	0.5	0.0	0.9	0.0	0.5	0.0	0.7	0.0	0.8	0.0
Caribbean	1035	0.4	0.0	0.6	0.0	0.4	0.0	0.4	0.0	0.7	0.0
Brazilian province	18	0.1	0.0	0.6	0.0	0.6	0.0	0.3	0.0	0.7	0.0

1.4. DISCUSSION

Coral reefs globally are highly dependent on radiation, but are also exposed to radiation stress when values exceed normal seasonal and inter-annual ranges (Coles & Brown, 2003). Stress, as used here, is the environmental exposure and does not distinguish the physiological

acclimatization or genetic adaptation that determines the corals and other organisms' sensitivity to these forces. The degree of sensitivity will determine how organisms counter these stresses and therefore our metric is only a comparative baseline of the forces that are exogenous to the reef organisms. This exposure measure alone will not have predictive power in determining responses to the environment, which requires the sensitivity and adaptive capacity of the organisms, but does provide a basis for understanding the forces that these organisms face.

The results suggest considerable spatial heterogeneity globally but also some clear groupings based on our metrics of radiation stress and reinforcing and reducing variables. The spatial heterogeneity of coral stressors and their influence on coral physiology provide a basis to tailor management strategies that can address locally relevant threats (Bellwood & Fulton, 2008; McClanahan *et al.*, 2009). Determining the specific spatial locations with lower or higher cumulative stress and with significant non-climate change related stressors can assist this prioritization process. Despite the difficulties of discriminating among stressors (Mora, 2008), the results of this study demonstrate the utility of disaggregating stress into various components to emphasize management strategies and to effectively reduce the degradation of coral reefs (Palumbi, 2005). The implications of this variability are discussed below in terms of the classification of reefs based on these variables and potential management recommendations
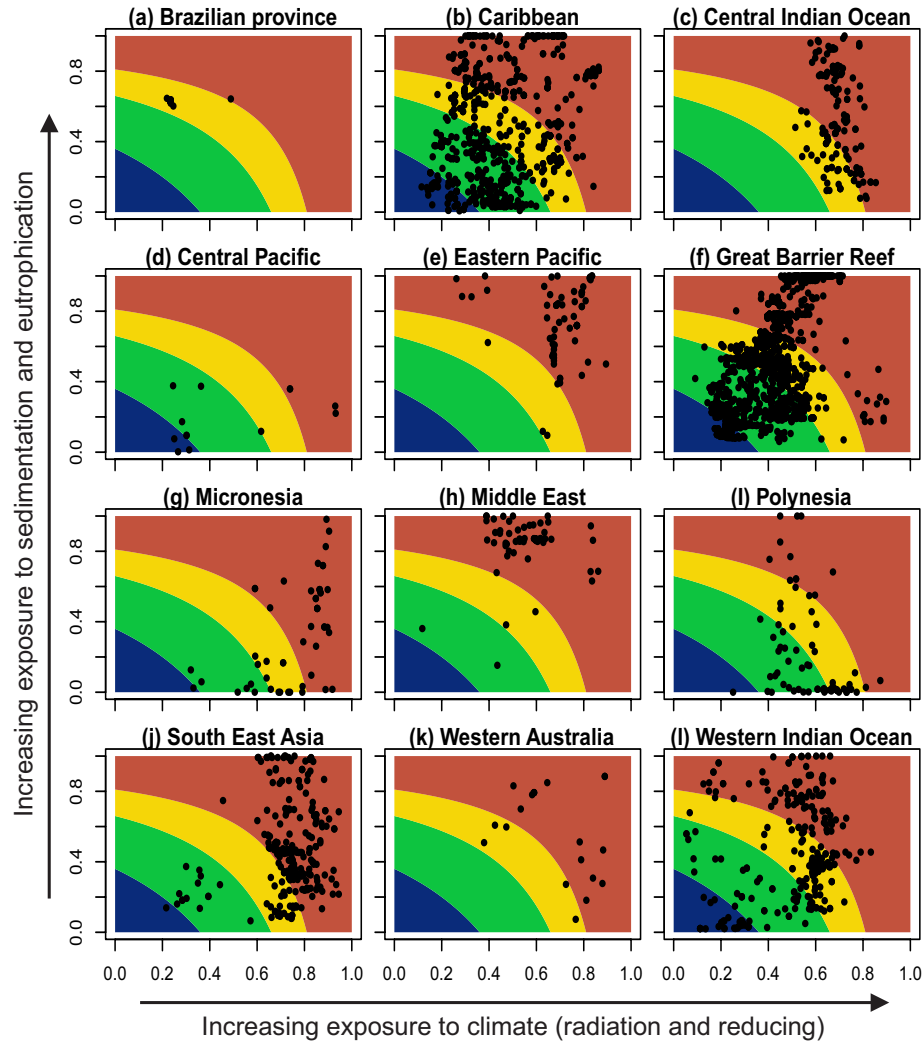
Figure 1.6: Exposure space bi-plots of reinforcing against combined radiation and reducing variables, with contours showing exposure grades (i.e. low, moderate, high, severe) based on the final exposure model.

There is increasing concern globally that enhanced runoff from human land uses is leading to the degradation of coral reefs (Fabricius, 2005). It has been argued from studies on the inshore reefs of GBR that poor

water quality lowers the radiation tolerance of scleractinian corals (Wooldridge, 2009). It has also been shown that high nutrient concentrations may often lead to increased bioerosion and to slowed growth and recovery rates of coral reefs (Fabricius, 2005; Carreiro-Silva *et al.*, 2009). Low water quality can reduce the stress of light and its interaction with temperature to increase bleaching response (Yentsch *et al.*, 2002; Coles & Brown, 2003). However, corals stressed by sedimentation and eutrophication may have a lower capacity to tolerate the effects of other stressors and recover slower, making these factors as overall reinforcing variables (Fabricius, 2005; Wooldridge & Done, 2009). Consequently, if these studies are relevant globally, sedimentation and eutrophication reinforce coral reef stress and improved water quality will increase regional-scale resilience to global climate change.

Our results indicate that sedimentation and eutrophication (reinforcing stresses) are common in all regions, but differ in their intensity and co-occurrence with radiation and reducing stressors.
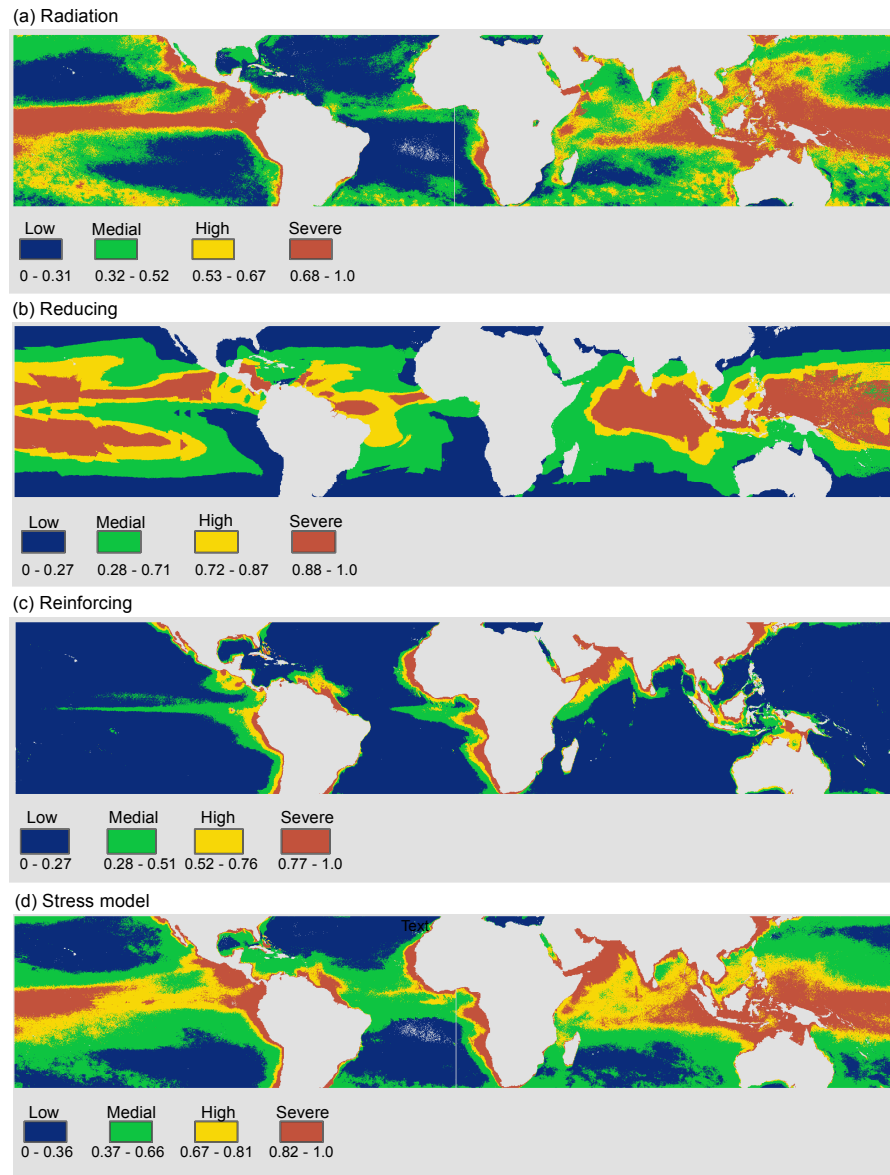
(a) Radiation

(b) Reducing

(c) Reinforcing

(d) Stress model

Figure 1.7: Composite layers for radiation, reducing, reinforcing stress categories, and the overall stress model (a, b, c & d respectively).

In the western Indian Ocean, coral locations exposed to high reinforcing stress correspond to those areas with high river runoff and sedimentation (McClanahan & Obura, 1997; Rakotoarison, 2003; Albietz, 2006; Fleitmann *et al.*, 2007) (Fig.1.6l, See Supplementary Information S1.4). These locations are exposed to moderate radiation stress but overall are severely exposed to high reinforcing effect of water quality from highland runoff. Local management of the coastal watershed in these areas is expected to shift the overall exposure towards lower severity grades. On the GBR, eutrophication is increasing principally due to land use in the adjacent coastal catchment area (Furnas, 2003; Devlin & Brodie, 2005; McKergow *et al.*, 2005; Cooper *et al.*, 2007). From our 1520 sample points in GBR, there is great variability but the majority of coral locations are moderately to highly exposed to water quality reinforcing stress (Fig.1.4, 1.7). Given that the exposure of GBR reefs to radiation stresses are relatively moderate (Fig.1.6f), a management strategy that improves water quality is predicted to increase reef resiliency (Bellwood *et al.*, 2004; Wooldridge & Done, 2009).

The central Indian Ocean lies within a different domain of exposure, where corals are exposed to high radiation stress but have little reinforcing stress, except in Sri Lanka and off India. Despite most of this region having small direct human impacts, synergistic effect of increased temperature and UV is the dominant stressor and has led to current significant coral declines associated with climatic anomalies (Sheppard, 1999). In the most remote areas of the Chagos Islands, there is also evidence for fast reef recovery after these disturbances, which may arise from the low reinforcing stresses (Sheppard *et al.*, 2008; Donner, 2009). Our results indicate that this region has low stress reducing effect from temperature variability and tidal amplitude, making it one of the most exposed to climate change alongside Micronesia and South East Asia.

In the Middle East, there was moderate to high radiation stress, with recent reports indicating exposure to high thermal anomalies (Selig *et al.*, 2010) and similar conditions for the future (Donner, 2009). Corals in the Middle East are also exposed to high levels of natural eutrophication, along with Western Australia, Eastern Pacific, and the GBR. Despite their exposure to extreme environments that are close to the limits of their thermal distribution (Baker *et al.*, 2008), less frequent bleaching disturbances have been predicted in the future (Donner, 2009). As a result, managing the highly eutrophic conditions and the chronic human impacts in these regions could possibly reduce coral decline.

In the Caribbean, coastal development—among other disturbances such as diseases and bleaching—has been associated with mortality of corals and the increase in macro algae (Mora, 2008; Schutte *et al.*, 2010). Our study shows that coral reefs in the south western and the western boundary of the Caribbean, including Belize, reefs off Panama, Costa Rica, Colombia and Venezuela, are severely exposed to stresses, primarily due to reinforcing stress and moderate radiation stress and compounded by a low reducing effect. In Belize for example, there has been reports of high coral decline due to nutrification, bleaching, and diseases among other factors (Aronson *et al.*, 2002; Mora, 2008), in agreement to our results indicating a high-severe exposure primarily due to reinforcing and radiation stresses (Fig.1.2, See Supplementary Information S1.4). Declines continue despite the integrated adaptive approach to marine protected area management currently in place since the late 1990's. This scenario provides an example of the difficulties of managing for both large-scale climate disturbances and the regulation of land-based sources of pollution and siltation in areas where the main sources of pollution are far away from the reefs (Gibson *et al.*, 1998; McClanahan & Muthiga, 1998).

While these results are largely expected to correspond to the observed degree or extent to which coral reefs are subject to the perturbations, including the proximity to river discharges, coastal cities and agricultural areas, they may not necessarily correlate with the current reef status and observed changes in the respective regions or specific coral reef locations. Internal elements of biological and ecological adaptive capacity (i.e. genetic and species diversity, dispersal and connectivity) and sensitivity (e.g. acclimatization, overall health) that are critical to such predictions are not considered here and may explain mismatches between exposure and vulnerability. Recent model predictions are indicating that adaptations of corals through physiological and genetic changes of corals and zooxanthellae will not match the rate of temperature increase from climate change under the business-as-usual scenarios (Baskett *et al.*, 2009). Environmental factors that counter the effects of radiation stressors or reduction of the reinforcing stress factors may play a greater role in the maintenance of the health of coral reefs.

1.4.1. Management implications

The global variability in coral exposure to stresses, as evidenced by the distribution of coral locations by region in the exposure space (Fig.1.6) portrays the degree to which various management strategies are locally relevant. For example, the variability of exposure among coral reef locations in the Caribbean, GBR, South East Asia, and western Indian Ocean indicate the potential for a high within-region dynamics (Fig.1.6). This offers an opportunity for spatially targeted management strategies to possibly reverse the well-documented significant decline of coral reefs in these regions (e.g. (Bruno *et al.*, 2007b)). While management can act to reduce the exposure to anthropogenic pressures, few if any practical large-scale options exist for reducing climate related stress. Under this framework, effective local management needs to target moving reef locations, especially those

that are moderately exposed to climate related stress, towards low reinforcing conditions through improved water quality.

1.4.2. Model limitations

The outputs of this study are constrained, among others, by the uncertainty conferred on the results of the membership functions and standardization algorithms. Insufficient or contradictory knowledge on the response of corals to environmental stimuli in the field and the local adaptation and species-specific responses to stress is the main limitation to creating predictive models. In addition, the use of proxies as a substitute for unavailable environment data, may limit the validity of the assumptions because of potential weak causation associated with correlation-based studies. For example, sedimentation and eutrophication proxy is used as a reinforcing variable and defined using a monotonically increasing sigmoid function, as suggested by some field studies (Wooldridge & Done, 2009). This however contradicts other findings that suggest increased turbidity, which may result from increased chlorophyll, reduces the depth penetration of harmful UVB (Dunne & Brown, 1996), thereby protecting corals. Similarly, high nutrients and heterotrophy associated with rich plankton and high chlorophyll may prevent the severity and impact of coral bleaching (McClanahan *et al.*, 2003; Anthony *et al.*, 2009). In addition, the results of localized studies may not necessarily scale to an entire region (Guidetti & Sala, 2007). The multiple interactive roles of turbidity is an example of the complex nature of multiple stressors, where even a single variable can be viewed mechanistically as multiple stressors with impacts of varying scales (Hughes & Connell, 1999).

Our model assumes a negative linear relationship between thermal stress and SST variability whereas the relationship may be more complex (Ateweberhan & McClanahan, 2010a). Other studies evaluating large variability areas have indicated large thermal stress

values in regions with the largest SST variability (Hughes *et al.*, 2003; Ateweberhan & McClanahan, 2010a). This could result in uncertainties in areas of high SST variability in the Arabian Sea, Arabian Gulf, Eastern Pacific, Western Australia and the coast of Brazil. Further, the boundaries of our study preclude several other factors that affect coral health and an ideal systems analysis with unlimited global data for multiple threats would consider. These include: ocean acidification; fishery exploitation; hydrodynamic disturbances; abundance of bio-eroders and corallivores; and coral community structure, among others.

While the low-moderate resolution remote sensing data used in this study demonstrates sufficient variability for explaining large-scale biological processes (Maina *et al.*, 2008; Selig *et al.*, 2010), a coarse grid ignores significant sub-grid details, and very often introduces approximations and uncertainties into model results (Isukapalli & Georgopoulos, 2001). The spatial and temporal aggregation, interpolation and integration of data from different spatial and temporal scales contribute to the errors from mismatch in spatial and temporal correlation structure (Burrough & McDonnell, 1998).

1.5. CONCLUSIONS

Despite the limitations described above, these results can be applied to specific reefs if they are downscaled to incorporate indicators of resilience at reef scale (West & Salm, 2003), (Maynard *et al.*, 2010). Through the framework presented, integrating many sources of spatially explicit data and scientific knowledge has identified global spatial gradients of radiation, sedimentation and eutrophication stressors and of the key factors that reduce these stresses. This provides a better understand how coral reefs might be managed better under conditions of environmental uncertainty and complexity.

There is high spatial variability of the relative exposures of corals to radiation and reinforcing stressors. Despite radiation stress being dominant, most reef locations identified as severely exposed due to radiation and reinforcing stress are expected to have a lower severity grade if the reinforcing effect from sedimentation and eutrophication were managed. Future studies should focus on incorporating additional coral threats such as acidification, the removal of grazers, and multiple interacting stresses. Enhancement of the knowledge base of the physiological response of corals to environmental stimulus can help improve future models.

1.6. ACKNOWLEDGEMENTS

1.7. SUPPLEMENTARY INFORMATION

S1.1 A summary of conceptual deductions of reef coral responses to environmental variables.

| Variable	Proxy/ derived variable	Response and direction	Reference	Proxy data Source
Sea surface temperature	Thermal Stress Anomaly	Positive correlation with coral bleaching and diseases	(Bruno *et al.*, 2007a; Selig & Bruno, 2010); Bruno	NOAA SST
	Sea surface temperature anomaly	Positive correlation with coral bleaching and diseases	(Bruno *et al.*, 2007a; Selig & Bruno, 2010)	(CoRTAD database)
	Long term mean	Positive correlation with bleaching	(McClanahan *et al.*, 2007a)	NOAA AVHRR
	SST variability	Negative correlation with bleaching; non-linear relationship; non linear relationship with coral growth and survival.	(Potts & Swart, 1984; McClanahan *et al.*, 2007b; Maina *et al.*, 2008; Ateweberhan & McClanahan, 2010b)	NOAA AVHRR, JCOMM, HADSST
Tides	Tidal variability	Large tidal variability may create stress tolerance in corals on shallow reefs.	(Brown, 1997; Anthony *et al.*, 2004; Storlazzi *et al.*, 2004; Anthony *et al.*, 2007)	FES2004 model
UV	Erythermal exposure	Tissue damage, stress on coral and zooxanthellae, reduced photosynthetic efficiency particularly in combination with elevated temperatures	(Dunne & Brown, 2001a; Fitt *et al.*, 2001; Jokiel *et al.*, 2004; Lesser & Farrell, 2004; Ferrier-Pages *et al.*, 2007)	TOMS
Wind speed	Wind speed and low wind (doldrums) duration	as wind speed falls, vertical mixing decreases, resulting in decreased evaporative cooling and transfer of deeper cool water, which increases the likelihood of thermal stress on corals	Hoegh-Guldberg 1999; Dunne and Brown 2001; Mumby et al. 2001	Sea winds Scaterometers
Particulate matter	Chlorophyll a	High chlorophyll levels may represent stressful eutrophic environments; high chlorophyll a concentration also may shade corals from the effects strong irradiation levels. High chlorophyll	(Szmant & Forrester, 1996; Fabricius, 2005; Weber *et al.*, 2006; Cooper *et al.*, 2007; Wooldridge, 2009)	Merged MODIS, MERIS, SeaWIFS

	is also associated with turbid coastal zones influenced by land drainage or sediment re-suspension. Here chlorophyll is used as an indicator of sedimentation and eutrophication.	
Total Suspended Matter (TSM)	Stresses corals; causes mortality to corals	(Cortes & Risk, 1985; Rogers, 1990; Nugues & Roberts, 2003; MERIS Fabricius *et al.*, 2005; Fabricius, 2005)

S1.2   A conceptual framework adopted for the analysis of ocean color data.
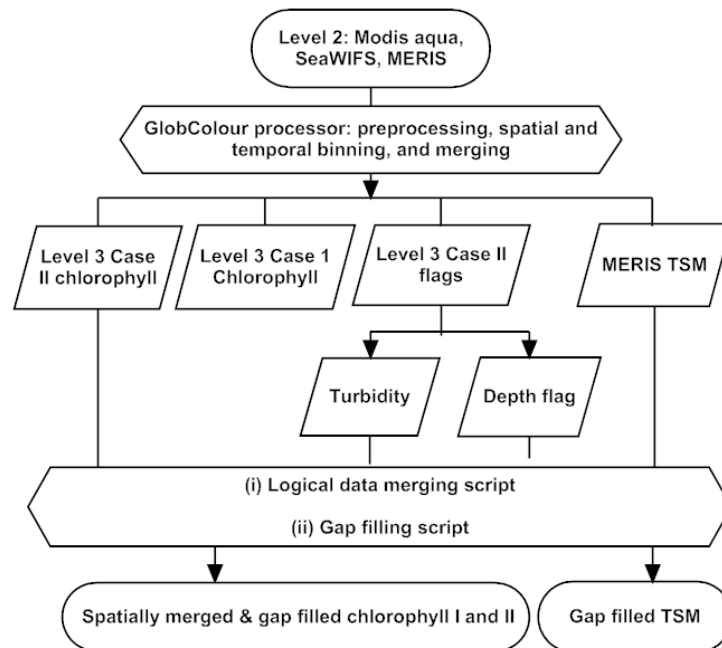
S1.3 Normal cumulative density functions fitted on respective environmental parameters (log transformed except for SST and UV).
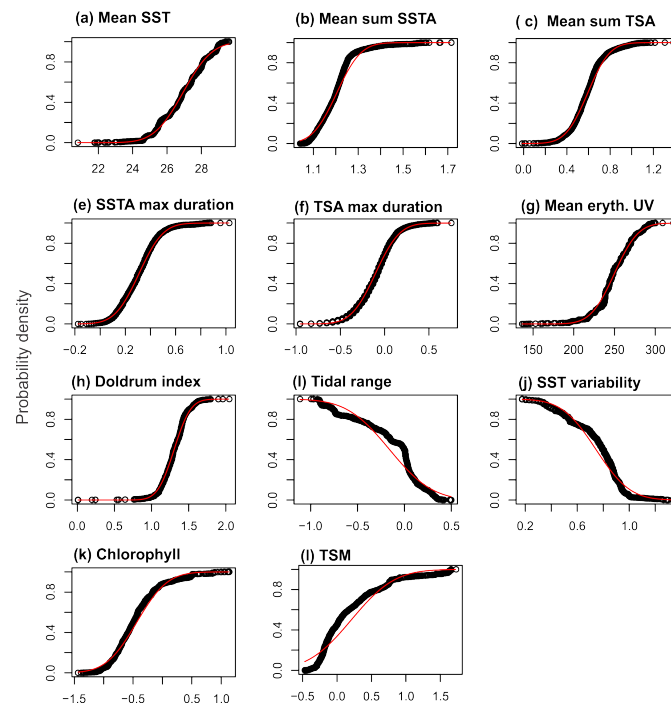
S1.4 A table of coral exposure indices i.e. radiation, reducing, reinforcing, each set of coordinates represents coral reef location within respective ocean provinces.

http://www.plosone.org/article/fetchSingleRepresentation.action?uri=info:doi/10.1371/journal.pone.0023064.s004

References

Adger, W.N. (2006) Vulnerability. *Global Environmental Change*, **16**, 268-281.

Albietz, J.M. (2006) Watershed protection for ecosystem services in the Makira Forest Area, Madagascar: a preliminary biophysical assessment.

An, P., Moon, W.M. & Rencz, A. (1991) Application of fuzzy set theory for integration of geological, geophysical and remote sensing data. *Canadian Journal of Exploration Geophysics*, **27**, 1-11.

Anthony, K., Connolly, S.R. & Hoegh-Guldberg, O. (2007) Bleaching, energetics, and coral mortality risk: effects of temperature, light and sediment regime. *Limnology and Oceanography*, **52**, 716-726.

Anthony, K.R.N. & Kerswell, A.P. (2007) Coral mortality following extreme low tides and high solar radiation. *Marine Biology*, **151**, 1623-1631.

Anthony, K.R.N., Ridd, P.V., Orpin, A.R., Larcombe, P. & Lough, J. (2004) Temporal variation of light availability in coastal benthic habitats: Effects of clouds, turbidity, and tides. *Limnology and Oceanography*, **49**, 2201-2211.

Anthony, K.R.N., Hoogenboom, M.O., Maynard, J.A., Grottoli, A.G. & Middlebrook, R. (2009) Energetics approach to predicting mortality risk from environmental stress: A case study of coral bleaching. *Functional Ecology*, **23**, 539-550.

Aronson, R.B., Macintyre, I.G., Precht, W.F., Murdoch, T.J.T. & Wapnick, C.M. (2002) The expanding scale of species turnover events on coral reefs in Belize. *Ecological Monographs*, **72**, 233-249.

Ateweberhan, M. & McClanahan, T.R. (2010a) Relationship between historical sea-surface temperature variability and climate change-induced coral mortality in the western Indian Ocean. *Marine Pollution Bulletin*, **60**, 964-970.

Ateweberhan, M. & McClanahan, T.R. (2010b) Relationship between historical sea-surface temperature variability and climate change-induced coral mortality in the western Indian Ocean. *Matine Pollution Bulletin*, **60**, 964–970.

Baird, A.H. & Marshall, P.A. (2002) Mortality, growth and reproduction in scleractinian corals following bleaching on the Great Barrier Reef. *Marine Ecology Progress Series*, **237**, 133-141.

Baker, A.C., Glynn, P.W. & Riegl, B. (2008) Climate change and coral reef bleaching: An ecological assessment of long-term impacts, recovery trends and future outlook. *Estuarine, Coastal and Shelf Science*, **80**, 435-471.

Baskett, M.L., Gaines, S.D. & Nisbet, R.M. (2009) Symbiont diversity may help coral reefs survive moderate climate change. *Ecological Applications*, **19**, 3-17.

Baskett, M.L., Nisbet, R.M., Kappel, C.V., Mumby, P.J. & Gaines, S.D. (2010) Conservation management approaches to protecting the capacity for corals to respond to climate change: A theoretical comparison. *Global Change Biology*, **16**, 1229-1246.

Bellwood, D.R. & Fulton, C.J. (2008) Sediment-mediated suppression of herbivory on coral reefs: Decreasing resilience to rising sea levels and climate change? *Limnology and Oceanography*, **53**, 2695-2701.

Bellwood, D.R., Hughes, T.P., Folke, C. & Nyström, M. (2004) Confronting the coral reef crisis. *Nature*, **429**, 827-833.

Boss, E. & Zaneveld, J.R.V. (2003) The effect of bottom substrate on inherent optical properties: Evidence of biogeochemical processes. *Limnology and Oceanography*, **48**, 346-354.

Brown, B.E. (1997) Adaptations of reef corals to physical environmental stress. *Advances in Marine Biology*, **31**, 221-299.

Brown, B.E., Dunne, R.P., Goodson, M.S. & Douglas, A.E. (2002) Experience shapes the susceptibility of a reef coral to bleaching. *Coral Reefs*, **21**, 119-126.

Bruno, J.F., Selig, E.R., Casey, K.S., Page, C.A., Willis, B.L., Harvell, C.D., Sweatman, H. & Melendy, A.M. (2007a) Thermal stress and coral cover as drivers of coral disease outbreaks. *PLoS Biol*, **5**, e124.

Bruno, J.F., Selig, E.R., Casey, K.S., Page, C.A., Willis, B.L., Harvell, C.D., Sweatman, H. & Melendy, A.M. (2007b) Thermal stress and coral cover as drivers of coral disease outbreaks. *PLoS Biology*, **5**, 1220-1227.

Burrough, P.A. & McDonnell, R.A. (1998) *Principles of Geographical Information Systems*,

Carilli, J.E., Norris, R.D., Black, B.A., Walsh, S.M. & McField, M. (2009) Local stressors reduce coral resilience to bleaching. *PLoS ONE*, **4**

Carpenter, K.E., Abrar, M., Aeby, G., Aronson, R.B., Banks, S., Bruckner, A., Chiriboga, A., Cortés, J., Delbeek, J.C., DeVantier, L., Edgar, G.J., Edwards, A.J., Fenner, D., Guzmán, H.M., Hoeksema, B.W., Hodgson, G., Johan, O., Licuanan, W.Y., Livingstone, S.R., Lovell, E.R., Moore, J.A., Obura, D.O., Ochavillo, D., Polidoro, B.A., Precht, W.F., Quibilan, M.C., Reboton, C., Richards, Z.T., Rogers, A.D., Sanciangco, J., Sheppard, A., Sheppard, C., Smith, J., Stuart, S., Turak, E., Veron, J.E.N., Wallace, C., Weil, E. & Wood, E. (2008) One-

third of reef-building corals face elevated extinction risk from climate change and local impacts. *Science*, **321**, 560-563.

Carreiro-Silva, M., McClanahan, T.R. & Kiene, W.E. (2009) Effects of inorganic nutrients and organic matter on microbial euendolithic community composition and microbioerosion rates. *Marine Ecology Progress Series*, **392**, 1-15.

Coles, S.L. & Brown, B.E. (2003) Coral bleaching - Capacity for acclimatization and adaptation. *Advances in Marine Biology*, **46**, 183-223.

Cooper, T.F., Uthicke, S., Humphrey, C. & Fabricius, K.E. (2007) Gradients in water column nutrients, sediment parameters, irradiance and coral reef development in the Whitsunday Region, central Great Barrier Reef. *Estuarine, Coastal and Shelf Science*, **74**, 458-470.

Cortes, J.N. & Risk, M.J. (1985) A reef under siltation stress: Cahuita, Costa Rica. *Bulletin of Marine Science*, **36**, 339-356.

Crabbe, M.J.C. (2008) Climate change, global warming and coral reefs: Modelling the effects of temperature. *Computational Biology and Chemistry*, **32**, 311-314.

Darling, E.S. & Côté, I.M. (2008) Quantifying the evidence for ecological synergies. *Ecology Letters*, **11**, 1278-1286.

Devlin, M.J. & Brodie, J. (2005) Terrestrial discharge into the Great Barrier Reef Lagoon: Nutrient behavior in coastal waters. *Marine Pollution Bulletin*, **51**, 9-22.

Donner, S.D. (2009) Coping with commitment: Projected thermal stress on coral reefs under different future scenarios. *PLoS ONE*, **4**

Dunne, R. & Brown, B. (2001a) The influence of solar radiation on bleaching of shallow water reef corals in the Andaman Sea, 1993-1998. *Coral Reefs*, **20**, 201-210.

Dunne, R.P. (2008) The use of remotely sensed solar radiation data in modelling susceptibility of coral reefs to environmental stress: Comment on Maina et al. [Ecol. Model. 212 (2008) 180-199]. *Ecological Modelling*, **218**, 188-191.

Dunne, R.P. (2010) Synergy or antagonism-interactions between stressors on coral reefs. *Coral Reefs*, **29**, 145-152.

Dunne, R.P. & Brown, B.E. (1996) Penetration of solar UVB radiation in shallow tropical waters and its potential biological effects on coral reefs; results from the central Indian Ocean and Andaman Sea. *Marine Ecology Progress Series*, **144**, 109-118.

Dunne, R.P. & Brown, B.E. (2001b) The influence of solar radiation on bleaching of shallow water reef corals in the Andaman Sea, 1993-1998. *Coral Reefs*, **20**, 201-210.

Eastman, J.R. (2003) *IDRISI Kilimanjaro: guide to GIS and image processing*. Clark Labs, Clark University Worcester.

Fabricius, K., De'ath, G., McCook, L., Turak, E. & Williams, D.M.B. (2005) Changes in algal, coral and fish assemblages along water quality gradients on the inshore Great Barrier Reef. *Marine Pollution Bulletin*, **51**, 384-398.

Fabricius, K.E. (2005) Effects of terrestrial runoff on the ecology of corals and coral reefs: Review and synthesis. *Marine Pollution Bulletin*, **50**, 125-146.

Ferrier-Pages, C., Richard, C., Forcioli, D., Allemand, D., Pichon, M. & Shick, J.M. (2007) Effects of temperature and UV radiation increases on the photosynthetic efficiency in four scleractinian coral species. *The Biological Bulletin*, **213**, 76.

Fitt, W.K., Brown, B.E., Warner, M.E. & Dunne, R.P. (2001) Coral bleaching: interpretation of thermal tolerance limits and thermal thresholds in tropical corals. *Coral Reefs*, **20**, 51-65.

Fleitmann, D., Dunbar, R.B., McCulloch, M., Mudelsee, M., Vuille, M., McClanahan, T.R., Cole, J.E. & Eggins, S. (2007) East

African soil erosion recorded in a 300 year old coral colony from Kenya. *Geophysical Research Letters*, **34**

Furnas, M. (2003) *Catchments and Corals: Terrestrial Runoff to the Great Barrier Reef*, 334.

Game, E.T., McDonald-Madden, E., Puotinen, M.L. & Possingham, H.P. (2008) Should we protect the strong or the weak? Risk, resilience, and the selection of marine protected areas. *Conservation Biology*, **22**, 1619-1629.

Gibson, J., McField, M. & Wells, S. (1998) Coral reef management in Belize: An approach through integrated coastal zone management. *Ocean and Coastal Management*, **39**, 229-244.

Guidetti, P. & Sala, E. (2007) Community-wide effects of marine reserves in the Mediterranean Sea. *Marine Ecology Progress Series*, **335**, 43-56.

Halpern, B.S., McLeod, K.L., Rosenberg, A.A. & Crowder, L.B. (2008) Managing for cumulative impacts in ecosystem-based management through ocean zoning. *Ocean and Coastal Management*, **51**, 203-211.

Herman, J.R., Krotkov, N., Celarier, E., Larko, D. & Labow, G. (1999) Distribution of UV radiation at the Earth's surface from TOMS-measured UV-backscattered radiances. *Journal of Geophysical Research D: Atmospheres*, **104**, 12059-12076.

Hoegh-Guldberg, O. (1999) Climate change, coral bleaching and the future of the world's coral reefs. *Marine and Freshwater Research*, **50**, 839-866.

Houk, P., Musburger, C. & Wiles, P. (2010) Water quality and herbivory interactively drive coral-reef recovery patterns in american samoa. *PLoS ONE*, **5**

Hughes, T.P. & Connell, J.H. (1999) Multiple stressors on coral reefs: A long-term perspective. *Limnology and Oceanography*, **44**, 932-940.

Hughes, T.P., Graham, N.A.J., Jackson, J.B.C., Mumby, P.J. & Steneck, R.S. (2010) Rising to the challenge of sustaining coral reef resilience. *Trends in Ecology and Evolution*, **25**, 633-642.

Hughes, T.P., Baird, A.H., Bellwood, D.R., Card, M., Connolly, S.R., Folke, C., Grosberg, R., Hoegh-Guldberg, O., Jackson, J.B.C., Kleypas, J., Lough, J.M., Marshall, P., Nyström, M., Palumbi, S.R., Pandolfi, J.M., Rosen, B. & Roughgarden, J. (2003) Climate change, human impacts, and the resilience of coral reefs. *Science*, **301**, 929-933.

Isukapalli, S.S. & Georgopoulos, P.G. (2001) Computational methods for sensitivity and uncertainty analysis for environmental and biological models. *New Jersey: Environmental and Occupational Health Sciences Institute*,

Jokiel, P.L., Rosenberg, E. & Loya, Y. (2004) Temperature stress and coral bleaching. *Coral Health and Diseases*, 401-428.

Kilpatrick, K.A., Podestá, G.P. & Evans, R. (2001) Overview of the NOAA/NASA advanced very high resolution radiometer Pathfinder algorithm for sea surface temperature and associated matchup database. *Journal of Geophysical Research C: Oceans*, **106**, 9179-9197.

Knowlton, N. & Jackson, J.B.C. (2008) Shifting baselines, local impacts, and global change on coral reefs. *PLoS Biology*, **6**, 0215-0220.

Le Provost, C., Lyard, F., Molines, J.M., Genco, M.L. & Rabilloud, F. (1998) A hydrodynamic ocean tide model improved by assimilating a satellite altimeter-derived data set. *Journal of Geophysical Research C: Oceans*, **103**, 5513-5529.

Legendre, P. & Legendre, L. (1998) Numerical Ecology: second english edition. *Developments in environmental modelling*, **20**

Lesser, M.P. & Farrell, J.H. (2004) Exposure to solar radiation increases damage to both host tissues and algal symbionts of corals during thermal stress. *Coral Reefs*, **23**, 367-377.

Li, A., Wang, A., Liang, S. & Zhou, W. (2006) Eco-environmental vulnerability evaluation in mountainous region using remote sensing and GIS - A case study in the upper reaches of Minjiang River, China. *Ecological Modelling*, **192**, 175-187.

Liu, X., Newchurch, M.J. & Kim, J.H. (2003) Occurrence of ozone anomalies over cloudy areas in TOMS version-7 level-2 data. *Atmospheric Chemistry and Physics*, **3**, 1113-1129.

Loya, Y. (1976) Effects of water turbidity and sedimentation on the community structure of Puerto Rican corals. *Bull. Mar. Sci.*, **26**, 450-466.

Lyard, F., Lefevre, F., Letellier, T. & Francis, O. (2006) Modelling the global ocean tides: Modern insights from FES2004. *Ocean Dynamics*, **56**, 394-415.

Maina, J., Venus, V., McClanahan, T.R. & Ateweberhan, M. (2008) Modelling susceptibility of coral reefs to environmental stress using remote sensing data and GIS models. *Ecological Modelling*, **212**, 180-199.

Maynard, J.A., Marshall, P.A., Johnson, J.E. & Harman, S. (2010) Building resilience into practical conservation: Identifying local management responses to global climate change in the southern Great Barrier Reef. *Coral Reefs*, **29**, 381-391.

McClanahan, T.R. (2002) The near future of coral reefs. *Environmental Conservation*, **29**, 460-483.

McClanahan, T.R. & Obura, D. (1997) Sedimentation effects on shallow coral communities in Kenya. *Journal of Experimental Marine Biology and Ecology*, **209**, 103-122.

McClanahan, T.R. & Muthiga, N.A. (1998) An ecological shift in a remote coral atoll of Belize over 25 years. *Environmental Conservation*, **25**, 122-130.

McClanahan, T.R., Ateweberhan, M., Omukoto, J. & Pearson, L. (2009) Recent seawater temperature histories, status, and

predictions for madagascar's coral reefs. *Marine Ecology Progress Series*, **380**, 117-128.

McClanahan, T.R., Ateweberhan, M., Muhando, C.A., Maina, J. & Mohammed, M.S. (2007a) Effects of climate and seawater temperature variation on coral bleaching and mortality. *Ecological Monographs*, **77**, 503-525.

McClanahan, T.R., Ateweberhan, M., Muhando, C., Maina, J. & Mohammed, S.M. (2007b) Effects of climate and seawater temperature variation on coral bleaching and mortality. *Ecolgical Monographs*, **77**, 503-525.

McClanahan, T.R., Sala, E., Stickels, P.A., Cokos, B.A., Baker, A.C., Starger, C.J. & Jones Iv, S.H. (2003) Interaction between nutrients and herbivory in controlling algal communities and coral condition on Glover's Reef, Belize. *Marine Ecology Progress Series*, **261**, 135-147.

McClanahan, T.R., Ateweberhan, M., Ruiz Sebastián, C., Graham, N.A.J., Wilson, S.K., Bruggemann, J.H. & Guillaume, M.M.M. (2007c) Predictability of coral bleaching from synoptic satellite and in situ temperature observations. *Coral Reefs*, **26**, 695-701.

McClanahan, T.R., Cinner, J.E., Maina, J., Graham, N.A.J., Daw, T.M., Stead, S.M., Wamukota, A., Brown, K., Ateweberhan, M., Venus, V. & Polunin, N.V.C. (2008) Conservation action in a changing climate. *Conservation Letters*, **1**, 53-59.

McKergow, L.A., Prosser, I.P., Hughes, A.O. & Brodie, J. (2005) Sources of sediment to the Great Barrier Reef World Heritage Area. *Marine Pollution Bulletin*, **51**, 200-211.

McKinlay, A.F. & Diffey, B.L. (1987) A reference action spectrum for ultraviolet induced erythema in human skin. *Human Exposure to Ultraviolet Radiation:Risks and Regulations, Elsevier, Amsterdam*,

Meesters, E.H., Bak, R.P.M., Westmacott, S., Ridgley, M. & Dollars, S. (1998) A fuzzy logic model to predict coral reef

development under nutrient and sediment stress. *Conservation Biology*, **12**, 957-965.

Mora, C. (2008) A clear human footprint in the coral reefs of the Caribbean. *Proceedings of the Royal Society B: Biological Sciences*, **275**, 767-773.

Morel, A. & Prieur, L. (1977) Analysis of variations in ocean color. *Limnol. Oceanogr.*, **22**, 709-722.

Morel, A. & Bélanger, S. (2006) Improved detection of turbid waters from ocean color sensors information. *Remote Sensing of Environment*, **102**, 237-249.

Mumby, P.J., Hastings, A. & Edwards, H.J. (2007) Thresholds and the resilience of Caribbean coral reefs. *Nature*, **450**, 98-101.

Mumby, P.J., Chisholm, J.R.M., Edwards, A.J., Andrefouet, S. & Jaubert, J. (2001) Cloudy weather may have saved Society Island reef corals during the 1998 ENSO event. *Marine Ecology Progress Series*, **222**, 209-216.

Mumby, P.J., Skirving, W., Strong, A.E., Hardy, J.T., LeDrew, E.F., Hochberg, E.J., Stumpf, R.P. & David, L.T. (2004) Remote sensing of coral reefs and their physical environment. *Marine Pollution Bulletin*, **48**, 219-228.

Nugues, M.M. & Roberts, C.M. (2003) Coral mortality and interaction with algae in relation to sedimentation. *Coral Reefs*, **22**, 507-516.

Palumbi, S.R. (2005) Environmental science: Germ theory for ailing corals. *Nature*, **434**, 713-715.

Parinet, B., Lhote, A. & Legube, B. (2004) Principal component analysis: An appropriate tool for water quality evaluation and management - Application to a tropical lake system. *Ecological Modelling*, **178**, 295-311.

Potts, D.C. & Swart, P.K. (1984) Water temperature as an indicator of environmental variability on a coral reef. *Limnology and Oceanography*, **29**, 504-516.

Qian, S.S., King, R.S. & Richardson, C.J. (2003) Two statistical methods for the detection of environmental thresholds. *Ecological Modelling*, **166**, 87-97.

Rakotoarison, H.F. (2003) Evaluation Economique des Bénéfices Hydrologiques du Programme Environment III a Madagascar. *Diplome d'Ingenieur Agronome Thesis, Université d'Antananarivo*, 72.

Rogers, C.S. (1990) Responses of coral reefs and reef organisms to sedimentation. *Marine ecology progress series. Oldendorf*, **62**, 185-202.

Schroeder, T., Behnert, I., Schaale, M., Fischer, J. & Doerffer, R. (2007) Atmospheric correction algorithm for MERIS above case-2 waters. *International Journal of Remote Sensing*, **28**, 1469-1486.

Schutte, V.G.W., Selig, E.R. & Bruno, J.F. (2010) Regional spatio-temporal trends in Caribbean coral reef benthic communities. *Marine Ecology Progress Series*, **402**, 115-122.

Selig, E.R. & Bruno, J.F. (2010) A Global Analysis of the Effectiveness of Marine Protected Areas in Preventing Coral Loss. *PLoS One*, **5**, e9278.

Selig, E.R., Casey, K.S. & Bruno, J.F. (2010) New insights into global patterns of ocean temperature anomalies: Implications for coral reef health and management. *Global Ecology and Biogeography*, **19**, 397-411.

Sheppard, C.R.C. (1999) Coral decline and weather patterns over 20 years in the Chagos Archipelago, central Indian Ocean. *Ambio*, **28**, 472-478.

Sheppard, C.R.C. (2003) Predicted recurrences of mass coral mortality in the Indian Ocean. *Nature*, **425**, 294-297.

Sheppard, C.R.C., Harris, A. & Sheppard, A.L.S. (2008) Archipelago-wide coral recovery patterns since 1998 in the Chagos Archipelago, central Indian Ocean. *Marine Ecology Progress Series*, **362**, 109-117.

Silvert, W. (1997) Ecological impact classification with fuzzy sets. *Ecological Modelling*, **96**, 1-10.

Smit, B. & Wandel, J. (2006) Adaptation, adaptive capacity and vulnerability. *Global Environmental Change*, **16**, 282-292.

Storlazzi, C.D., Ogston, A.S., Bothner, M.H., Field, M.E. & Presto, M.K. (2004) Wave-and tidally-driven flow and sediment flux across a fringing coral reef: Southern Molokai, Hawaii. *Continental Shelf Research*, **24**, 1397-1419.

Szmant, A.M. & Forrester, A. (1996) Water column and sediment nitrogen and phosphorus distribution patterns in the Florida Keys, USA. *Coral Reefs*, **15**, 21-41.

Vasilkov, A., Krotkov, N., Herman, J., McClain, C., Arrigo, K. & Robinson, W. (2001) Global mapping of underwater UV irradiances and DNA-weighted exposures using Total Ozone Mapping Spectrometer and Sea-viewing Wide Field-of-view Sensor data products. *Journal of Geophysical Research C: Oceans*, **106**, 27205-27219.

Vasilkov, A.P., Herman, J.R., Ahmad, Z., Kahru, M. & Mitchell, B.G. (2005) Assessment of the ultraviolet radiation field in ocean waters from space-based measurements and full radiative-transfer calculations. *Applied Optics*, **44**, 2863-2869.

Veron, J.E.N., Hoegh-Guldberg, O., Lenton, T.M., Lough, J.M., Obura, D.O., Pearce-Kelly, P., Sheppard, C.R.C., Spalding, M., Stafford-Smith, M.G. & Rogers, A.D. (2009) The coral reef crisis: The critical importance of <350 ppm CO2. *Marine Pollution Bulletin*, **58**, 1428-1436.

Wang, H., Hladik, C.M., Huang, W., Milla, K., Edmiston, L., Harwell, M.A. & Schalles, J.F. (2010) Detecting the spatial and temporal variability of chlorophylla concentration and total suspended solids in Apalachicola Bay, Florida using MODIS imagery. *International Journal of Remote Sensing*, **31**, 439-453.

Weber, M., Lott, C. & Fabricius, K.E. (2006) Sedimentation stress in a scleractinian coral exposed to terrestrial and marine sediments with contrasting physical, organic and geochemical properties. *Journal of Experimental Marine Biology and Ecology*, **336**, 18-32.

West, J.M. & Salm, R.V. (2003) Resistance and Resilience to Coral Bleaching: Implications for Coral Reef Conservation and Management. *Conservation Biology*, **17**, 956-967.

Williams, G.J., Aeby, G.S., Cowie, R.O.M. & Davy, S.K. (2010) Predictive modeling of coral disease distribution within a reef system. *PLoS ONE*, **5**

Wooldridge, S.A. (2009) Water quality and coral bleaching thresholds: Formalising the linkage for the inshore reefs of the Great Barrier Reef, Australia. *Marine Pollution Bulletin*, **58**, 745-751.

Wooldridge, S.A. & Done, T.J. (2009) Improved water quality can ameliorate effects of climate change on corals. *Ecological Applications*, **19**, 1492-1499.

Yentsch, C.S., Yentsch, C.M., Cullen, J.J., Lapointe, B., Phinney, D.A. & Yentsch, S.W. (2002) Sunlight and water transparency: Cornerstones in coral research. *Journal of Experimental Marine Biology and Ecology*, **268**, 171-183.

Zadeh, L.A. (1975) The concept of a linguistic variable and its application to approximate reasoning-I. *Information Sciences*, **8**, 199-249.

Zhang, H.M., Bates, J.J. & Reynolds, R.W. (2006) Assessment of composite global sampling: Sea surface wind speed. *Geophysical Research Letters*, **33**

Zhang, H.M., Reynolds, R.W., Lumpkin, R., Molinari, R., Arzayus, K., Johnson, M. & Smith, T.M. (2009) An integrated global observing system for sea surface temperature using satellites and in situ data: Research to operations. *Bulletin of the American Meteorological Society*, **90**, 31-38.

Zhao, D., Xing, X., Liu, Y., Yang, J. & Wang, L. (2010) The relation of chlorophyll-a concentration with the reflectance peak near 700 nm in algae-dominated waters and sensitivity of fluorescence algorithms for detecting algal bloom. *International Journal of Remote Sensing*, **31**, 39-48.

3. ENVIRONMENTAL CONTROLS AND GLOBAL DISTRIBUTION PATTERNS OF HARD CORAL ENDOSYMBIONTS

ABSTRACT

Aim: Quantifying the ecological niches of coral symbiont clades is essential for understanding environmental controls on their geographical ranges and the coral species that associate with them.

Location: Global coral reefs.

Methods: We characterize the biogeography of *Symbiodinium* clades A to D using published records of locations in which they were found *in hospite* with scleractinian corals. Environmental variables at each location were used to construct climatic niche models. These variables included sea surface temperature (SST), photosynthetic active radiation (PAR), and total suspended solids (TSS). SST was further characterized by its magnitude (maximum, minimum, median), variability (standard deviation), distribution (skewness, kurtosis), and the frequency and intensity of SST anomalies. Climatic niche characteristics were quantified by applying kernel smoothers to densities of species occurrence in gridded environmental space.

Results: *Symbiodinium* in clades A and D were the most tolerant of high temperatures and indistinguishable in their gross niche characteristics (niche equivalency tests, p=0.20). Nevertheless, they do have two characteristically different thermal tolerance strategies with clade A having a wide distribution in the Caribbean and associations with high levels of PAR and SST but not associated with intense and frequent warm SST anomalies, which is more typical of tropical and clade D distributions. Clade C had a pandemic distribution, which included observations in high latitude coral communities and predicted to occur over a wide range of environments. On the other hand, clade B tended to occur only in

cooler high latitude environments with high seasonal fluctuations in temperature and irradiance (negatively skewed SST and low PAR).

Main conclusions: Differences in climatic niche characteristics among clades indicate that *Symbiodinium* clade C is a widely distributed generalist, clade A is spatially limited generalist, D is a tropically distributed environmental specialists, and clade B is a high latitude distributed specialist.

Key words: biogeography; climate change; climatic niche; symbiosis; niche characteristics

3.1. INTRODUCTION

Ocean temperature is rising at a rate thought to be too rapid for the evolutionary adaptation of corals (Veron et al., 2009). Nevertheless, changes in the abundance of thermally tolerant symbionts associating with corals may be a short-term response (Buddemeier & Fautin 1993; Baker 2003; Baker et al. 2004; Berkelmans & van Oppen 2006; Baird et al., 2007; Jones et al. 2008; Silverstein et al., 2012). Quantifying differences in environmental controls on *Symbiodinium* clades and their subsequent geographical range limits is expected to improve understanding of the scope and limits to this potential change. Climatic niche modeling is a robust approach for quantifying the "realized niche" (Colwell & Rangel, 2009), as well as the potential for ranges to shift in response to global warming (Broennimann et al., 2007; Holt, 2009). In the context of this study, the niche represents the set of environmental abiotic forces experienced by a single clade living within a scleractinian coral host within a particular region (Grinnell, 1917) and implicitly includes the influence of biotic interactions, both of the clades and the coral hosts.

The genus *Symbiodium* is highly diverse and comprises at least nine phylogenetically distinct clades (A–I) with multiple sub clades or 'types', within these clades (Rowan & Powers 1991; LaJeunesse 2005; Pochon & Gates, 2010). Scleractinian corals primarily associate with *Symbiodinium* in clades A-D, although clades F and G have infrequently been recorded (Baker, 2003; Rodriguez-Lanetty et al., 2004; LaJeunesse et al., 2010). Coral species often host multiple symbiont taxa (Baker, 2003; Baker & Romanski 2007, Baird et al. 2007; Putnam et al., 2012; Silverstein et al., 2012) contrary to an earlier paradigm of symbiont specificity (Trench 1989, 1992; Goulet 2006, 2007). Corals can have multiple symbiont clades in individual colonies, as well as within single host species; in such cases, one clade tends to dominate (Baker & Rowan, 1997; Mieog et al. 2007; Correa et al. 2009; Silverstein et. al. 2012). Flexibility in mutualists can expand

the host's tolerance to environmental variation and thereby increase the host's environmental niche (Poisot et al., 2011). Similarly in corals, symbiotic flexibility is perceived as a mechanism by which corals may acquire thermally tolerant symbionts to compensate for changing temperatures (Buddemeier & Fautin 1993; Baker et al. 2004; Silverstein et al., 2012). The stability of this change and long-term benefits of this flexibility remains to be determined (Little et al. 2004; Stat & Gates 2011; Putnam et al., 2012; McClanahan et al. in review).

Bioclimatic models, generated by combining species occurrence data with spatially explicit environmental data are increasingly being used to understand the environmental conditions associated with the geographic distribution of species and how distributions might be expected to change over time (Broennimann et al., 2006, 2012; Warren et al., 2008). Our study focuses on the potential sensitivity of corals to global warming and provides a baseline for future predictions. However, given several uncertainties about the nature of coral-algal symbiotic association, we do not take the next step and explicitly predict future geographic distributions (Araújo & Guisan, 2006). Despite the potential benefits for conservation planning, attempts to model these distributions have been limited (Oliver & Palumbi, 2011), perhaps owing to challenges of modeling niches in marine environments (Araújo & Guisan, 2006; Robinson et al., 2011).

Previous studies have quantified the relative influence of climatic factors on observed occurrences of *Symbiodinium* at a range of spatial scales (LaJeunesse et al., 2010; Cooper et al., 2011). For instance, a regional-scale analysis found that the geographic ranges of different *Symbiodinium* on the Great Barrier Reef (GBR) are shaped predominantly by macroclimate, with SST and light as important predictors of these ranges (Cooper et al., 2011). In the Western Indian Ocean, temperature parameters are important for predicting distribution, particularly of clade D (Baker et al., in prep/submitted).

At the smaller scale of an individual reef system, however, local factors, such as tides, depth, and geomorphology modify macroclimate to determine the distribution of symbionts (e.g., Rowan & Knowlton 1995; Sampayo et al., 2007). Turbidity and light have been reported to influence the occurrence and relative abundance of some symbiont clades (Toller et al. 2001; LaJeunesse et al., 2010). In particular, clade D has been associated with high turbidity and extreme SST, whereas clade C is less sensitive to temperature variance and is widely distributed (Baker 2003; Rowan, 2004; Baker et al. 2004; Stat & Gates, 2011).

This study aimed to investigate the relationships between environmental variables and the common *Symbiodinium* clades living in scleractinian corals, and their potential current distributions within coral reefs globally. Specifically, our analysis addressed the following questions: (i) what are the climatic gradients or niches that potentially separate *Symbiodinium* clades; (ii) what are the characteristics of the clade climatic niches; and (iii) what are the global spatial distribution patterns of *Symbiodinium* clades A-D in scleractinian corals? Our evaluation used a global compilation of *Symbiodinium* occurrence (Franklin et al., 2012) with spatially explicit abiotic variables of SST, PAR, and TSS derived from satellite imagery. We evaluated the niche characteristics by examining the relative shapes of the clades response curves and quantifying environmental overlap, niche similarity, and mean niche positions and breadth along environmental gradients using the ordination of the occurrence and environmental data matrices.

3.2. MATERIALS AND METHODS

3.2.1. *Symbiodinium* occurrence data

The clade occurrence data for clades A-D were extracted from a global online spatially explicit database (GeoSymbio, Franklin et al., 2012), and were supplemented by more recent observations (Yang et al. 2012, Lien et al. 2012, Zhou et al. 2012). A global presence-absence (true absence) matrix was generated consisting of 335 distinct locations where sampling of coral hosts was conducted (Fig.3.1, 3.2). The clade prevalence (presence/absence ratio) was: A = 30/335, B = 34/335, C = 180/335, and D = 91/335. We illustrate our method diagrammatically in Fig.3.1.

Comparisons between clade occurrence data and the spatial distribution of coral reefs globally developed by Veron (2009) highlighted areas of potential sampling bias; that is, sampling was particularly poor in several regions, including the coral triangle (Indonesia, Philippines, Papua New Guinea), the Mediterranean, the west coast of Africa (in Cape Verde and the Gulf of Guinea), and in the Pacific Islands (Fig.3.2). This bias can potentially distort modeled distributions. Nonetheless, such biases have been shown to be minimal when true absence data is used (Barbert-Massin et al., 2012), which is the approach we adopted here.

Clade prevalence (n=4)	A 30/335	B 34/335	C 180/335	D 91/335
	(i)	(ii)	(iii)	
Predictor variable set (n=3)	max SST stddev SST skewness SST mean TSA PAR TSS	max SST min SST skewness SST mean TSA PAR TSS	median SST skewness SST TSA PAR TSS	
Model fitting & accuracy tests (n= 8 x 11)	Algorithms: GLM GAM MARS MDA CTA GBM ANN RF 80% training x 10 repetitions 20% test N = 1056 runs			
Projections	- Projecting to new area			
Ensemble projections	- Weighted sum by AUC - Committee averaging			

Figure 3.1: Modeling framework showing data used in modeling and the steps, including the prevalence of the respective clades in the observation data; the predictor data sets; BNM algorithms employed, and spatial projection and finally the ensemble projection steps. All clades were modeled using predictor variable sets i, ii, & iii. 264 models were calibrated for each clade, for a total of 1056 runs overall
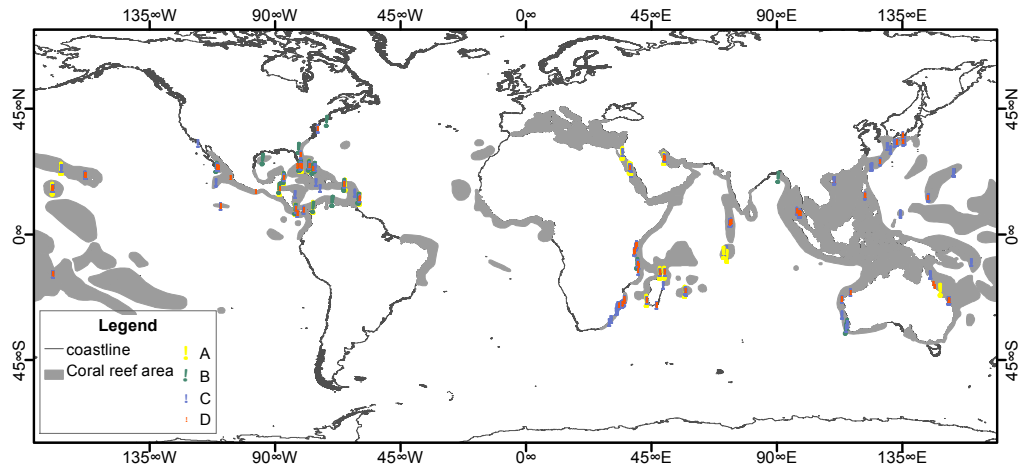
Figure 3.2: Current global distribution of coral reefs (after Veron, 2009), and the known locations of the Symbiodinium clades A-D, based on Geosymbio database (after Franklin et al. 2012). Yellow points represent clade A; green = clade B; blue = clade C; red = clade D

3.2.2. Environmental data

We derived three categories of environmental data from ocean satellite observations and databases: 1) sea surface temperature [SST], 2) turbidity [TSS] (2002-2010), and 3) photosynthetically active radiation [PAR]. These variables were specifically chosen due to their relevance to physiological processes, productivity, and responses to stress (Maina et al. 2008). Oceanic satellite observations allow for the measurement of a variety of ocean characteristics including SST, PAR, phytoplankton chlorophyll-*a*, total suspended solids (TSS), and colored dissolved organic matter (CDOM) (Morel & Prieur, 1977; Hedley et al., 2012). However, application of these data in coastal environments, in particular in coral reef areas, is limited by the complexity of the water optical properties in these regions (Hedley et al., 2012). To derive oceanographic parameter estimates to correct for these

problems, geophysical values for deep-water pixels were assumed for adjacent shallow areas (<30m) (Maina et al., 2011).

Table 3.1: Definition of the codes for the environmental variables considered in the study

Code	Description
mean TSA	Deviations of 1 week where the temperature was 1 °C or greater than the mean maximum climatological week or the long-term average warmest week from 1982 to 2009 (Selig et al. 2010)
mean SSTA	Observed weekly a averaged temperature is $\geq$ 1 °C warmer than weekly climatological value; SSTA's are typical deviations from typical weekly temperatures (Selig et al., 2010)
TSA max	Annual maximum TSA averaged over 27 years
TSA freq	Count of TSA events in a year averaged over 27 years
SSTA max	Annual maximum SSTA averaged over 27 years
SSTA freq	Count of SST anomalies events in a year averaged over 27 years
min SST	2.5 percentile of SST time series
median SST	Median of SST time series
max SST	97.5 percentile of SST time series
SST stdev	Standard deviation of SST time series

SST skewness	Skewness of the distribution of SST time series
SST kurtosis	kurtosis (peakedness of the distribution) of SST time series
Chl	Arithmetic median of chlorophyll-*a* time series
TSS	Arithmetic median of TSS time series
PAR	Arithmetic median photosynthetic active radiation

We obtained weekly data of SST for the period 1982-2009, for the globe at a resolution of ~4x4km. These data were aggregated to capture long-term SST magnitude (97.5th percentile, median, and 2.5th percentile); distribution (skewness and kurtosis); and variability (standard deviation). Total suspended solids (TSS, mg/l) and chlorophyll-*a* concentration monthly time series (2002-2010) derived from this database were pooled to median values. Photosynthetically active radiation (PAR) monthly time series data (2002-2010) were obtained from the Globcolour database (http://hermes.acri.fr/GlobColour) and pooled to median values of the time series. All variables were tested for collinearity (Table 3.1, see Supplementary Information S3.1). To reduce multicollinearity among predictors, we examined the variance inflation factors (VIFs) between the predictor variables and set a conservative threshold of VIF = 3 relative to suggested 5 or 10 to indicate multicollinearity (Cranet & Surle, 2002). On this basis, from Table 3.1, we created three sets of predictor variables by selecting different combinations of the least correlated variables (Fig.3.1, see Supplementary Information S3.1).

3.2.3. Model fitting

Eight climatic niche model algorithms (CNMs) incorporated in BIOMOD package (Thuiller et al., 2003) in R (http://www.R-project.org) were applied, where each of the three environmental data sets were used a predictors of the clade presence-absence response (Fig.3.1). These CNMs included three regression methods (GLM: generalized linear model, GAM: generalized additive model, and MARS: multiple adaptive regression splines), two classification methods (FDA: fixed discriminant analysis and CTA: classification tree analysis), and three machine learning methods (ANN: artificial neural networks, GBM: generalized boosted model, and RF: random forest) (see Thuiller et al., 2003 for details). In the absence of independent test data, we split the data randomly into calibration (80%) and validation (20%) datasets, where the calibration data were used to generate the models that were then tested with validation data. In addition, ten cross-validation runs were performed for each combination of predictor data, model algorithm, and symbiont clade, as outlined by Thuiller et al. (2009). We used non-independent data for model evaluation; therefore the level of model accuracy is interpreted as a measure of sensitivity of the outputs relative to the initial data (Araújo et al., 2005; Araújo & Guissan, 2006).

Outputs from BIOMOD for the respective CNMs included *Symbiodium*-environment response curves, prediction accuracy, and variable importance standardized across all the models (Thuiller et al., 2009). The model performance was measured using the "area under curve" (AUC) of the receiver operating characteristic plots (Hanley & McNeil, 1982). Values of AUC can range from 0.5 for models with no predictive power, to 1.0 for models with perfect predictive power (Araújo et al., 2005). We retained models with AUC values ≥ 0.7, which were considered to have fair to excellent predictive power (Hosmer & Lemeshow, 2000).

To estimate the importance of individual variables, an independent randomisation procedure was used to compare each variable across the eight models (Thuiller et al., 2009). We used simulated occurrences from each of the model runs to generate response curves. Following Thuiller et al. (2009) we used a consensus approach, that weighted each model based on its AUC, was applied to generate ensemble maps of the predicted probability of occurrence of each clade (Thuiller et al., 2009).

3.2.4. Niche characteristics

We tested five characteristics of the climate niches occupied by each clade, including: (1) overlap (the amount of environmental space shared by two clades); (2) equivalency (whether niches are more equivalent or identical than expected by chance [Knouft et al., 2006; Pfenninger et al., 2007; Warren et al., 2008]); (3) similarity (whether niches are more similar than would be expected by chance [Warren et al., 2008]); (4) position (the absolute distance between the mean location of a given clade along a gradient and the mean of the gradient [MacNally, 1995]); and (5) breadth (i.e. the range of the environmental variable occupied by the niche). Niche equivalency and similarity tests use different approaches to assess niches of clades: the former is a measure of the degree to which niche overlap is constant when randomly reallocating the occurrences of both clades in their respective niches, while the later examines whether the overlap between observed niches for pairs of clades is different from the overlap between the observed niche for one clade and randomly selected niche from the second clade.

To assess the above characteristics of niches, we used the approach described by Broennimann et al. (2012). First, we conducted principal component analysis (PCA) on environmental data for variables listed in Table 3.1 from the global coral reef areas. Second, using the first

two PC axes, a multivariate space was created and gridded into 100 x 100 grid cells. Third, for each clade, a kernel density function was applied to determine a smoothed density of occurrences in this gridded environmental feature space. Finally, we calculated the five niche characteristics.

To quantify niche overlap, Schoener's D was calculated for each clade pair combination (Schoener, 1968; Warren et al., 2008). This metric ranges from 0 (no overlap) to 1 (complete overlap). Niche equivalency and similarity were then computed from Schoener's D (Broennimann et al., 2012), which involved permuting histograms of the D statistic of niche overlap based on the simulated occurrences. If the D statistic based on observed occurrences falls within the density of 95% of the D statistics from the simulated occurrences, the null hypothesis of niche equivalency cannot be rejected (Broennimann et al., 2012). Similarly, the test of niche similarity is also based on 100 repetitions. If the overlap from observed data is greater than 95% of the overlap of the simulated occurrences, the clades occupy environments that are more similar to each other than expected by chance.

The mean position of the different clades in the environmental space was calculated by randomly sampling the environmental space weighted by the niche density. These were permuted 100 times to compute mean niche positions (i.e., niche centroids), which were then compared between clades using the Wilcoxon paired sample signed rank test statistic. Finally, niche breadth was calculated from the variance of the positions of each occurrence on the first and second axes of the PCA analysis (Thuiller et al., 2004; Broennimann et al., 2007).

3.3. RESULTS

3.3.1. Global spatial distribution patterns of *SYMBIODINIUM*

The models' predictive accuracy (AUC) indicates that of the 264 models per clade (8 CNM's x 3 environmental datasets x 11 repetitions), clade A had the lowest proportion (16%) of models with AUC values above the threshold of 0.7 (see Supplementary Information S3.2). Approximately half of the models for clades B, C and D were above this AUC threshold (53, 46 and 31%, respectively). The lower number of models with high predictive accuracies for clade A was likely an artifact of the relatively low prevalence in observation data.

Spatial projections indicated differential patterns in the distribution of suitable habitat (i.e. realized niche) for symbiont clades. Realized niche for clade C is projected as widely distributed, with high occurrence probabilities in all coral reef areas (Fig.3.3). Clade D is projected to have the second-widest realized niche, with relatively high probabilities in northern Australia, the eastern Pacific, eastern Africa, southwest Indian Ocean, the Red Sea, Indonesia and the Arabian Gulf, among other areas (Fig.3.3, see Supplementary Information S3.3). Coral reefs at high latitudes (i.e. in the Caribbean and in southern Australia) are projected to contain climatic niche for clade B, while for clade A these areas are projected to occur in the Red Sea, SW Indian Ocean, GBR & NW Australia, eastern Pacific, and in the Caribbean, and southeast Asia among other areas (Fig.3.3, see Supplementary Information S3.3)
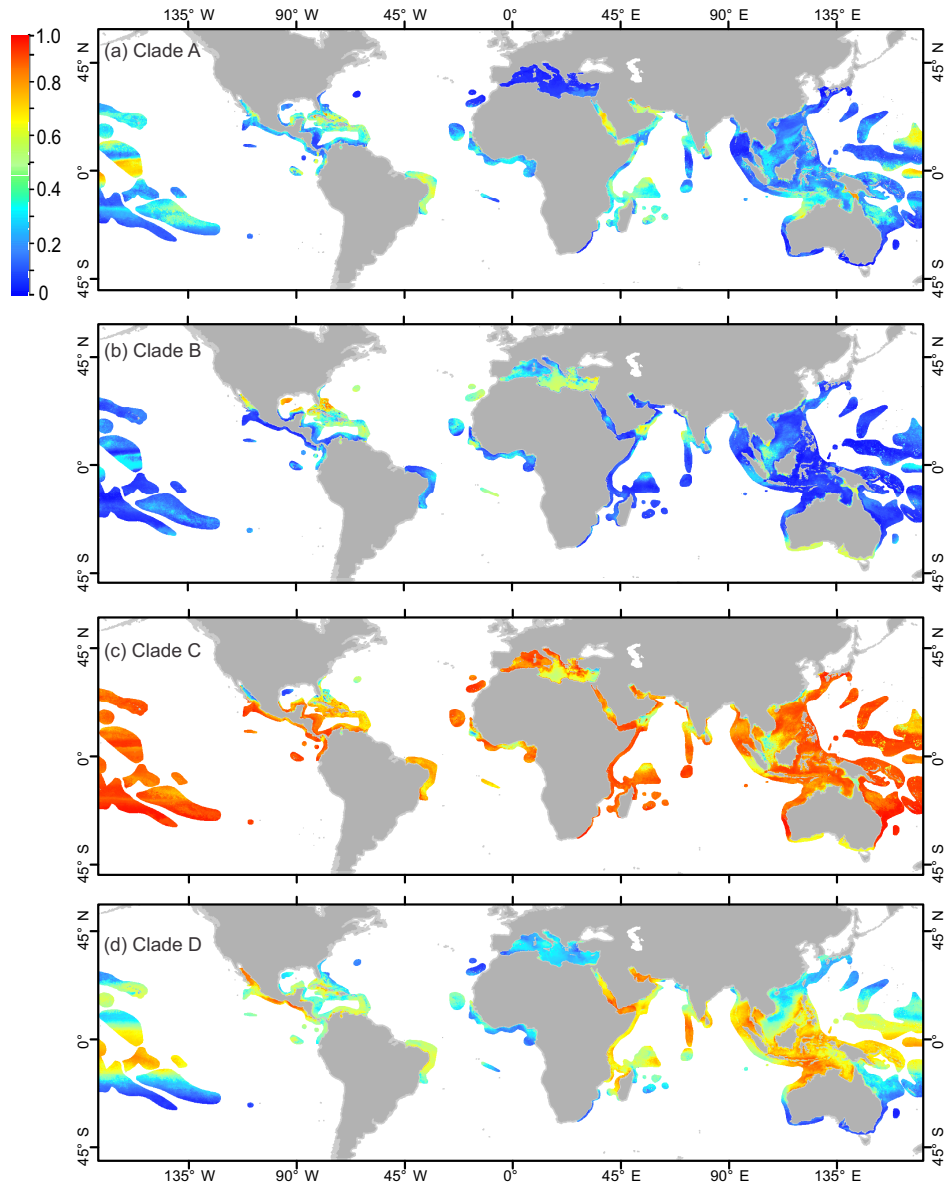
Figure 3.3: Ensemble maps of climatically suitable habitat for the Symbiodinium clades A-D

3.3.2. Climatic gradients separating niches among clades

For clade D, maximum and median SST, PAR, and SST variability were the most important predictors of occurrence (Fig.3.4). Minimum SST, PAR and median SST were most important for clade A, TSA, maximum and median SST for clade C, and TSA, maximum and median SST and turbidity for clade B (Fig.3.4). Occurrence patterns over gradients of SST magnitude were variable, with clades B and D indicating a propensity towards extreme low and high SST magnitude, respectively (Fig.3.5). Along the maximum SST gradient, clade A displayed a right skewed with flat slope distribution. Along minimum SST this clade displayed a bimodal distribution with the two peaks possibly representing two sub-populations of clade A, which differ in SST tolerance. Clade C displayed a wide, "generalist" realized niche breadth along the SST maximum gradient and PAR, with a high probability of occurrence along the maximum SST and PAR ranges of the study area (Fig.3.5). Clade C occurrence also displayed a right skewed response along median and minimum SST's. In contrast, clades A and B displayed narrower, "specialized" niche positions with respect to temperature magnitude and variability, with bell-shaped unimodal response curves, and relatively narrow niche breadths across the SST magnitude gradient (Fig.3.5). Clade A also showed a high probability of occurrence for locations with negatively skewed temperature distributions, In contrast, clades B and C showed a right skewed and unimodal, centrally-located distribution respectively, with the latter having a wide breadth along the SST skewness gradient.
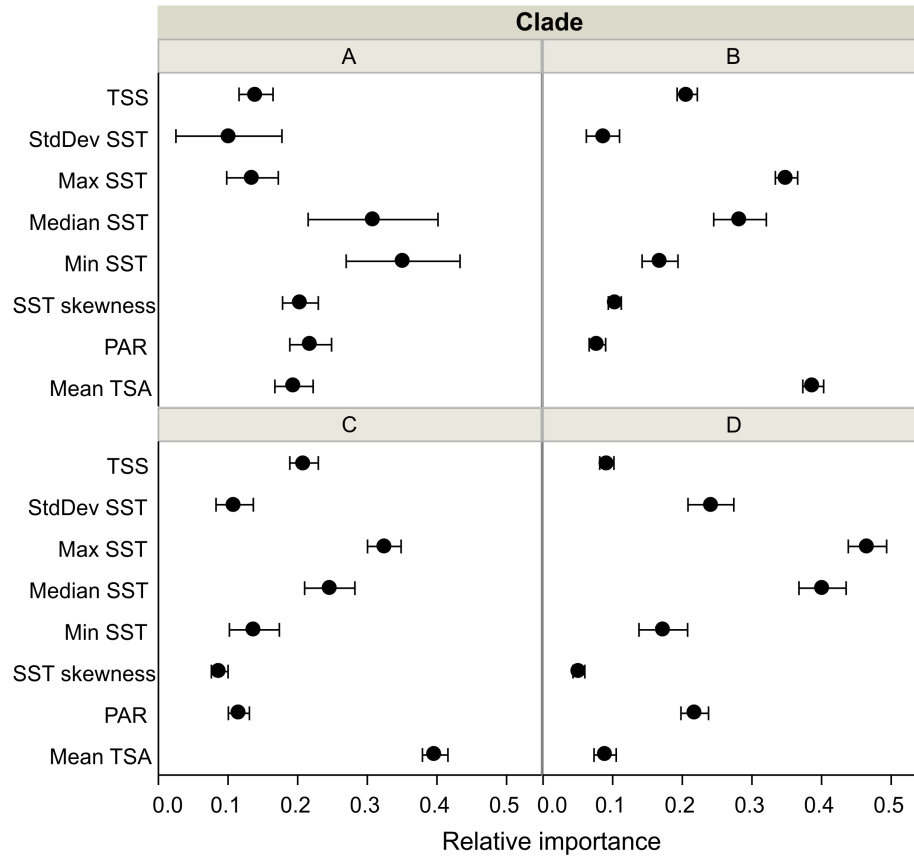
Figure 3.4: Relative importance of the predictor variables for each clade based on 387 models with prediction accuracy ≥ AUC 0.7

Along the PAR gradient, clades A, B, and D showed clear niche separation, where clades A and D displayed an association for high PAR, and clade B showed an association for the lower end of the PAR range. Along the turbidity gradient, occurrence probability for clade C declined marginally, probabilities for clades A, B increased markedly over the turbidity gradient, while clade D displayed a unimodal distribution peaked at relatively low levels of turbidity (Fig.3.5).
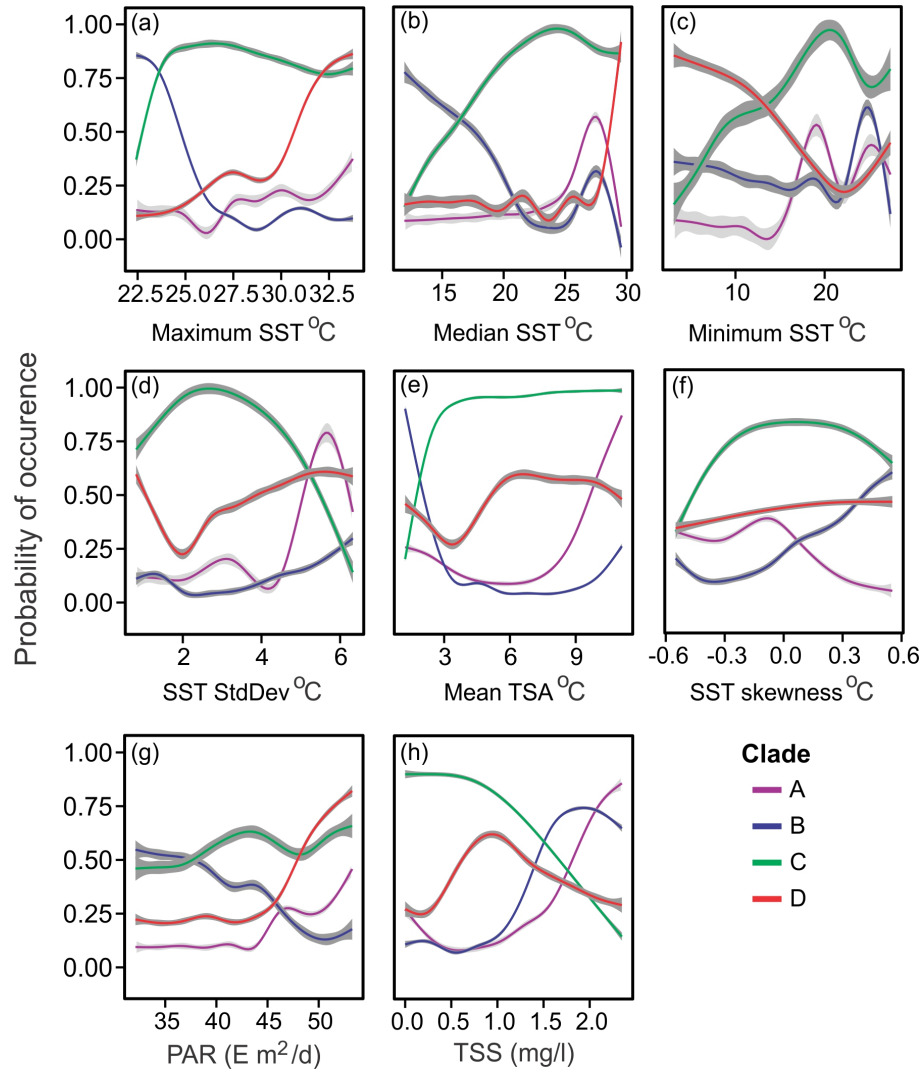
Figure 3.5: Response curves for each clade, illustrating their respective probability of occurrence along the gradients of (a) maximum SST (b) median SST (c) minimum SST (d) SST standard deviation (e) mean TSA (f) SST skewness (g) PAR (h) TSS. A GAM smoother was fitted across response from all selected models. Uncertainty estimated from repetition runs and different models is plotted in light grey

3.3.3. Differences in the niche characteristics of different clades

Correlations between PCA axes and environmental variables indicated that the principal component axis 1 (PC1) was significantly and negatively associated with SST anomalies and temperature magnitude, which accounted for 34% of the variability (Table 3.2). Principal component axis 2 (PC2), explained 32% of the variability, and was positively correlated with variables representing SST magnitude and light, and negatively correlated with SST variability. PC2 also correlated negatively with SST anomalies metrics associated with deviations from typical weekly temperatures (i.e., SSTA), and was not significantly correlated with more extreme anomalies associated with deviations from the mean maximum climatological week (i.e., TSA) (Table 3.1, 3.2). Small values of PC1 represent high SSTs and extreme frequency and intensity of SST anomalies. In contrast, small values of PC2 represent extreme high frequency of SST anomalies and SST variability, while large values represent extreme high temperatures and PAR (Table 3.2; Fig.3.6).

Niche occupancy tests show that clades tended to occupy environmental niches that were less similar than random (rejection of niche similarity, $p < 0.05$). Although dissimilar, the niche equivalency tests suggest that the clades climatic niches were more identical than expected by chance ($p > 0.05$), except clades C and D, which were significantly less identical (i.e., rejection of niche equivalency tests, $p < 0.05$) (Fig.3.6, see Supplementary Information S3.4). Clades A and D being the most identical compared to other pair-wise combinations (niche equivalency tests, $p = 0.2$).
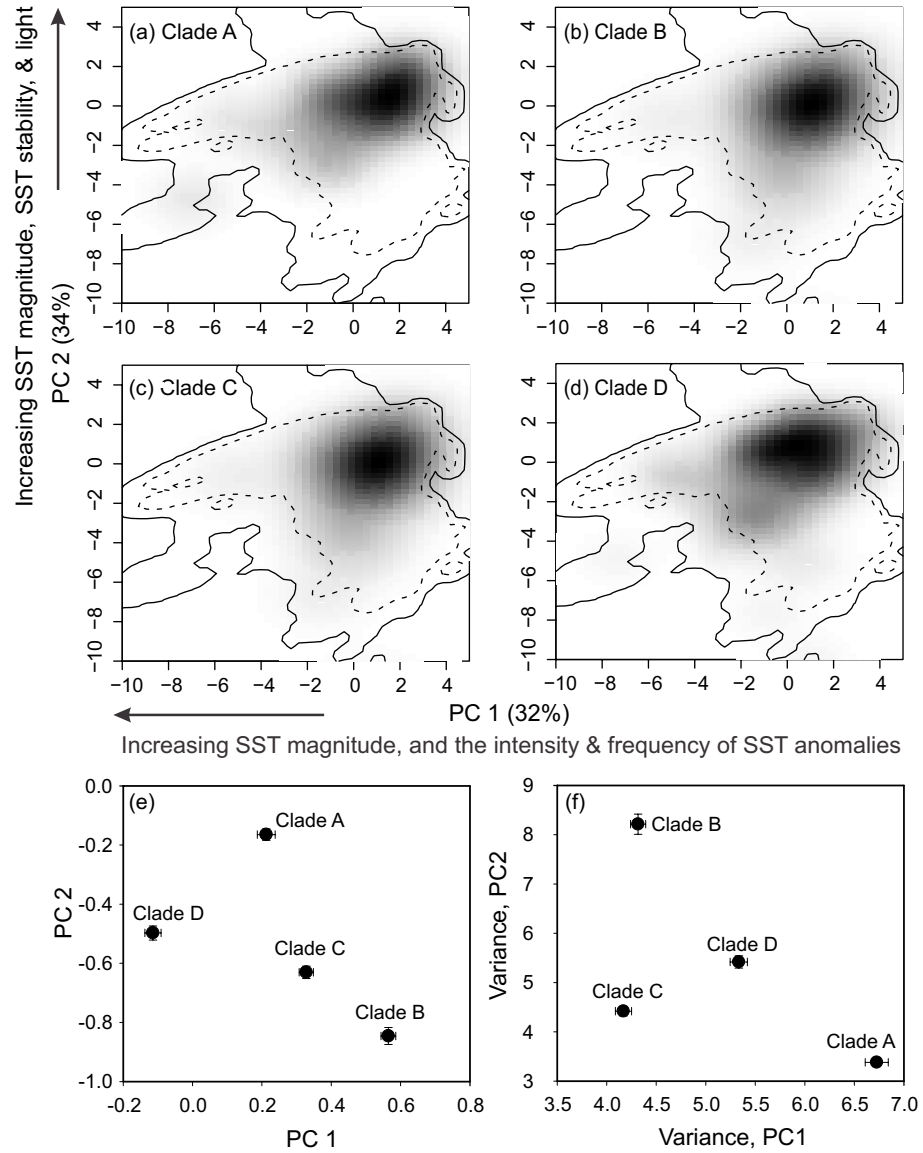
Figure 3.6: Realized niche of Symbiodinium spp. clades A-D, along the first two axes of the PCA; and average niche positions, or the niche centroids for the respective clades along (e) PC1 and (f) PC2 axes. The solid and dashed contours illustrate respectively

Table 3.2: Coefficients of correlation between environmental variables and axes 1 and 2 of the principal component analysis

Variable category	Variable code	Correlation coefficient, r	
		PC1 (34%)	PC2 (32%)
SST anomalies	mean TSA	-0.9	0.2
	mean SSTA	-0.7	-0.6
	TSA freq	-0.9	0.0
	SSTA freq	-0.7	-0.6
	TSA max	-0.9	-0.1
	SSTA max	-0.7	-0.7
SST magnitude	median SST	-0.4	0.9
	min SST	-0.3	0.9
	max SST	-0.5	0.6
SST variability	SST Stdev	0.2	-0.8
SST distribution	SST skewness	0.2	-0.2
	SST kurtosis	-0.1	0.2
Light	PAR	-0.2	0.6

Each pair-wise comparison of the niche centroids and niche breadths along PC1 and PC2 revealed significant difference for all pairs ($P<0.05$) (Fig.3.6e,f). Along PC1, clade B's niche position had the highest scores, while clade D's had the lowest, indicating a niche occupancy for the two clades on the opposite extremes of the

environmental conditions represented by PC1 (i.e. SST magnitude, frequency and intensity of SST anomalies). Niche centroids for clades A and C along this axis were centrally positioned (Fig.3.6e). Along PC2, niche positions for clades A and B were on the opposite extremes, with clade A having the lowest scores on this axis, followed by D, C, B in ascending order. This ranking indicates that clades A and D have a high propensity to occur at high SSTs and irradiance (positively correlated with PC2); that are relatively stable over time (SST variability negatively correlated with PC2). Clade B had the widest niche breadth along the PC2 axis and a narrow niche breadth along the PC1 axis, while clade A had the highest breadth on PC1 and lowest on PC2 axis. Clades C and D had relative moderate niche breadth along both PC axes. The wide niche breadth for clade A indicates a generalist strategy with respect to the environmental conditions, while the narrow niche breadth for clade B suggests specialization.

3.4. DISCUSSION

3.4.1. Global distributions and niche characteristics

The study finds evidence for differences in the environmental niches of the four studied *Symbiodinium* clades, with clade C being a widely distributed generalist, clade D being a tropically distributed specialist, clade A being a spatially restricted generalist, and clade B as a spatially restricted specialist. *Symbiodinium* clade C is the most widely distributed clade in scleractinia and has been reported in many coral reef regions, including the eastern Pacific (LaJeunesse, 2005; Franklin et al. 2012; Baker & Rowan 1997), GBR and western Australia (Cooper et al., 2011; Silverstein et al., 2011), western Indian Ocean (LaJeunesse et al., 2010), and central Pacific (Stat et al. 2009; Putnam et al. 2012). The response curves associated with SST magnitude and irradiance range for coral reef locations show that clade C can tolerate the current breadth of these variables. Our results show that the

climatically suitable habitat for clade C extends to all areas where coral reefs are found including the understudied high latitudinal outlying coral communities (Lien et al., 2007) (Fig.3.3). Although Indo-Pacific corals are more commonly associated with clades C and D, while Caribbean corals are more commonly associated with clades A and B (Baker & Rowan 1997; Baker 2003; LaJeunesse et al. 2003; Silverstein et al. 2012), some strains of clade C are very prevalent in the Atlantic (LaJeunesse 2005). Our study validates these observations and predicts climatically suitable habitat for clade C in the southern and western Caribbean (Fig.3.3).

The climate niche for clade D was defined by extreme temperature associated with high frequency and intensity of SST anomalies, and high irradiance (Figs.3.3, 3.5, 3.6). Locations projected to have suitable climate include NW Australia, the Red Sea, the Maldives, and parts of the coral triangle (SE Asia), western Indian Ocean, eastern and central Pacific, among others (Fig.3.2, 3.3). Notably, in the Caribbean relatively fewer locations are projected to have suitable climate for clade D. This is consistent with earlier reports of clade B dominance over other clades in this region (Baker & Rowan, 1997; LaJeunesse et al. 2003, 2005). Locations in the Caribbean with relatively higher probabilities of occurrence for clade D include Florida, Belize, NW Caribbean, Cuba and the Cayman islands in the northern Caribbean, and in the southern Caribbean among other areas (Fig.3.3d, see Supplementary Information S3.3). Clade D occurrence has previously been reported in the in Florida Keys and US Virgin islands (Correa et al. 2009). In the Indo Pacific, clade D has been recorded in east Africa in the western Indian Ocean (LaJeunesse et al. 2010; Visram & Douglas, 2006), and its distribution in the Indo-Pacific may perhaps occur over a relatively wider scale than currently reported (Fig.3.3, see Supplementary Information S3.3).

Our results indicate that the climatic niche for clade B is relatively small (Fig.3.3, 3.6), with the greatest occupancy in the Caribbean, and in the western and southern Australia. In the Indo-Pacific, clade B is mostly absent, with patchy high probability of occurrences in the eastern Pacific, Arabian Gulf, GBR and sections of Coral Triangle (Fig.3.3). Furthermore, the response curves associated with SST magnitude (Fig.3.5a,b,c) and niche position and breadth tests (Fig.3.6e,f) indicate that the climatic niche of this symbiont clade includes relatively low SST and PAR. This is consistent with previous studies, which have showed that clade B is adapted to cooler temperate environments with greater seasonal fluctuations in temperature and irradiance (Rodriguez-Lanetty et al., 2001; Thornhill et al., 2008; Silverstein et al., 2011). However, there are patches of suitable climate within the tropical Indo-Pacific, where clade B has been found, especially in the western Indian Ocean (Visram & Douglas, 2006), possibly suggesting that some types within this clade could be suited to warmer areas.

Relative to tropical environments, corals in cooler temperate environments, such as those areas with suitable climate for clade B, are poorly studied. This is despite these environments harboring a considerable number of corals species (Veron et al., 2009; Lien et al., 2012). Temperate corals that are tolerant of low temperatures often harbor *Symbiodinium* in clades B and D (Lien et al., 2007; Silverstein et al., 2011; Lien et al., 2012). However, our models did not project these areas to contain suitable climate for clade D. On the contrary, our results suggest that clade D is well adapted to suboptimal high temperature and SST anomaly conditions, while clade B is suited for suboptimal low SST conditions (Figs.3.5, 3.6e).

Despite being uncommon in our dataset, clade A was relatively widely distributed in the Caribbean, and has also been found in the western Indian Ocean, Mediterranean, Red Sea, and GBR (Visram & Douglas,

2006). Our models identified some locations in the western and central Indian Ocean (east Africa, Seychelles, western Madagascar, Andaman Sea) as having suitable climate for these symbionts (see Supplementary Information S3.3). High PAR, high SST with moderate stability and a negatively skewed distribution pattern characterize the climatic niche of this clade. Clade A exploits a narrow climatic niche breadth along PC2, and occurs more generally along the SST anomalies and gradient (i.e. wide niche breadth along PC1). This may explain the localized specialization and the rare occurrence of this clade in coral reefs areas.

While the climatic niches of clades A and D were less distinguishable compared to other pair-wise combinations of clades (niche equivalency tests, p=0.2), niche similarity tests indicate that the respective climatic niches are less similar (P<0.05). High SST and irradiance characterize climatic niches for both clades, albeit at different magnitudes. Moreover, the high temperatures which form part of clade A's niche were not associated with intense SST anomalies, as is the case with clade D (Fig.3.6). Therefore, clade A potentially has thermal tolerance traits, albeit at a lower degree than clade D. This has also been observed in experimental conditions where clade A has been found to confer thermal tolerance to corals exposed to short-term increases in temperature (Rodolfo-Metalpa et al., 2006). Further, clade A may provide photo-protective capabilities, e.g. production of mycosporine-like amino acids (Banaszak et al., 2006) that results in higher tolerance of high irradiance and thermal stress (Reynolds et al., 2008; Suggett et al., 2008); consistent with our results which show clade A's propensity for PAR. In the Caribbean, where clade A prevalence is high relative to the Indo-Pacific, corals experience more frequent but less severe bleaching events, while in the Indo-Pacific bleaching events have been described as less frequent but more severe (Baker 2004b; LaJeunesse et al., 2012). These differences may be linked to the dominance of

clades A and D in the respective regions, and their differences in thermal tolerance traits.

3.4.2. Conservation implications

Symbiosis recombination (i.e., switching or shuffling) in corals has been suggested as a potential mechanism by which corals might respond to climate change (Buddemeier & Fautin 1993). To apply this hypothesis to genetic conservation however, key issues that need to be resolved include, among others, (i) an understanding of the host-symbiont interactions including 'specificity', and (ii) the potential current distribution ranges and climatic niche characteristics of both coral hosts and their *Symbiodinium*, and (iii) how these niches are likely to reorganize spatially as a result of rising temperatures. The first of these issues has been the subject of recent quantitative study (e.g., Silverstein et al., 2012; Putnam et al., 2012). By addressing the second issue, we provide a baseline that can be used to project how climatically suitable habitat may be re arranged in the future. This, in turn, may help identify locations in which conservation approaches may be effective. Similarly it provides a guide for determining where conservation investments may be more successful, or where management or restoration efforts may yield the greatest benefits.

3.4.3. Limitations and future directions

All models are sensitive to the quality and quantity of the underlying data. A major assumption made in this study is that the data used for the calibration represent a random sample of the entire dataset (Araújo & Guissan, 2006). The observation data are climatically biased as there were large areas without samples, especially in the coral triangle, Mediterranean, Polynesia and SW Atlantic (Brazil). Despite the effect of such biases being minimal when true absence data is used (Barbert-Massin et al., 2012); model extrapolations to these areas should be viewed with caution. To justify the acceptance of the models, we tested

the ability of the models to fit the training data. While this is a common practice, model-testing using independent data when available is preferred when describing the distributions of species, understanding the relationships with environmental data and prediction and extrapolation to new spatial and temporal domains.

Model outputs are primarily driven by the choice of predictor variables entering the models (Araújo & Guisan, 2006). The variables chosen here have a physiological basis with respect to corals (Maina et al. 2008), however it is possible some important predictor variables may have been left out due to inadequate knowledge and data availability (Robinson et al., 2011). Significantly, the subject organism for this analysis is an endosymbiont, and more rarely free-living, hence its biogeography is nested within that of the coral host. While this study assumes that many (if not all) coral species are physiologically capable of hosting a variety of symbionts, it is also clear that the degree to which corals realize this diversity varies by host species, and the complexity of these associations is still being analyzed (Putnam et al., 2012; Silverstein et al., 2012). Therefore, the bio-climate modeling approach employed here should be a process where future iterations incorporate new field data. Despite these limitations, our results provide an opportunity to identify geographic gaps for potential surveys. They also provide a baseline to monitor how the diversity and distribution of symbionts may change in response to global climate change. Further sampling and testing of the models with independent data will increase the confidence that can be placed in these projections.
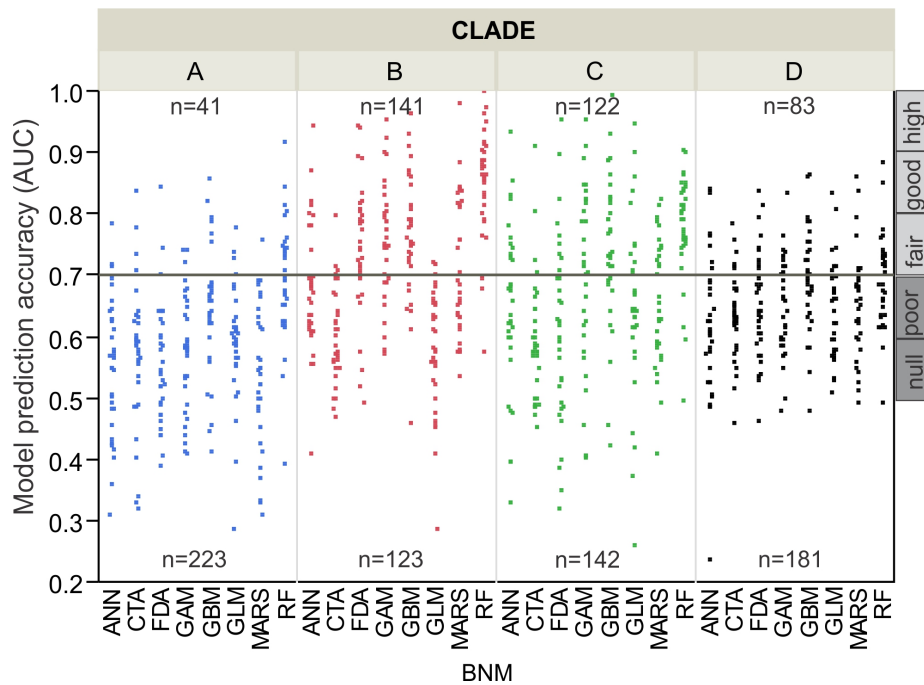
3.5. ACKNOWLEDGEMENTS

3.6. SUPPLEMENTARY INFORMATION

S3.1 Correlation coefficient matrix for pairwise predictor variables

	mean TSA	Mean SSTA	TSA max	TSA freq	SSTA	SSTA	min SST	media n SST	max SST	SST stde	SST	SST	Chl	PAR
mean TSA	1	0.4	0.8	0.9	0.2	0.4	0.2	0.2	0.3	-0.2	0.0	0.5	0.1	0.2
Mean SSTA	0.4	1	0.5	0.6	0.9	1.0	-0.4	-0.3	0.2	0.5	0.1	0.0	0.2	-0.2
TSA max	0.8	0.5	1	0.9	0.5	0.5	-0.1	0.0	0.2	0.1	0.0	0.3	0.1	0.0
TSA freq	0.9	0.6	0.9	1	0.4	0.5	-0.1	0.0	0.2	0.1	0.1	0.3	0.1	0.1
SSTA max	0.2	0.9	0.5	0.4	1	0.9	-0.4	-0.2	0.2	0.5	0.0	0.0	0.1	-0.3
SSTA freq	0.4	1.0	0.5	0.5	0.9	1	-0.5	-0.3	0.2	0.6	0.1	-0.1	0.3	-0.4
min SST	0.2	-0.4	-0.1	-0.1	-0.4	-0.5	1	0.9	0.5	-0.9	-0.1	0.6	-0.1	0.6
median SST	0.2	-0.3	0.0	0.0	-0.2	-0.3	0.9	1	0.7	-0.7	-0.2	0.5	0.0	0.6

max SST	0.3	0.2	0.2	0.2	0.2	0.2	0.5	0.7	1.0	-0.1	-0.1	0.2	0.1	0.3
SST stdev	-0.2	0.5	0.1	0.1	0.5	0.6	-0.9	-0.7	1	1.0	0.1	-0.6	0.1	-0.6
SST skewne	0.0	0.1	0.0	0.1	0.0	0.1	-0.1	-0.2	-0.1	1	1.0	0.1	0.0	0.0
SST kurtosi	0.5	0.0	0.3	0.3	0.0	-0.1	0.6	0.5	0.2	-0.6	1	1	0.0	0.3
Chl	0.1	0.2	0.1	0.1	0.1	0.3	-0.1	0.0	0.1	0.1	0.0	0.0	1	-0.1
PAR	0.2	-0.2	0.0	0.1	-0.3	-0.4	0.6	0.6	0.3	-0.6	0.0	0.3	-0.1	1

S3.2 Predictive accuracy (AUC) for all models showing relative proportions of the models with predictive accuracy above and below a threshold of AUC ≥ 0.7

S3.3 Histograms illustrating the observed niche overlap between paired clades (bars with diamond) and simulated niche overlaps (grey bars) on which tests of niche equivalency of the paired clades (column 1), and niche similarity of the paired clades (columns 2 and 3) are calculated from 100 iterations. The significance tests of the differences between the observed and simulated are shown (ns=not significant, ***=p<0.05)
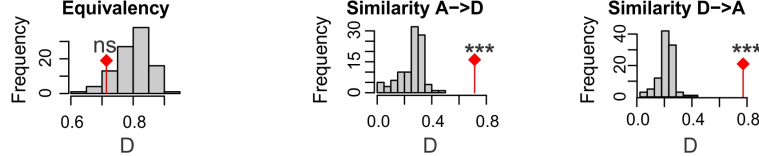
(a) clade A vs B; overlap statistic D = 0.67
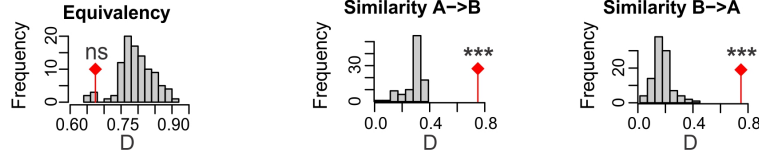
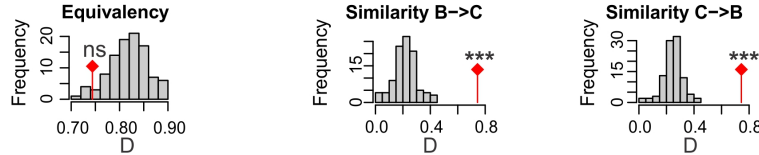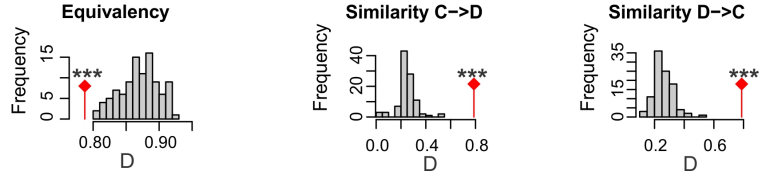(b) clade A vs C; overlap statistic D = 0.75
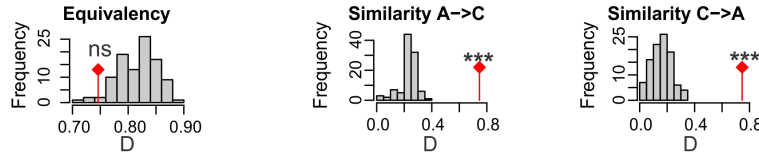
(c) clade A vs D; overlap statistic D = 0.71

(d) clade B vs C; overlap statistic D = 0.74

(e) clade C vs D; overlap statistic D = 0.79

References

Araújo, M.B., Pearson, R.G., Thuiller, W. & Erhard, M. (2005) Validation of species-climate impact models under climate change. Global Change Biology, 11, 1504-1513.

Araújo, M.B. & Guisan, A. (2006) Five (or so) challenges for species distribution modeling, Journal of Biogeography, 33, 1677-1688.

Baird, A.H., Cumbo, V.R., Leggat, W. & Rodriguez-Lanetty, M. (2007) Fidelity and flexibility in coral symbioses. Marine Ecology Progress Series, 347, 307–309.

Baker, A.C. & Rowan, R. (1997) Diversity of symbiotic dinoflagellates (zooxanthellae) in scleractinian corals of the Caribbean and Eastern Pacific. Proceedings of the 8th International Coral Reef Symposium, 2, 1301–1306.

Baker, A.C. (2003) Flexibility and specificity in coral-algal symbiosis: diversity, ecology, and biogeography of Symbiodinium. Annual Review of Ecology Evolution and Systematics, 34, 661-689.

Baker AC (2004) Diversity, distribution and ecology of Symbiodinium on coral reefs and its relationship to bleaching resistance and resilience. In: Coral Health and Disease (Rosenberg E & Loya Y, eds.), Springer-Verlag, New York, Berlin, pp. 177-194

Baker, A.C., Starger, C.J., McClanahan, T.R., & Glynn, P.W. (2004) Coral's adaptive response to climate change. Nature, 430, 741.

Baker, A.C. & Romanski, A.M. (2007) Multiple symbiotic partnerships are common in scleractinian corals but not octocorals. Marine Ecology Progress Series, 335, 237-242.

Banaszak, A.T., Santos, M.G.B., LaJeunesse, T.C., Lesser, M.P. (2006) The distribution of mycosporine-like amino acids (MAAs) and the phylogenetic identity of symbiotic dinoflagellates in cnidarian hosts from the Mexican Caribbean.

Journal of Experimental Marine Biology and Ecology, 337, 131–146.

Barbet-Massin, M., Jiguet, F., Albert, C.H. & Thuiller, W. (2012) Selecting pseudo-absences for species distribution models: how, where and how many? Methods in Ecology Trends and Evolution, 3, 327-338.

Berkelmans, R. & van Oppen, M.J.H. (2006) The role of zooxanthellae in the thermal tolerance of corals: a 'nugget of hope' for coral reefs in an era of climate change. Proceedings of the Royal Society B, 273, 2305 – 2312.

Broennimann, O., Thuiller, W., Hughes, G.,Midgley, G., Robert, J. M., . Alkemades, R., & Guisan, A. (2006) Do geographic distribution, niche property and life form explain plants' vulnerability to global change? Global Change Biology, 12, 1079–1093.

Broennimann, O., Treier, U.A., Müller-Schärer, H., Thuiller,W., Peterson, A.T. & Guisan, A. (2007) Evidence of climatic niche shift during biological invasion. Ecology Letters, 10, 701–709.

Broennimann, O., Fitzpatrick, M.C., Pearman, P.B., Petitpierre, B., Pellissier, L., Yoccoz, N.G., Thuiller, W., Fortin, M.J., Randin, C., Zimmermann, N.E., Graham, C.H., & Guisan, A. (2012) Measuring ecological niche overlap from occurrence and spatial environmental data. Global Ecology and Biogeography, 21, 481–497.

Buddemeier, R.W. & Fautin, D.G. (1993) Coral bleaching as an adaptive mechanism. BioScience, 43, 320 –326.

Cooper, F.T., Berkelmans, R., Ulstrup K.E., Weeks, S., Radford, B., Jones, A.M., Doyle, J., Canto, M., O'Leary, R.A., Madeleine, J.H. & van Oppen, M.J.H. (2011) Environmental factors controlling the distribution of Symbiodinium harboured by the coral Acropora millepora on the Great Barrier Reef. PLOS ONE, 6: e25536.

Correa, A.M.S., McDonald, D.M., & Baker, A.C. (2009) Development of clade-specific Symbiodinium primers for quantitative PCR (qPCR) and their application to detecting clade D symbionts in Caribbean corals. Marine Biology, 156, 2403-2411.

Colwel, R.K. & Rangel, T.F. (2009) Hutchinsons duality: the once and future niche. PNAS, 106, 19651-19658.

Cranet, T.A. & Surle, G.A. (2002) Model-dependent variance inflation factor cutoff values. Quality Engineering 14, 391–403.

Franklin, E.C., Stat, M., Pochon, X., Putnam, H.M. & Gates, R.D. (2012) GeoSymbio: a hybrid, cloud-based web application of global geospatial bioinformatics and ecoinformatics for Symbiodinium–host symbioses. Molecular Ecology Resources, 12, 369–373.

Goulet, T.L. (2006) Most corals may not change their symbionts. Marine Ecology Progress Series, 321, 1–7.

Goulet, T.L. (2007) Most scleractinian corals and octocorals host a single symbiotic zooxanthella clade. Marine Ecology Progress Series, 335, 243-248.

Grinnell, J. (1917) The niche-relationships of the California Thrasher. Auk, 34, 427–433.

Hanley, J.A. & McNeil, B.J. (1982) The meaning and use of the Area under a Receiver Operating Characteristic (ROC) Curve. Radiology, 143, 29-36.

Hedley, J.D., Roelfsema, C.M., Phinn, S.R. & Mumby, P.J. (2012) Environmental and sensor limitations in optical remote sensing of coral reefs: Implications for monitoring and sensor design. Remote Sensing, 4, 271-302.

Holt, R.D. (2009) Up against the edge: invasive species and test beds for basic questions about evolution in heterogeneous environments. Molecular Ecology, 18, 4347– 4348.

Hosmer, D.W. & Lemeshow, S. (2000) Applied Logistic Regression, second ed.   John Wiley & Sons.

Jones, A.M., Berkelmans, R., van Oppen, M.J.H., Mieog, J.C. & Sinclair, W. (2008) A community change in the algal endosymbionts of a scleractinian coral following a natural bleaching event: field evidence of acclimatization. Proceedings of the Royal Society B, 275, 1359-1365.

Knouft, J. H., J. B. Losos, R. E. Glor, and J. J. Kolbe. (2006) Phylogenetic analysis of the evolution of the niche in lizards of the Anolis sagrei group. Ecology, 87, S29–S38.

La Jeunesse, T.C., Loh, W.K.W., Van Woesik, R., Hoegh-Guldberg, O., Schmidt,

G.W. & Fitt, W.K. (2003) Low symbiont diversity in southern Great Barrier

Reef corals relative to those of the Caribbean. Limnology and Oceanography, 48, 2046–2054.

LaJaunesse, T.C. (2005) "species" radiations of symbiotic dinoflagellates in the Atlantic and the Indo-Pacific since the Miocene-pliocene transition. Molecular Biology and Evolution, 22, 570-581.

LaJeunesse, T.C., Pettay, D.T., Sampayo, E.M., Phongsuwan, N., Brown, B., Obura, D.O., Hoegh-Guldberg, O. & Fitt, W.K. (2010) Long-standing environmental conditions, geographic isolation and host-symbiont specificity influence the relative ecological dominance and genetic diversification of coral endosymbionts in the genus Symbiodinium. Journal of Biogeography, 37: 785-800.

Lien, Y-T., Nakano, Y., Plathong, S., Fukami, H., Wang, J-T. & Chen, C.A. (2007) Occurrence of the putatively heat-tolerant Symbiodinium phylotype D in high-latitudinal outlying coral communities. Coral Reefs, 26, 35–44.

Lien, Y-T., Fukami, H. & Yamashita, Y. (2012) Symbiodinium clade C dominates zooxanthellate corals (Scleractinia) in the temperate region of Japan. Zoological Science, 29, 173-180.

Little, A.F., van Oppen, M.J.H., & Willis, B.L. (2004) Flexibility in algal endosymbioses shapes growth in reef corals. Science, 304, 1492-1494.

Maina, J., Venus, V., McClanahan, T.R. & Ateweberhan, M. (2008) Modeling susceptibility of coral reefs to environmental stress using remote sensing data and GIS models. Ecological Modelling, 212, 3-4.

Maina, J., McClanahan, T.R., Venus, V., Ateweberhan, M. & Madin, J. (2011) Global gradients of coral exposure to environmental stresses and implications for local management. PLoS ONE, 6, e23064.

MacNally, R.C. (1995) Ecological versatility and community ecology. Cambridge University Press, Cambridge, New York.

Mieog, J.C., van Oppen, M.J.H., Cantin, N.E., Stam, W.T. & Olsen, J.L. (2007) Real-time PCR reveals a high incidence of Symbiodinium clade D at low levels in four scleractinian corals across the Great Barrier Reef: implications for symbiont shuffling. Coral Reefs 26, 449-457.

Morel, A., Prieur, L. (1977) Analysis of variations in ocean color. Limnology and Oceanography, 22, 709–722.

Oliver, T. & Palumbi, S.R. (2011) Do fluctuating temperature environments elevate coral thermal tolerance? Coral Reefs, 30, 429-440.

Pfenninger, M., Nowak, C. & Magnin, F. (2007) Intraspecific range dynamics and niche evolution in Candidula land snail species. Biological Journal of the Linnean Society, 90, 303–317.

Pochon, X. & Gates, R. D. (2010) A new Symbiodinium clade (Dinophyceae) from soritid foraminifera in Hawai'i. Molecular Phylogenetics and Evolution, 56, 492-497.

Poisot, T., Bever, J.D., Nemri, A., Thrall, P.H. & Hochberg, M.E. (2011) A conceptual framework for the evolution of ecological specialization. Ecology Letters, doi: 10.1111/j.1461-0248.2011.01645.x

Putnam, H.M., Stat, M., Pochon, X. & Gates, R.D. (2012) Sensitivity in scleractinian corals endosymbiotic flexibility associates with environmental. Proceedings of The Royal Society B., doi: 10.1098/rspb.2012.1454.

Reynolds, J.M., Bruns, B.U., Fitt, W.K., & Schmidt, G.W. (2008) Enhanced photoprotection pathways in symbiotic dinoflagellates of shallow-water corals and other cnidarians. Proceedings of the National Academy of Sciences, 105, 13674-13678.

Robinson, L.M., Elith, J., Hobday, A.J., Pearson, R.G., Kendall, B.E., Possingham, H.P. & Richardson, A.J. (2011) Pushing the limits in marine species distribution modeling: lessons from the land present challenges and opportunities. Global Ecology and Biogeography, 20, 789–802.

Rodolfo-Metalpa, R., Richard, C., Allemand, D., Bianchi, C.N., Morri, C. & Ferrier-Pagès, C. (2006) Response of zooxanthellae in symbiosis with the Mediterranean corals Cladocora caespitosa and Oculina patagonica to elevated temperatures. Marine Biology, 150, 45-55.

Rodriguez-Lanetty, M., Loh, W., Carter, D., & Hoegh-Guldberg, O. (2001) Latitudinal variability in symbiont specificity within the widespread scleractinian coral Plesiastrea versipora. Marine Biology, 138, 1175–1181.

Rodriguez-Lanetty, M., Krupp, D., & Weis, V.M. (2004) Distinct ITS types of Symbiodinium in clade C correlate to

cnidarian/dinoflagellate specificity during symbiosis onset. Marine Ecology Progress Series, 275, 97-102.

Rowan, R. (2004) Thermal adaptation in reef coral symbionts. Nature, 430, 742.

Rowan, R. & Powers, D.A. (1991) A molecular genetic classification of zooxanthellae and the evolution of animal-algal symbioses. Science, 251, 1348–1351.

Rowan, R. & Knowlton, N. (1995) Intraspecific diversity and ecological zonation in coral-algal symbiosis. Proceedings of the National Academy of Sciences USA, 92, 2850-2853.

Sampayo, E.M., Franceschinis, L., Hoegh-Guldberg, O., & Dove, S. (2007) Niche partitioning of closely related symbiotic dinoflagelates. Molecular Ecology, 16, 3721-3733.

Selig, E.R., Casey, K.S., & Bruno, J.F. (2010) New insights into global patterns of ocean temperature anomalies: implications for coral reef health and management. Global Ecology and Biogeography, 19, 397-411.

Schoener, T.W. (1968) Anolis lizards of Bimini: resource partitioning in a complex fauna. Ecology, 49, 704-726.

Stat, M. & Gates, R.D. (2011) Clade D Symbiodinium in scleractinian corals: A "nugget" of hope, a selfish opportunist, an ominous sign, or all of the above? Journal of Marine Biology, doi:10.1155/2011/730715.

Stat, M., Pochon, X., Cowie, R.O.M., Gates, R.D. (2009) Specificity in communities of Symbiodinium in corals from Johnston atoll. Marine Ecology Progress Series, 386, 83-96.

Silverstein, R.N., Correa, A.M.S., Lajeunesse, T.C., & Baker, A.C. (2011) Novel algal Symbiont (Symbiodinium spp.) diversity in the reef corals of Western Australia. Marine Ecology Progress Series, 422, 63-75.

Silverstein, R.N., Correa, A.M.S., & Baker, A.C. (2012) Specificity is rarely absolute in coral-algal symbiosis: implications for coral response to climate change. Proceedings of the Royal Society B., 279, 2609-2618.

Suggett, D.J., Warner, M.E., Smith, D.J., Davey, P., Hennige, S. & Baker, N.R. (2008) Photosynthesis and production of hydrogen peroxide by Symbiodinium (Pyrrhophyta) phylotypes with different thermal tolerances. Journal of Phycology, 44, 948-956.

Thornhill, D.J., Kemp, D.W., Bruns, B.U., Fit, W.K., Gregory & Schmidt, W. (2008) Correspondence between cold tolderant and temperate biogeography in a western Atlantic Symbiodinium (Dinophyta) lineage. Journal of Phycology, 44, 1126-1135.

Thuiller, W. (2003) BIOMOD – optimizing predictions of species distributions and projecting potential future shifts under global change. Global Change Biology, 9, 1353-1362.

Thuiller, W. (2004) Patterns and uncertainties of species range shifts under climate change. Global Change Biology, 10, 2020-2027.

Toller, W.W., Rowan, R. & Knowlton, N. (2001) Zooxanthellae of the Montastraea annularis species complex: patterns of distribution of four taxa of Symbiodinium of different reefs and across depths. Biological Bulletin, 201, 348-359.

Trench RK (1989) Genetic basis of specificity in dinoflagellate-invertebrate symbiosis. NTIS Order No.: AD-A209 812/7/GAR. Contract N00014-88-K-0463.

Trench RK (1992) Microalgal-invertebrate symbiosis, current trends. Encyclopedia of Microbiology, 3, 129-142.

Veron, J.E.N., DeVantier, L.M., Turak, E., Green, A.L., Kininmonth, S.,

Stafford-Smith, M., & Peterson, N. (2009) Delineating the coral triangle. Galaxea, 11, 91-100.

Visram, S. & Douglas, A.E. (2006) Molecular diversity of symbiotic algae (zooxanthellae) in scleractinian corals of Kenya. Coral Reefs, 25, 172-176.

Warren, D.L., Glor, R.E. & Turelli, M. (2008) Environmental niche equivalency versus conservatism: quantitative approaches to niche evolution. Evolution, 62, 2868–2883.

Yang, S.Y., Keshavmurthy, S., Obura, D., Sheppard, C.R.C., Visram, S. & Chen, C.A. (2012) Diversity and distribution of Symbiodinium associated with Seven common coral species in the Chagos Archipelago, Central Indian Ocean. PLOS ONE, 7, e35836.

Zhou, G., Huang, H., Lian, J., Zhang, C. & Li, X. (2012) Habitat correlation of Symbiodinium diversity in two reef-building coral species in an upwelling region, eastern Hainan Island, China. Journal of the Marine Biological Association of the United Kingdom, doi:10.1017/S0025315411001548.

4. LINKING CORAL RIVER RUNOFF PROXIES WITH CLIMATE VARIABILITY, HYDROLOGY AND LAND-USE IN MADAGASCAR CATCHMENTS

ABSTRACT

Understanding the linkages between coastal watersheds and adjacent coral reefs is expected to lead to better coral reef conservation strategies. Our study aims to examine the main predictors of environmental proxies recorded in near shore corals and therefore how linked near shore reefs are to the catchment physical processes. To achieve these, we developed models to simulate hydrology of two watersheds in Madagascar. We examined relationships between environmental proxies derived from massive *Porites* spp. coral cores (spectral luminescence and barium/calcium ratios), and corresponding time-series (1950-2006) data of hydrology, climate, land use and human population growth. Results suggest regional differences in the main environmental drivers of reef sedimentation: on annual time-scales, precipitation, river flow and sediment load explained the variability in coral proxies of river discharge for the northeast region, while El Niño-Southern Oscillation (ENSO) and temperature (air and sea surface) were the best predictors in the southwest region.

4.1. INTRODUCTION

The decline of coral reefs has been attributed to multiple and interacting global and local pressures. These pressures include pollutants from terrestrial sources (Gardner *et al.*, 2003; Wilkinson, 2004), overfishing (Mumby *et al.*, 2006; Mora, 2010), and changes in sea surface temperature (SST) and seawater pH (Hoegh-Guldberg *et al.*, 2007; Eakin *et al.*, 2009; Fabricius *et al.*, 2011; Pandolfi *et al.*, 2011). Coral reef ecosystem changes occur at different spatial scales, where local factors may exacerbate the effects of global processes, and temporal scales, where longer-term trends may be obscured by short-term, inter-annual and seasonal variability (Chabanet *et al.*, 2005; Habeeb *et al.*, 2005; Darling *et al.*, 2010). Understanding the linkages between local and global processes in coastal watersheds and adjacent reef ecosystems is expected to lead to better coral reef conservation strategies (Jupiter, 2006; Richmond *et al.*, 2007; Prouty *et al.*, 2010). Furthermore, the development of long-term records of the physical environment of coastal watersheds, adjacent coral reef ecosystems, and linkages between them will help contextualize recent observations and help to identify the likely causes.

In Madagascar, several interacting environmental factors have changed over the past few decades, including air and sea surface temperature, storm frequency, rainfall quantity and intensity, soil erosion and sediment yield, river discharge, land cover, cropping systems, urbanization, coastal turbidity, and exploitation of reef fisheries (Hofmann *et al.*, 2005; Alory *et al.*, 2007; Zhang *et al.*, 2007; Kuleshov *et al.*, 2008; Mavume *et al.*, 2009). For example, there has been extensive deforestation over the past 5 decades attributed to charcoal exploitation, cropland expansion, mining and increased logging (Sussman *et al.*, 1994; Harper *et al.*, 2007). The decline in forest cover is coincident with human population increase, loss of biodiversity in the forests (Ingram & Dawson, 2005; Hannah *et al.*, 2008), and a significant decline in coral cover (Harris *et al.*, 2010;

Bruggemann *et al.*, 2012) over the same period. Long-term monitoring of environmental change may provide early warnings of environmental regime shifts (Carpenter *et al.*, 2011). Furthermore, a better understanding of environmental changes and how they interact may provide opportunities to change resource management practices and avoid irreversible and un-desirable ecological changes (Lindenmayer *et al.*, 2011).

In Madagascar, long-term records of river discharge are sparse and the majority of sub-catchments are un-gauged. In such cases, hydrological models are required to provide spatial information for environmental management decision-making (Lu *et al.*, 2006). Here we use STREAM hydrological model (Spatial Tools for River basins, Environment and Analysis of Management options; (Aerts *et al.*, 1999); (Bouwer *et al.*, 2006)) and N-SPECT (Nonpoint-Source Pollution and Erosion Comparison Tool) (Eslinger *et al.*, 2005) to reconstruct historical river discharge and sediment load in Madagascar catchments. STREAM is a grid-based spatial water balance model that describes the hydrological cycle of a drainage basin as a series of storage compartments and flows (Bouwer *et al.*, 2006). Using monthly time step climate data as input, STREAM has successfully been applied in catchments of varying size in different parts of the world (e.g. (Aerts & Bouwer, 2002); (Bouwer *et al.*, 2006)).

Environmental proxy records, such as those laid down annually in the skeleton of massive *Porites* coral species, can augment model-based reconstructions and instrumental observations (Felis & Pätzold, 2003); (Grottoli & Eakin, 2007; Prouty *et al.*, 2010). We utilize two of these environmental proxies related to sediment load and river flow: the barium/calcium ratio (Ba/Ca; (McCulloch *et al.*, 2003) and the luminescence green/blue ratio (G/B;(Grove *et al.*, 2010)), as indicators of environmental variability and long-term changes over the last five decades. Temporal variability of Ba/Ca in coral skeletons in near-shore

areas has been shown to correspond with terrestrial sediment loading (Alibert *et al.*, 2003; Prouty *et al.*, 2010; Lewis *et al.*, 2011; Lewis *et al.*, 2012). Barium (Ba) is dissolved into the drainage catchment and adsorbed to suspended sediments (clay minerals), which are then transported to coastal waters via rivers. As salinity increases, Ba desorbs from the suspended sediment due to the higher ionic strength of seawater. Ba diluted by seawater is thought to follow a conservative mixing pattern (Sinclair & McCulloch, 2004), and thus can act as a tracer for riverine sediment input into the ocean.

When placed under ultra-violet (UV) light, slices from inshore massive corals often display bright luminescent lines that have been linked to river flood plumes from coastal catchments and hence have the potential to provide a long-term record of hinterland precipitation (Isdale *et al.*, 1998; Lough, 2011). Coral luminescence is thought to result from the incorporation of soil-derived humic acids transported to the reef during major flood events (Lough *et al.*, 2002; Jupiter *et al.*, 2008; Grove *et al.*, 2010). Here, we apply spectral luminescence scanning (SLS) of coral cores that uses the UV emission wavelength of the green (humic acid signal) relative to blue portions (skeletal density signal) of the electromagnetic spectrum, expressed as green/blue (G/B) ratio, as an indicator of the relative amount of humic acids in river runoff reaching the reef (Grove *et al.*, 2010). Temporal variability in the Ba/Ca and G/B ratios (or luminescence intensity) has been successfully associated with a watershed's historical rainfall, erosion and river flow (Grove *et al.*, 2010; Lough, 2011).

This study aims to evaluate the relationships between climate variables (i.e. air and sea surface temperature, precipitation, ENSO (El Niño-southern oscillation), population growth, land use change, hydrology, and environmental proxies derived from cores of coral colonies in the northeast (NE) and southwest (SW) Madagascar catchments. We develop hydrological models to reconstruct river discharge and

sediment yield in these catchments and examine the relative importance of climatic versus anthropogenic processes as drivers of river flow and terrestrial sediment discharge. We test whether river discharge signals are recorded at the reef scale in Madagascar and discuss the validity of coral proxies as reliable recorders of environmental change. Further, we investigate evidence of change points or significant events, seasonality, and inter-annual and long-term trends in the time series of environmental and coral proxy data. We test the following hypotheses:

I.   There is significant covariation between coastal climate, hydrology, land use (forest cover), population size and coral river runoff proxies.

II.   Changes in coastal climate (precipitation, air and sea surface temperature), hydrology, forest cover, and population size significantly explain the variability in changes in coral river runoff proxies (i.e. Ba/Ca and G/B).

4.2. METHODS

4.2.1. Study area

The island of Madagascar lies between 13-25ºS in the south-western Indian Ocean, extending roughly 1600 km in north-south direction and 500 km across. The western side is dominated by coastal plains and the transition between the west and the east coast plateaus consists of mountains >1500 m high. The east coast is wet and humid throughout the year, owing to orographic uplift of trade winds (Nassor & Jury, 1998). In the highlands the weather is determined by the dynamic interaction of trade winds, monsoon flow and the subtropical anticyclones, and a hot rainy season occurs during the Southern Hemisphere summer. Tropical cyclones and floods affect the NE and SW from November to May. The rainfall season starts in late December, with a convective peak in mid-February that declines by the

end of March (Jury & Pathack, 1991). The cooler dry season occurs between June to October when climate is dominated by SE trade winds; it lasts up to 2 months longer in the SW of Madagascar compared to the NE. Annual total rainfall varies from 3700 mm in the east to 400 mm in the west and SW. Our study watersheds are located in the SW and in the NE. The Onilahy and Fiherenana rivers drain the SW watershed, while Antainambalana River, which flows into Antongil Bay drains the NE watershed (Fig.4.1).

4.2.2. Hydrological modeling

Given the sparse observational long-term hydrological data for Madagascar, we employed STREAM to simulate monthly and annual river discharge patterns in the NE and SW regional watersheds (Aerts *et al.*, 1999; Bouwer *et al.*, 2006). STREAM simulates the water balance for each grid using a limited number of parameters, including spatial-temporal precipitation and temperature data, elevation, land-cover and soil water storage capacity (Aerts & Bouwer, 2002) (Supplementary Information 4.1, 4.2).
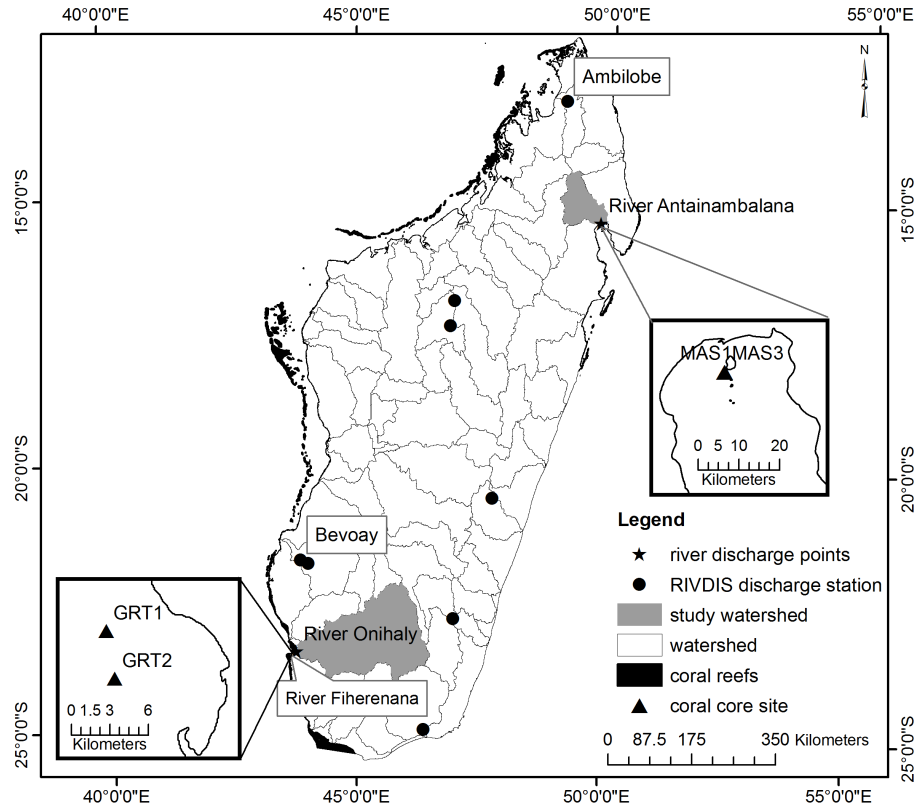
Figure 4.1: Map of Madagascar showing all the watersheds, coral reefs, the northeast (NE) and southwest (SW) study basins, locations of the respective main rivers draining these basins, and river discharge observational stations (black filled dots). The location of the calibration (Bevoay) and validation stations (Ambilobe) for the hydrological model are indicated

A configuration of the STREAM model was developed and run for the whole of Madagascar for 1950-2006. The model provided output time series of average monthly discharge in m^3/s for selected locations. These locations included outlet points of the Antainambalana and Onilahy Rivers, which drain the NE and SW watersheds, respectively, and eight gauging stations (Fig.4.1), for which data were available in the RivDIS database

(http://daac.ornl.gov/RIVDIS/rivdis.shtml)(Vorosmarty *et al.*, 1998). The lengths of these records vary widely among stations. The Bevoay station on the Mangoky River had the longest time series (total of 310 months, intermittently between 1952-1994), and is relatively close to the SW watershed. Consequently, data from this station were used to calibrate the STREAM model by adjusting the various model coefficients to optimize the simulated monthly hydrographs (Aerts *et al.*, 1999). The performance of the model was tested at every stage using the model efficiency coefficient (NSE) (Nash & Sutcliffe, 1970), a widely used statistic in hydrological studies. NSE ranges between negative infinity and 1, where values between 0 and 1 are considered satisfactory, but values <0 indicate poor performance (see e.g. (Moriasi *et al.*, 2007)). Respective discharge volumes were also compared by calculating the ratio of modeled to observed values. STREAM outputs were subsequently validated using the Ambilobe river discharge station in the North of Madagascar (Fig.4.1).

Sediment yield per unit area was computed using the Non-Point Source Pollution and Erosion Comparison Tool (N-SPECT) developed by the National Oceanic and Atmospheric Administration (NOAA) (http://www.csc.noaa.gov/digitalcoast/tools/nspect/index.html). It combines data on elevation (Lehner *et al.*, 2008), slope (Nam *et al.*, 2003), soils (FAO/IIASA/ISRIC/ISSCAS/JRC 2009), precipitation (Mitchell & Jones, 2005), rainfall erosivity (Vrieling *et al.*, 2010), and land cover (Harper *et al.*, 2007) to derive estimates of runoff, erosion, and pollutant sources (nitrogen, phosphorous, and suspended solids) from across the landscape, as well as estimates of sediment and pollutant accumulation in stream and river networks. The N-SPECT tool was run for each year from 1950-2006 to obtain estimates of annual sediment yield per unit area in mt/year (see Supplementary Information 4.1 and 4.2 for details on input parameters).

4.2.3. Coral sampling and analysis

Coral cores were drilled in March and April 2007 from massive colonies of *Porites* spp. at water depths between 4-6 m along the southern fringing reef slope at Nosy Mangabe Island in Antongil Bay (NE Madagascar) (Fig.4.1) (Grove *et al.*, 2010). Two of these cores (MAS1 and MAS3), drilled ~300 m apart and both located 7 km from the river Antainambalana's mouth, are utilized in this study. The river plume directly disperses towards the core sites, as described in detail in (Grove *et al.*, 2010). Two coral cores from SW Madagascar (GRT1 and GRT2) were drilled in March 2008 at 3 m depth on the inner slope of the *Grand Récif* of Toliara (GRT) (Fig.4.1). The GRT, located <2 km seaward of Toliara town, is a major barrier reef system of the southwestern Indian Ocean. It stretches over 19 km (23°20 - 23°30 S) between the Fiherenana River in the north and the Onilahy River in the south (Fig.4.1) and represents approximately 33 km^2 of structurally diverse shallow reef area. Coral core GRT-1 is located 15.7 km north of the Onilahy river mouth and 11.2 km south of the Fiherenana River mouth, whereas GRT-2 is located 12.5 km north of the Onilahy River and 19.9 km south of the Fiherenana River.

A detailed description of the coral core sample preparation and analysis is given in (Grove *et al.*, 2010). In brief, coral cores were sectioned lengthwise into 7 mm thick slabs, rinsed several times with demineralised water, blown with compressed air to remove any surficial particles and dried for more than 24 hours in a laminar flow hood. Annual bands were visualised by X-radiograph-positive prints and luminescence imagery to produce an initial chronology based on annual density and luminescence bands (Grove *et al.*, 2010). All coral slabs from the four cores were cleaned with sodium hypochlorite (NaOCl, 10-13% reactive chloride; Sigma-Aldrich Company) for 24 hours to remove residual organics that might quench luminescence. Spectral luminescence scanning (SLS) was performed on bleached coral slabs using a line-scan camera fitted with a Dichroic beam

splitter prism, separating light emission intensities into three spectral ranges: red (R), green (G) and blue (B) (Grove *et al.*, 2010). We subsequently calculated the Green/Blue (G/B) ratio that reflects the changing humic acid/aragonite skeletal density ratio in the coral skeleton. To obtain Ba/Ca ratios at 40 μm intervals, slabs of the coral cores from NE Madagascar were analyzed by laser ablation inductively coupled plasma mass spectrometry (LA ICP-MS) at the Australian National University in Canberra, following the methods described by (Fallon *et al.*, 2002). We use 56 years (1950-2006) from the NE coral G/B and Ba/Ca data (cores MAS1 and MAS3). LA ICP-MS analyses on the SW Madagascar corals were done at the Max-Planck-Institut (MPI) für Chemie in Mainz (Germany). A detailed description of the LA ICP-MS procedure applied is given by (Mertz-Kraus *et al.*, 2009). Analysis in both laboratories utilized either NIST SRM 614 or 612 glasses as reference material. This approach has been shown to result in reliable, reproducible element concentrations in carbonate material (e.g., (Fallon *et al.*, 2002; Mertz-Kraus *et al.*, 2009)). Age models for both Ba/Ca and G/B ratios were based on the driest month in any given year (lowest Ba/Ca and G/B) in local rainfall and subsequent linear interpolation between the October anchor points using AnalySeries 2.0 (Paillard *et al.*, 1996) to a monthly time scale (for details see, (Grove *et al.*, 2010)). The G/B and Ba/Ca time series for the NE cover 1950 to 2006, and the Ba/Ca data for the SW cover 1976 to 2008 (GRT1) and 1975 to 2008 (GRT2).

4.2.4. Data analysis

Principal component analysis (PCA) was used to examine covariance and common temporal variations among hydrological variables (annual average discharge and sediment load), climatic variables (annual average sea surface temperature (hereafter SST), air temperature (hereafter AT), annual precipitation, the Niño3.4 SST anomaly index (i.e. an indicator of the strength of tropical Pacific ENSO events: http://www.cpc.ncep.noaa.gov/data/indices/), and the coral proxies for

river flow and sediment load (G/B and Ba/Ca) from NE and SW watersheds. Given the temporal autocorrelation inherent in time series data, we used PCA to reduce the dimensionality of the data matrix by finding uncorrelated principal components (PCs) that together account for much of the variance in the original variables(Jackson, 1991).

For each variable and watershed, time series data were aggregated on an annual basis using the November-October water year. For the NE, data for 11 variables were available in monthly time steps for 56 years (1950-2006) (Supplementary Information 4.2). For the SW, G/B data could not be used (see Supplementary Information 4.3); Ba/Ca time series were available at monthly time steps for 31 years (1976-2006). Consequently, for each region PCA was performed with seven environmental variables at 56 and 31 yearly time steps, respectively. PCA was repeated with the coral proxies, where four time series (two Ba/Ca and two G/B) and two time series (both Ba/Ca) were the input data for the NE and the SW, respectively. To estimate the association of each of the variables with the PCs, we performed pairwise correlations. To identify possible change points and their synchrony in the environmental multivariate and coral proxies time series, we applied the widely-used sequential t-test method (Rodionov, 2004) of environmental and coral proxies' PC's that explained >10 % variability. A cut-off regime length of 10 years was chosen and default settings were used for the other parameters (probability = 0.1; Huber parameter = 1; no weighting). Bivariate plots of standardized absolute values of the environmental and coral proxies were also constructed.

To investigate the presence of seasonality in the time series, we used autocorrelation, a mathematical feature that identifies seasonality in time series, and present graphs showing correlations between values in a time series and those at a fixed time interval later (Davis, 1986). By investigating how a time series correlates with itself at different time lags, autocorrelation detects non-randomness in data using

autocorrelation function, *R*(Box & Jenkins, 1976). An autocorrellogram is produced when the lags are plotted as a histogram at lags of *1, 2….t.* (Davis, 1986). The equations and methodology of autocorrelation function has been described in (Chatfield, 2003). For each variable, we also graphed the averaged absolute values for each month.

Finally, we employed generalized linear models (GLM) to determine which environmental variables explained the variability in coral runoff proxies in each watershed. Climate, land use, population and hydrologic variables were used as the predictors of coral proxies. Due to the temporal ordering of the data, pre-processing steps, i.e. z-score standardization and detrending, were carried out before fitting GLMs (Zuur *et al.*, 2003). Detrending removes any temporal trend, which can be confounding and can lead to spurious relationships, while z score standardizing ensures that the time series' statistical properties such as mean, variance, and autocorrelation are all constant over time. Because we were primarily interested in variables driving changes in coral proxies at yearly time-scales, we used first order differencing to detrend all z score standardized time-series data.

Multicollinearity among predictor variables may have adverse effects on estimated coefficients in a multiple regression (Mansfield & Helms, 1982). To detect the existence of multi-collinearity in our data, variance inflation factors (VIF) were computed. VIFs specify how much of a regressor's variability is explained by the remaining regressors in the model due to correlation among those regressors (Craney & Surles, 2002). A very conservative cut-off value of VIF = 3 was adopted relative to suggested values of 5 or 10 (Craney & Surles, 2002). High multi-collinearity was detected due to high correlation between river flow, sediment load, and precipitation in both regions. Consequently these variables were used interchangeably in a model with uncorrelated variables.

Further, regression equations that use time series data often contain lagged variables (e.g., (Zuur *et al.*, 2003; Lui *et al.*, 2007)). In our context, lags may be due to uncertainties in the environmental data, hydrological models, alignment error in time series elements, dating of the environmental proxies, and time delays in biological processes ((Barnes, 1993)) among other factors, which could lead to temporal mismatch in data consequently concealing relationships. Therefore, we introduced 0-3 year lags (*Lag=t+0...3*) on predictor variables in the GLM process where GLM was repeated for each lag. For the NE, 4 models (*Lag=t+0...3*) were run three times (i.e. each time with precipitation, sediment load or river flow) for each response coral proxy data. Similarly, for the SW, 4 models were run three times for Ba/Ca. During the GLM stepwise process, predictor variables are added and dropped in several iterations until the best model is achieved based on the Akaike Information Criterion (AIC) model selection method (Zuur *et al.*, 2009). To ensure robustness of the model estimates, residuals were examined for autocorrelation using the Durbin–Watson test (Durbin & Watson, 1971); no autocorrelation was found. We report only significant models in Table 4.2.

4.3. RESULTS

4.3.1. Calibration and validation

Calibration of hydrological model (STREAM) results at Bevoay, based on 25 years of model simulation, are given in Figures 4.2a and c. When simulations were compared with observed monthly averaged hydrographs of the respective catchments using the calibration tests (NSE and modeled/observed ratio), values were close to one, indicating good agreement. The validation of the annual hydrograph at Ambilobe (Figs.4.2b,d) also shows good seasonal agreement. However the absolute amount of annual modeled discharge was slightly lower than observed (NSE 0.73). Comparisons of observed/modeled annual discharges over time (Fig.4.2, bottom panels) also revealed that the

model performed well in both the calibration and validation stations with occasional mismatches in observed/modeled peak values (Figs.4.2c,d). At Bevoay, the prediction at annual time scales was significant and explained a substantial part of the observed variance (56%), but the values of intercept (>0) and slope (<1), suggest a systematic discrepancy. Since we had no objective guidance to further adjust our model parameters, we accepted this difference: our model overestimates discharges above ~ 800 m^3/s.

4.3.2. Relationships among variables

PCA of environmental variables for the NE and SW revealed considerable covariance, with PC 1 and PC 2 in each region, together accounting for over 65% of the total variation in the multivariate samples (Table 4.1). In the NE, sediment yield, precipitation, river flow, forest cover, and population were highly correlated with PC 1 (39%) (Table 4.1) (r ≥ 0.6). Also AT and SST correlated moderately (r = 0.4-0.5) with PC 1 and highly (r ≥ 0.6) with PC 2 (29%). AT and SST covaried negatively with precipitation and with hydrological variables in PC 2. ENSO (Niño3.4 Index) correlated moderately with PC 1 and 2, and highly with PC 3 (15%) (Table 4.1), alongside forest cover, SST, and population growth. In the SW (Table 4.1), PC 1 (44%) was comprised mainly of temperature, population and forest cover, while PC 2 (30%) was comprised of precipitation, river flow and sediment load. PC 3 (12%) was highly correlated with ENSO (r = 0.9) and moderately with precipitation (r = 0.2). Comparisons of the PC's in the two regions indicate similarities and differences. Forest cover and population in both regions were highly prominent in PC 1. However, hydrological variables and precipitation associated with PC 1 in the NE were replaced by AT and SST in the PC1 in the SW.
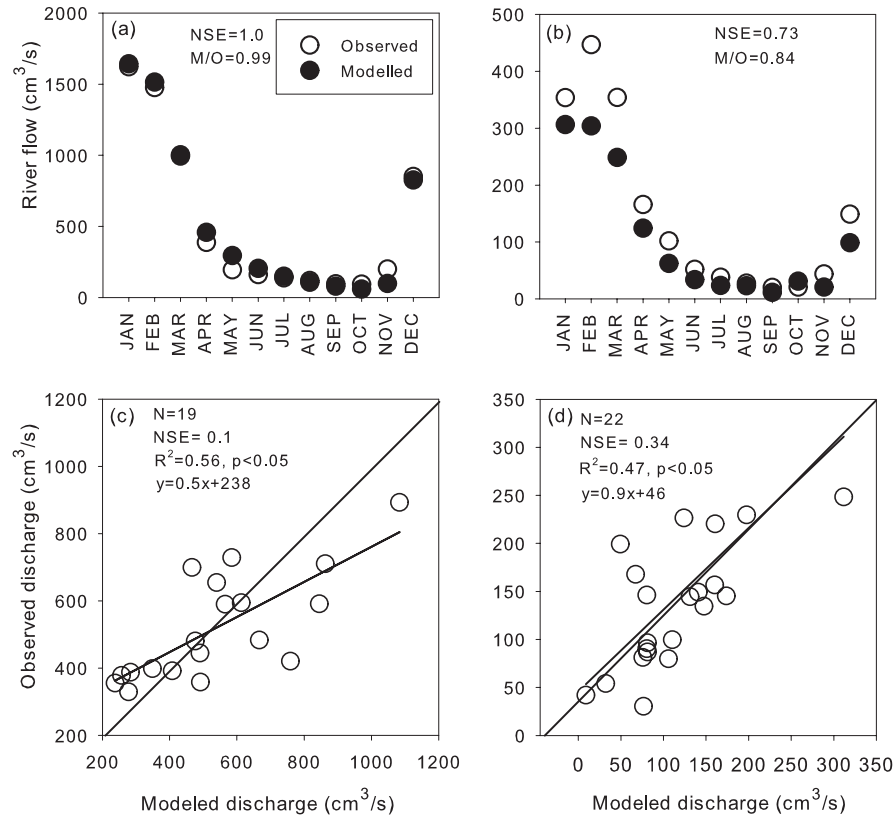
Figure 4.2: Plots of observed against modeled discharge at monthly and annual aggregation levels at calibration and validation stations. Hydrograph and mean monthly average for each year for the calibration station (Bevoay, a and c), and for the validation station (Ambilobe, b and d) are shown. NSE index (see text) values and the model/observation ratio are presented, the latter is shown only for hydrographs. The regression line indicates the deviation of the modeled discharge relative to the diagonal line

Table 4.1: Correlation coefficients between leading three PCs for each region and various environmental and coral proxy time series. Bold values are statistically significant at the 95% confidence level.

Principal components	Northeast			Southwest		
	PC 1	PC 2	PC 3	PC 1	PC 2	PC 3
Contribution ratio (%)	39.4	29.3	15.1	43.7	30.4	11.6
Precipitation	**0.6**	**0.7**	**0.3**	0.0	**0.9**	**0.2**
Sediment load	**0.7**	**0.5**	-0.1	0.0	**0.8**	-0.1
River flow	**0.6**	**0.8**	**0.2**	-0.1	**1.0**	0.1
Forest cover	**-0.8**	**0.3**	**0.5**	**-0.9**	-0.1	0.1
Population	**0.8**	**-0.2**	**-0.5**	**0.9**	0.1	-0.1
Air temperature	**0.5**	**-0.7**	0.1	**0.9**	-0.1	-0.1
Sea surface temperature	**0.4**	**-0.6**	**0.4**	**0.9**	0.0	0.0
Niño3.4 index	**0.5**	**-0.4**	**0.6**	**0.3**	-0.1	**0.9**
Ba/Ca MAS1 (GRT1)	**0.6**	**-0.2**	**-0.3**	**0.4**	**0.2**	0.0
Ba/Ca MAS 3 (GRT2)	**0.3**	-0.1	**-0.3**	0.1	0.1	0.0
G/B MAS1	**0.6**	-0.1	**-0.2**			
G/B MAS 3	0.1	0.0	-0.1			

Coral proxies, except G/B MAS 3, correlated highly with environmental PC 1, while Ba/Ca also correlated marginally with PC 3. For the SW, only one of the two Ba/Ca records (GRT1) correlated significantly with PC 1 and PC 2 (Table 4.1). For the NE, both proxies in MAS 1 highly (positively) correlated with PC1, while MAS3 Ba/Ca was moderately correlated with PC1. G/B and Ba/Ca in MAS1 were negatively correlated to PC2, which is mostly dominated by temperature, precipitation and river flow. Environmental proxies in both cores were also negatively associated with PC3, dominated mostly by ENSO, temperature, forest and land cover. For the SW, only one of the two Ba/Ca records (GRT1) correlated significantly with PC

1 (dominated by AT, SST, ENSO, forest cover and population growth). The same core showed significant but relatively lower correlation with SW PC2 (dominated by river flow, sediment load and precipitation, Table 4.1). These results suggest that precipitation and hydrology, both influenced by anthropogenic catchment alteration, are the key environmental drivers in the NE, but a significant contribution of temperature and ENSO is also evidenced. In the SW, forest cover, population growth, AT, SST and ENSO represent the main environmental drivers.

Table 4.2: Generalized linear model (GLM) outputs showing models that significantly explain the variation in each of the coral proxy variables in the NE and SW regions. GLM selects variables for deletion or inclusion based on Akaike Information Criterion (AIC)''; given a set of models for the data, the preferred model is the one with the minimum AIC value

Dependent variable	Model AIC	Predictor	t-value	p
Northeast				
Ba/Ca $_{(t+2)}$	326	Precipitation	4.2	0.00
	327	Sediment load	3.2	0.00
	329	River flow	4.1	0.00
G/B $_{(t+0)}$	347	Air temperature	3.5	0.00
		Precipitation	1.9	0.05
		Niño3.4 index	-2.0	0.05
	349	Air temperature	3.59	0.00
		Sediment load	2.48	0.01
		Niño3.4 index	-1.85	0.07
	350	Air temperature	3.5	0.00
		River flow	1.7	0.095
		Niño3.4 index	-1.9	0.06

G/B (t+2)	338	River flow	3.1	0.00
	338	Sediment load	3.1	0.00
	340	Precipitation	2.7	0.01
Southwest				
Ba/Ca (t+1)	182	Air temperature	3.0	0.00
		Niño3.4 index	-3.5	0.00

Change point analysis of environmental and coral proxies PCs for the respective regions revealed significant changes at various points in the time series (Fig.4.3). In the NE, environmental PC 1 shows positive change points in 1958, 1982, 1991, 2002 (Fig.4.3a). The 1991 and 2002 change points did approximately correspond, albeit with a lag of 2-3 years, with coral proxy PC 1 (65%), which showed positive shifts in 1988 and 2000 respectively (Figs.4.3a,d). The 1958-change point appeared in both environmental parameters' PC 1 and coral proxies PC 2 (18%) (Figs.4.3a,e). NE forest cover was negatively associated with environment PC 1, while the other variables were positively associated with PC1 (hydrology, precipitation, and population, Table 4.1). Thus, the stepwise change in hydrology, precipitation, and population growth reflects an increasing trend while a declining trend is observed for forest cover (Figs.4.4, 4.5). In the SW, PC 1 showed step-like positive changes during 1969, 1977, 1987, and 1997 (Fig.4.3f). The last two change points approximately corresponded with those depicted by the trends in the two coral proxies in 1989 and 1999 (Figs.4.3i,j). The positive step like change in PC1 represents an increasing trend for temperature and population growth and a decrease in forest cover.

4.3.3. Seasonal variability in observational, modeling and coral data

Figure 4.6 illustrates the seasonal dynamics of the modeled discharge, the coral proxies and several other environmental indicators for both

catchments. Visual inspection of the seasonal dynamics indicates high synchrony among the hydrological variables (Figs.4.6a,b), precipitation and discharge, and between the two regions, with peak values during the wet season between January to March and lowest values in the dry season between September/October (Figs.4.6a,b). Climatic differences between the NE and SW in hydrological variables are also evident. During wet months, precipitation and discharge is higher in the NE than in the SW (Figs.4.6a,b). The NE is wet throughout the year with relatively high discharge. The discharge in the SW shows a sharp peak around February whereas peak discharge in the NE is more evenly distributed throughout the rainy season (Fig.4.6b). AT and SST showed an almost similar seasonal timing as hydrological variables: the highest temperatures occurred between January to March and the lowest temperatures between August and September (Figs.4.6e,f). The average SSTs of the warmest and coldest months in the NE region were higher than in the subtropical SW region, which has higher temperature variability than the NE. From October to March, AT is higher in the SW than the NE (Fig.4.6f).
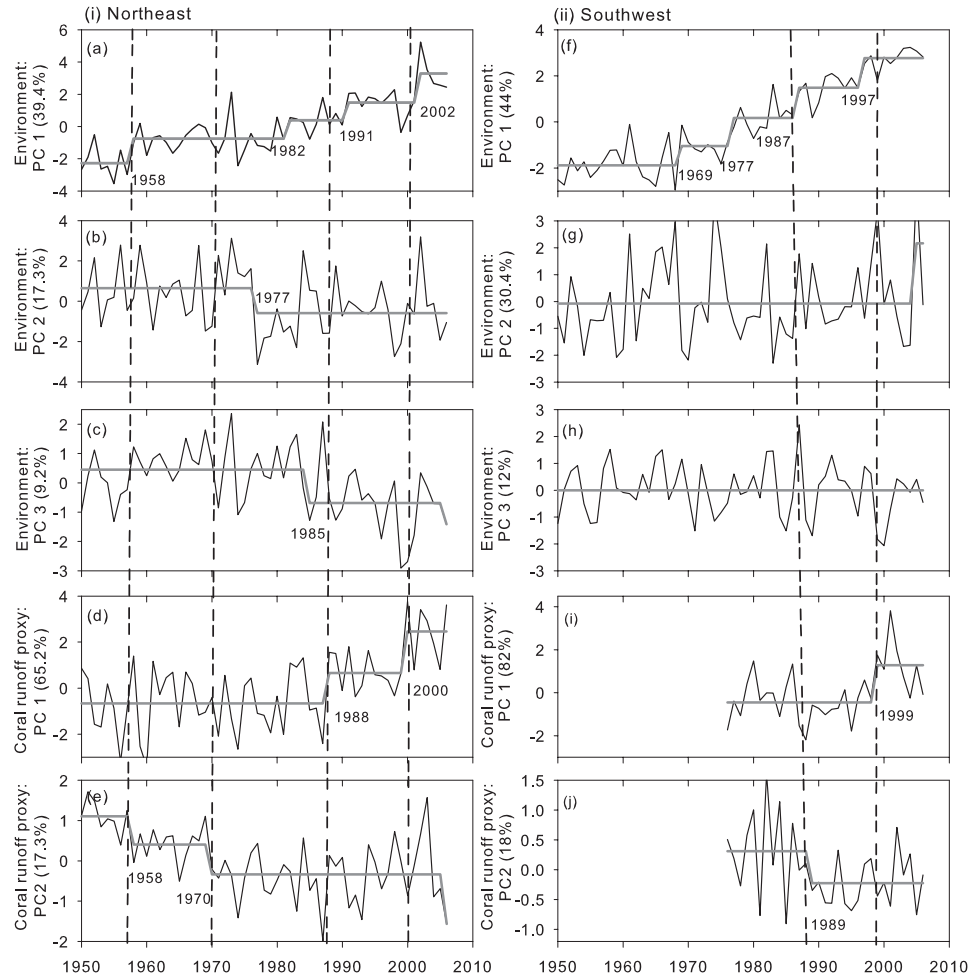
Figure 4.3: Long term trend and change-point analysis of the first three principal components of the environment data time series (a, b, c, f, g, h); and of coral proxies for river flow and sediment load (d, e, i, j) with Rodionov's sequential t-test for (i) NE, and (ii) SW regions. The grey line indicates the regime and significance shifts are at p < 0.01, while the vertical dotted lines depict points of significant shifts in any of the PC's

Coral Ba/Ca (for NE and SW cores) and G/B (for NE cores only) show a seasonal pattern of high values between January to April, which were also the wettest and warmest months of the year with high rainfall/discharge (Figs.4.6c,d). Coral proxy signals were lowest for September and October in the NE and SW consistent with the peak dry season in hydrological variables. The contrast between the wet and dry season in Ba/Ca is strongest for the GRT1 core in the SW (Fig.4.6c). The G/B ratio (only available for the NE cores) displays a more pronounced seasonal signal (Fig.4.6d). Overall, the seasonal signals of both coral proxies are in line with the seasonal discharge and precipitation patterns. Ba/Ca and G/B signals remain relatively high for the months following the peak discharge. Proxy signal differences between the NE and SW were also evident. Ba/Ca signals observed in the SW were higher than in the NE during the peak runoff season (Fig.4.6c). This is consistent with the contrasting amplitude of the seasonal variation in precipitation and river flow between the two regions.

Autocorrelograms for hydrological variables, precipitation, temperature, and coral proxies clearly showed a pronounced sine-like waveform and correlation coefficients (secondary y-axis) that attain a minimum at a lag of 6 months and a maximum at lags 1 and 12, typical of annual seasonal cycle (Fig.4.6, right panel). The maximum value of the graphed autocorrelation coefficient (R), when statistically significant, indicates the periodicity of the time series. All R-values were significant, indicating high similarity within respective months. Pairwise Pearson's correlation coefficients between individual cores (G/B, Ba/Ca) and environmental variables are also reported in Supplementary Information 4.4.
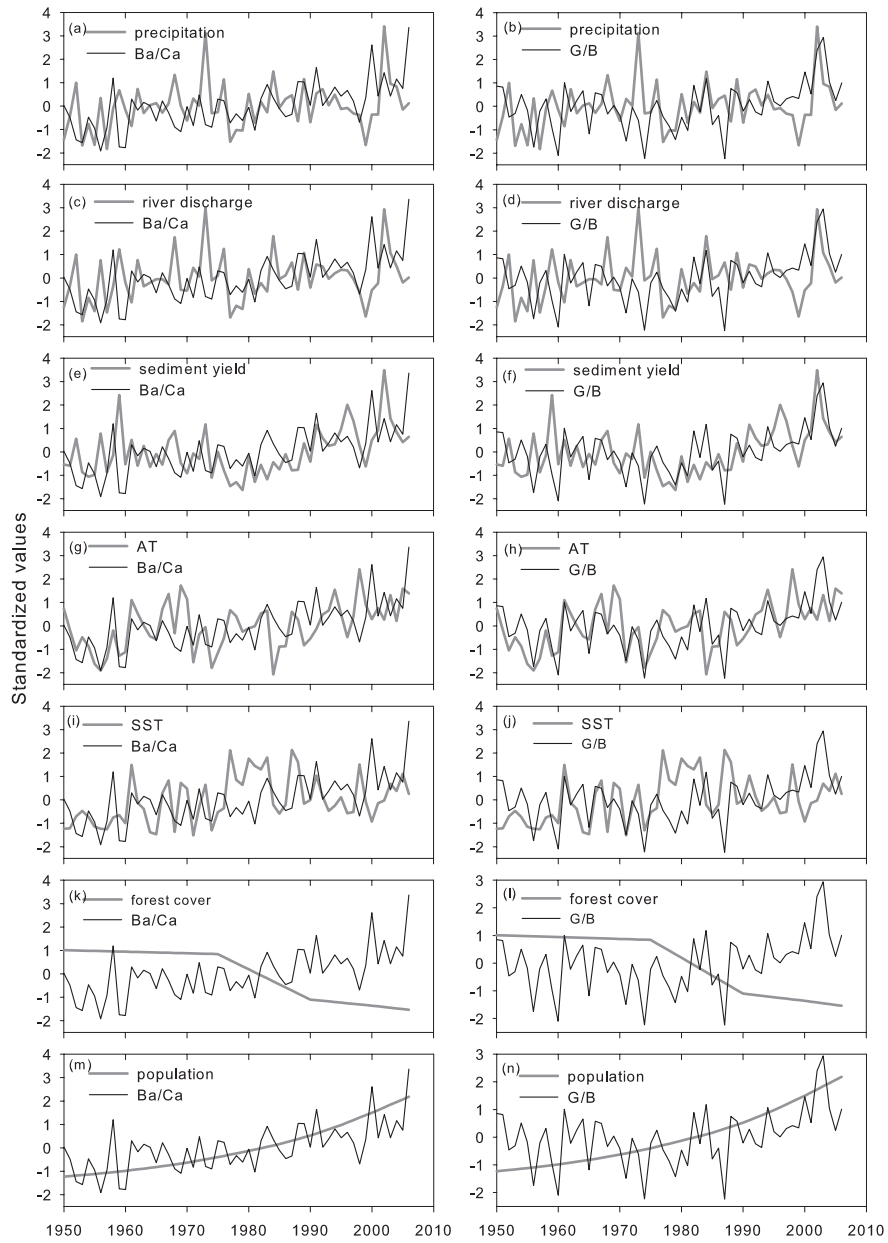
Figure 4.4: Annual standardized time series of environmental variables and coral proxies for the NE. The grey line is an environmental variable, while the thin line is a Ba/Ca or G/B

repeated on all plots. The two coral Ba/Ca, and G/B time series were averaged by calculating the arithmetic mean of the standardized time series
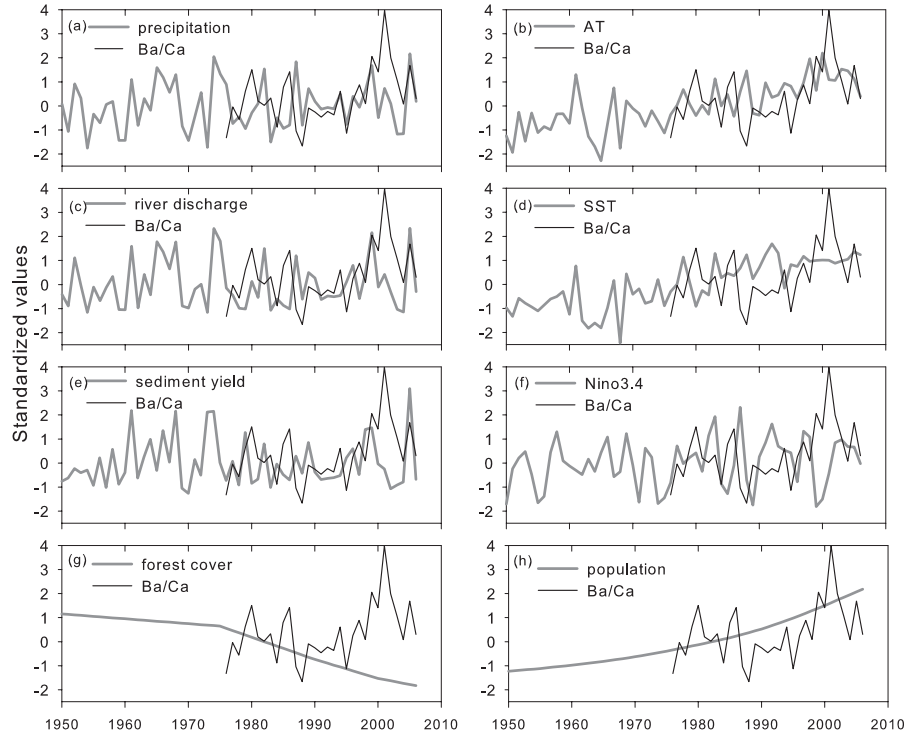

Figure 4.5: Annual standardized time series of environmental variables and coral proxies for the SW. The grey line is an environmental variable, while the thin line is a Ba/Ca repeated on all plots. The two coral Ba/Ca time series were averaged by calculating the arithmetic mean of the standardized time series

Multiple regressions to investigate environmental drivers of coral proxies from the NE catchment indicate that precipitation, sediment load, and river flow (in this order of importance) best explained the yearly changes in Ba/Ca (Table 4.2). These results were obtained at *lag = t+2*, as *lag's =t+0... t+1* yielded no significant results. When

multiple regressions were repeated with G/B as the response variable, three variable combinations were found to significantly explain the yearly variability in G/B (*lag=t+0*), sediment yield (interchangeably with precipitation and river flow), AT and ENSO (Table 4.2). In these three models, ENSO has a negative influence on G/B while sediment load and temperature showed a positive influence (Table 4.2). Regressions at *lags =t+0…1* showed no significant results, while at *lag = t+2,* only hydrological variables and precipitation significantly explained the variability of Ba/Ca (Table 4.2). In the warmer and drier SW catchment, AT and ENSO form a model that significantly explains the variability in Ba/Ca, having opposite effects (*at lag=t+1*). Unlike in the NE, sediment yield and discharge do not significantly explain the variability of Ba/Ca. This is consistent with the PCA results using un-detrended data, which showed a less dominant role of hydrological variables relative to temperature in the SW.
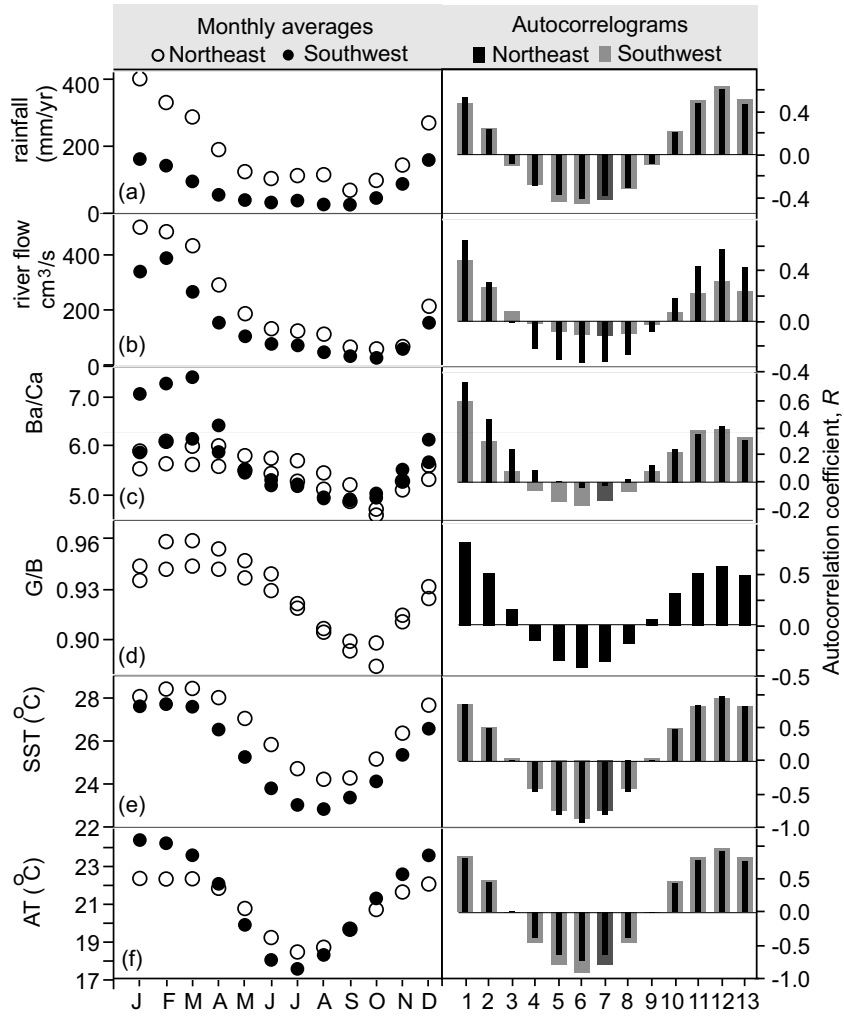
Figure 4.6: Average seasonal cycles of environmental parameters and coral geochemical proxies for NE and SW regions in Madagascar. Note that G/B (panel d) is only available for NE. Panels on the right are the autocorrelograms for each variable, with autocorrelation coefficients indicated on the secondary y-axis. Thirteen periods are shown on the autocorrelograms to illustrate that maximum value occurs at period 12 indicating an annual seasonal cycle and periodicity of the time series

4.4. DISCUSSION

We investigated the linkages between watershed characteristics (climate, land use, population, and hydrological variability), and environmental proxy records derived from coral skeletons (Ba/Ca and G/B) in NE and SW catchments of Madagascar, in the SW Indian Ocean. Previous studies have found correlation between precipitation, river discharge and suspended sediment load with the coral river runoff proxies (luminescence intensity, Ba/Ca), the concept underpinning reconstructions of historical rainfall, river flow and the amount of sediment in river flow (e.g., (McCulloch *et al.*, 2003; Lough, 2011)). We analyzed for potential or likely association between these variables in Madagascar and investigated possible causative roles of environmental drivers of changes that have occurred over the past 5 decades.

We confirm that in Madagascar catchments, precipitation, sediment load and river flow are associated with coral proxies from adjacent reefs at historical time scales, further extending the work of (Grove *et al.*, 2010; Grove *et al.*, 2012) in the NE catchments. We established that the seasonal river discharge signal is well recorded in both Ba/Ca and G/B ratios, where coral proxies values remain elevated during several months after the peak discharge has occurred (Grove *et al.*, 2012). This is possibly due to the time delay in plume dispersion and the incorporation of the proxies into the coral skeleton. Similar results were reported by (Barnes, 1993) and (Jupiter, 2006) for the Great Barrier Reef.

Results indicate, overall, that there is significant covariance between forest cover, population, river flow, sediment load, and the coral environmental proxies at annual and seasonal time scales. For the NE, changes in river discharge, sediment yield, precipitation, ENSO and temperature (AT, SST) were the main predictors of the variability in

Ba/Ca and G/B; for the SW, changes in AT and ENSO were the significant predictors. Strong coral proxy signals were associated with increases in precipitation and hydrological indices (Table 4.2) in the NE. In both regions, while ENSO negatively influenced the variability in coral proxies, AT positively influenced the variability of Ba/Ca. Relationships between river discharge and coral proxy signals have been confirmed in other regions, (e.g. (McCulloch *et al.*, 2003; Jupiter, 2006; Prouty *et al.*, 2010)), but the role of temperature (AT, SST) and ENSO in determining such proxies has not been clearly established. Earlier studies (e.g. (Lea *et al.*, 1989; Shen *et al.*, 1992; Fallon *et al.*, 1999)) have proposed, yet not verified, that the Ba distribution coefficient between coral and seawater is temperature dependent. Our study does confirm a causative role of temperature (AT, SST) and ENSO in both regions, albeit through different processes: NE corals may be responding to more extreme discharge, whereas in the SW coral Ba/Ca is responding directly to temperature (AT and/or SST) changes, which are directly sensitive to ENSO (Nicholson & Selato, 2000).

The hydrological variables (precipitation, discharge, sediment yield), and coral proxies for the NE were highly synchronized in terms of the long-term trends as revealed by the time series plots (Figs. 4.4, 4.5) and by the PCA analyses (Table 4.1, Fig.4.3). The increase in sediment yield since the late 1970s/early 1980's in the NE is also reflected in precipitation and river discharge, consistent with both coral Ba/Ca and G/B (Fig.4.4). This adds confidence to our coral proxy reconstructions in terms of the changes in the long-term trends in sediment yield. We can confirm that the postulated increase in Ba/Ca and G/B by (Grove *et al.*, 2010) is indeed related to an overall increase in sediment yield.

In the SW, Ba/Ca indicates a lower baseline signal from the late 1980's to mid 1990's, and a sharp increase in late 1990's, possibly related to the wetter conditions following the dry 1997/98 El Niño year (Fig.4.5)

(Zhong *et al.*, 2005). PCA revealed significant covariance of precipitation, sediment and discharge with only one core (GRT1). Further, the temporal trend of the averaged SW cores (Figs.4.5) corresponds to those of sediment and discharge during the late 1980's and early 1990's, which was a relatively dry decade with low sediment yield and river discharge. Unlike in the NE, sediment yield, discharge and precipitation did not significantly explain Ba/Ca variability in the two SW cores. However, given that ENSO explained the Ba/Ca variability in this region (Table 4.2) and its known influence on precipitation ((Nicholls, 1988)), a role of precipitation and hydrology on Ba/Ca changes can still be inferred for this region.

The seemingly lack of explanatory power by the hydrology and precipitation in the SW may be explained by the vast extent of the SW watershed, which ranges from the eastern mountains with annual rainfall of 1200 mm, to the lowland coastal plains with only 100 mm (Fig.4.1). The rivers Onilahy and Fiherenana, which drain the SW watershed, originate from the eastern plateaus and transport sediment loads even when most of the SW region is dry. The Onilahy River is likely the most important source of sediments reaching the GRT, due to the main direction of southerly winds that distribute the river plumes northwards. The SW reefs have a complex and shallow architecture, with large intertidal zones. These provide ideal conditions for resuspension of fine sediments, driven by the strong tidal currents, sea winds and the frequent cyclones (Bruggemann *et al.*, 2012). In contrast, cores from the NE are from a reef with a much simpler structure, in form of a shallow fringing reef surrounding a small island and directly exposed to the river plume, which directly disperses towards that fringing reef. Given that the NE and SW regions are prone to frequent storms and cyclones (Nassor & Jury, 1998), sediment resuspension could lead to 'committed sedimentation' from accumulation of the past sediment deposits whose signals can be recorded by corals at the time of resuspension, even when there is no

rainfall or new deposition (Jupiter *et al.*, 2008; Prouty *et al.*, 2010). Resuspension of sediments could be a secondary source of dissolved Ba for the corals in the SW enhancing Ba/Ca seasonality, and may contribute to temporal mismatch and lack of correlation between hydrology and proxy signals. Coral Ba/Ca in areas not influenced by terrestrial discharge are known to display seasonal signals that have been related to seasonal upwelling ((Lea *et al.*, 1989; Tudhope *et al.*, 1996)), which can be generated by zonal winds that are influenced by ENSO cycles (Fallon *et al.*, 1999). However, upwelling as a secondary driver of high Ba/Ca seasonality in the SW is not supported by recent monitoring data for the same region (Bruggemann *et al.*, 2012).

We observed mismatches between the interannual variability in either river discharge or sediment load and coral runoff proxies (Figs.4.4, 4.5). These were also evident in the GLM's where predictor variables performed better with the introduction of 1-2 year lags (Table 4.2), indicating possible alignment errors in the time series data and/or physical process in the hinterland and differences in local environmental influences. Similar results were observed for the Great Barrier Reef ((McCulloch *et al.*, 2003)), e.g. when dry years were followed by wet years, the erosive potential increased due to the loss of groundcover. Consequently increased suspended sediment loads and elevated coral Ba/Ca signals were observed even in years with average precipitation and river discharge (McCulloch *et al.*, 2003). Examples in our coral proxy data time series in the NE (Fig.4.4) include the dry mid 1950s which was followed by wet years in late 1950s leading to a spike in sediment load, and the dry 1997/1998 period which was followed by a relatively wet period and high sediment yield. These drought-breaking rain and floods that increase sediment discharge can distort the otherwise linear relationship between river discharge, sediment yield and coral proxy signals. Similarly, consecutive wet years result in lower erosion due to the soil saturation and subsequently low runoff proxy signals during wet years ((Alibert *et al.*, 2003;

McCulloch *et al.*, 2003)). Our results for the NE and SW catchments show evidence for non-linear relationships between precipitation and sediment yield on inter-annual, decadal and longer time scales (Figs.4.4, 4.5).

The timing of the change points in environmental variables (NE: 1958, 1991, 2002; SW: 1987, 1997) did roughly correspond to those observed in river runoff proxies (NE: 1958, 1988, 2000; SW: 1989, 1999), although within 2-3 years lag times in response to environmental changes (Figs.4.4, 4.5). These alignment errors can also be due to uncertainties from proxy dating; time averaging of proxy signals with skeletal growth; and catchment soil moisture characteristics. Coincidentally, the years 1977, 1982, 1987, 1991, 1997, and 2002 were strong El Niño years, while 2000 was a La Niña year (Chen *et al.*, 2004). It appears that some of the significant change points are associated with ENSO, further highlighting the role of ENSO on tropical coastal ecosystems in the western Indian Ocean (Zinke *et al.*, 2004; Zinke *et al.*, 2005).

Indeed, the tropical Pacific imparts substantial climate variability to the western Indian Ocean (Zinke *et al.*, 2005), where the warm phase of ENSO is associated with droughts, while the cold phase is associated high rainfall (Zhong *et al.*, 2005). ENSO's indirect influence on rainfall has been shown to occur most consistently in south-western Africa (15°S to 32°S)(Nicholson & Selato, 2000; Zhong *et al.*, 2005). The ENSO/rainfall relationships are manifestations of the influence of ENSO on these Indian and Atlantic oceans ((Nicholoson, 1997; Goddard & Graham, 1999; Nicholson *et al.*, 2001)). During the first half of La Nina episodes (warm phase), there is a tendency for anomalously dry conditions. As with El Nino, the La Nina signal is strongest during the second half of the episode (cold phase), but in contrast to El Nino, the rainfall is abnormally high (Nicholson & Selato, 2000).

Our results show that in both regions, the ENSO cycle is an important factor in explaining the variability of coral runoff proxies (G/B in the NE; Ba/Ca in SW) (Table 4.2). Given that ENSO is not highly correlated with rainfall (Table 4.1), it appears that ENSO influence is most significant during extreme high or low runoff in specific years that are associated with either phases of the ENSO. Similarly, Ward et al. (2010) found that ENSO has a greater impact on extreme discharge years than on years with mean annual discharge. ENSO variations have been shown to correlate with discharge in many parts of America, Australia, northern Europe, and parts of Africa and Asia (Dettinger *et al.*, 2000), reinforcing the postulation that global weather patterns captured by the ENSO have a significant forcing on both stream-flows and coastal ecosystems around the world (Ward *et al.*, 2010). Recent work in Madagascar (Ingram & Dawson, 2005) and in continental Africa (Anyamba *et al.*, 2001) showed a negative influence of ENSO on vegetation cover. Further, (Zinke *et al.*, 2004) showed evidence for the influence of ENSO on SST in the nearby Ifaty lagoon in the SW of Madagascar, where ENSO years after the 1970's were characterized by high SST and low rainfall. This is consistent with our GLM results, which showed a negative impact of ENSO on coral Ba/Ca in the SW.

Overall, our results corroborate the hypothesis that there are strong linkages between watersheds' climate variability, hydrology, forest cover, population growth and the adjacent coral reefs. Changes in forest cover in the respective watersheds and population size were not directly connected to coral runoff proxies, and they did not significantly predict the variability in coral proxy signals in both regions as shown by the regression models. They did however highly co-vary with coral runoff signals and with the hydrological variables. This suggests that changes in land use and increased population density might govern the long-term trends in sediment yield and coral environmental proxy data, but that these are slow processes. They interact with climatic changes through precipitation to influence the

amount of sediment transported through river runoff, which is subsequently deposited in coastal waters and reflected in elevated Ba/Ca and G/B in corals. This reinforces the need to incorporate terrestrial land use management in the design of coral reef protection networks.

4.5. ACKNOWLEDGEMENTS

4.6. SUPPLEMENTARY INFORMATION

S4.1 Description of the data used as input for STREAM and N-SPECT hydrological models

Precipitation and temperature data: The University of East Anglia's Climate Research Unit (CRU) hosts precipitation and temperature databases (Version 3.1) (Mitchell & Jones, 2005). These data are gridded at ~55 km spatial resolution for Madagascar and run monthly from 1901-2008. Together with the crop maps, STREAM utilizes land temperature distribution in the catchment to estimate potential evapotranspiration in the catchment, based on the Thornthwaite & Mather (1957) approach (Aerts et al., 1999). Temperature and precipitation data (1901-2008) were downloaded from the Climate Research Unit (CRU) website and extracted for Madagascar.

Rainfall erosivity: Rainfall erosivity is a measure of the erosive force of rainfall, and a required input of the RUSLE. Often, the large-scale rainfall erosivity mapping in data-poor regions is based on interpolation of erosivity values derived from rain gauge data (Vrieling et al., 2010). Indices used to estimate the rainfall erosivity include the R-factor (Renard & Freimund, 1994); the Fournier Index (FI) and the modified Fournier Index (MFI) (Vrieling et al., 2010). MFI was found to provide good spatial estimates of annual erosivity in Africa when used with the monthly satellite-based precipitation (Vrieling et al., 2010). Annual spatial maps of MFI were therefore computed with CRU precipitation data described above and used as the inputs to Eq. 4.1 (Supplementary Information 4.1).

Land use: Land cover maps were developed from multi-temporal vegetation maps from Harper et al. (2007). These maps, centered at 1950, 1970, 1990, 2000 and 2005 were developed from aerial photographs from1949-1957 (Blasco, 1965) and from Landsat imagery

from 1972-1979, 1989-1996, 1999-2001, and 2002-2005, respectively. These vegetation distribution maps are based on two classes: forested and non-forested areas. For our modelling purposes, the non-forested areas needed to be assigned to a land cover class. To achieve this, a land use map for Africa (Africover), developed in 2006 by the European Space Agency (ESA), was optimized for Madagascar and superimposed on the vegetation maps. As a result the non-forested areas were filled with the land cover class of the Africover map. This procedure maintained the forested class and assumed new classes for the non-forested areas. These land-use maps were in turn used to generate crop factor maps (Aerts & Bouwer, 2005), which STREAM utilizes for determining potential and actual evapotranspiration. The land cover maps were re-classified to the crop factor maps for use in STREAM, using the crop factor values adapted from Aerts & Bouwer (2005).

N-SPECT utilizes the land cover maps in a slightly different way. Each land cover type, such as forest, grassland, or cultivated land has an associated cover-factor or C-factor. The C-factor indicates relative erosion rate for the given land cover. For example, cultivated land, with a C-factor of 0.240 is rated as being 60 times more affected by erosion than forest, which has a C-factor of 0.004. In the absence of locally derived C-factors for Madagascar, we adopted the default values provided by NOAA in N-SPECT.

Soil data: Soil data were obtained from Version 1.1 of the Harmonized soil database of the world (FAO/IIASA/ISRIC/ISSCAS/JRC 2009). STREAM utilizes the water holding capacity of the soil as one of the input variables. The soil database was used in a reclassification procedure to develop the water holding capacity map for input in STREAM (Aerts & Bouwer, 2005). N-SPECT utilizes the two variables derived from soil data. First, it uses Hydrologic Soil Groups (HSG's). First, soils are classified into four hydrologic soil groups to

indicate the minimum rate of infiltration obtained for bare soil after prolonged wetting (Nam et al., 2003). Using the soil types in the soil database, a soil hydrologic group map for Madagascar was derived using a reclassification procedure. Second, it calculates the soil erodibility factor (K-factor), representing the susceptibility of soil to erosion by rainstorms, expressed as a function of sand, silt, clay and organic carbon concentrations, derived using reclassification procedures within the soil database. A low K-factor (about 0.05 to 0.2) indicates a high resistance to erosion and a high K-factor (0.4 or higher) indicates easily erodible soil. The K-factor was computed using equation 4.2 given in Supplementary Information 4.1.

Elevation data: STREAM utilizes the flow direction map and the digital elevation model (DEM) maps as inputs. Hydrologically corrected DEMs in 500 m resolution were downloaded from hydroSHEDS's website (Lehner et al., 2008). N-SPECT utilizes the DEM as an input for slope steepness (S) and slope length (L), which are RUSLE parameters. Their role is to adjust erosion rates based on topography, assigning higher rates to longer or steeper and lower rates to shorter or flatter slopes (Nam et al., 2003). N-SPECT also utilizes the DEM to delineate watersheds.

S4.2 Summary of data properties and sources as well as the equations used for derived variables

Data/derived variable	Time period	Spatial resolution	References
Precipitation data			
CRU, monthly mean	1901-2006	0.5^o	Mitchel & Jones, 2005
Rainfall erosivity (MFI)[1]			Vrieling et al., 2010
$$MFI = \frac{1}{p}\sum_{i=1}^{12} p_i^2$$			*(Equation 4.1)*
Land cover maps			
Forest cover maps	1950-2005	30 m	Harper et al., 2007
Land cover map	2006	300 m	http://www.esa.int
Land temperature	1901-2006	55 km	Mitchel & Jones, 2005
Sea surface temperature	1901-2006	111 km	Rayner et al., 2003
Soil			
Harmonized soil database of the world		Vector	FAO/IIASA/ISRIC /ISSCAS/JRC (2009)

Soil erodibility factor (K factor)[2]   Nam et al., 2003

$K =$
$\left[0.2 + \right.$
$\left. 0.3 \exp\left\{-0.026 SAN\left(1-\frac{SIL}{100}\right)\right\}\right]\left(\frac{SIL}{CL+SIL}\right)^{0.3}\left(1-\frac{0.25C}{C+\exp(3.7-2.9C)}\right)\left(1-\frac{0.7SN1}{SN1+\exp(-5.5+22.9)}\right)$

$K =$
$\left[0.2 + 0.3exp\left\{-0.026SAN\left(1-\frac{SIL}{100}\right)\right\}\right]\left(\frac{SIL}{CL+SIL}\right)^{0.3}\left(1-\frac{0.25C}{C+\exp(3.7-2.9C)}\right)\left(1-\right.$
$\left.\frac{0.7SN1}{SN1+\exp(-5.5+22.9SN1)}\right)$ *(Equation 4.2)*

Elevation data		
hydroSHEDS	500 m	Lehner et al., 2008
Climate indices		
Niño3.4		
Sea surface temperature (Hadley meteorological office)	55 km	Rayner et al., 2003

[1]p is the average rainfall (mm) of the month with the highest rainfall

[2]SAN, SIL, CL and C are (%) of sand, silt, clay and organic carbon contents of the soil respectively, SN1=1-SAN/100

Niño3.4 Index derived from http://www.cpc.ncep.noaa.gov/data/indices/

S4.3 Description of G/B luminescence for the SW catchment

Analysis of G/B for the coral cores GRT1 and GRT2 revealed no humic acid runoff for this semi-arid catchment. The theory behind this conclusion can be found in Grove et al. (2010). In brief, when we simultaneously analyse the luminescence intensity in the 'Green' (G) domain, the 'Blue' (B) domain and the G/B ratio, we expect to find that both G and G/B signals increase in parallel when humic acids are flushed into the system and are taken up by the coral. In other words, the G signal increases relative to the 'Blue" (B) domain, with the latter being related to skeletal density. When a coral is not influenced by humic acid runoff, the G/B will decrease while G increases. This is due to the aragonite coral skeletal density. As a high skeletal density band will cause G to increase, it also causes less B to be scattered by the skeleton giving an apparent increase in B relative to G, i.e. a decrease in G/B. This is what we observed for the corals GRT1 and GRT2. Therefore, G/B at this site cannot be used to reconstruct river flow.

S4.4 Pairwise correlation coefficients of monthly (annual time-step for sediment load, forest cover and population) data for the variables used in the analysis in both regions

	River flow	Ba/Ca (MAS1)	Ba/Ca (MAS3)	G/B(MAS1)	G/B(MAS3)	SST	AT	Rainfall	Nino3.4	Sediment	Population
Northeast											
Ba/Ca (MAS1)	0.3										
Ba/Ca (MAS3)	0.3	0.6									
G/B (MAS1)	0.4	0.6	0.6								
G/B (MAS3)	0.4	0.5	0.6	0.7							
SST	0.6	0.3	0.4	0.6	0.6						
AT	0.5	0.2	0.3	0.4	0.4	0.9					
Rainfall	0.9	0.3	0.2	0.3	0.3	0.6	0.6				
Niño3.4	0.0	0.0	0.0	0.1	0.0	0.1	0.1	0.1			
Sediment	0.6	0.3	0.2	0.4	0.2	-0.1	0.1	0.6	0.1		
Population	0.2	0.7	0.4	0.6	0.1	0.3	0.5	0.2	0.2	0.4	
Forest cover	-0.2	-0.7	-0.4	-0.6	-0.1	-0.3	-0.4	-0.2	-0.2	-0.4	-1.0
Southwest											
Ba/Ca (GRT1)	0.3										
Ba/Ca (GRT2)	0.2	0.4									
SST	0.4	0.5	0.4								
AT	0.3	0.4	0.3			0.9					
Rainfall	0.8	0.3	0.2			0.6	0.6				
Niño3.4	-0.1	-0.1	-0.1			0.0	0.1	0.0			
Sediment	0.6	0.2	0.1			-0.1	0.0	0.5	-0.1		
Population	0.0	0.5	0.3			-0.2	0.7	0.1	0.2	0.0	
Forest cover	0.0	-0.5	-0.2			-0.8	-0.7	-0.1	-0.2	0.0	-1.0

References

Aerts, J. & Bouwer, L. (2002) Calibration and validation for the wider Perfume River Basin in Vietnam. In, pp. 35-35. RIKZ/Coastal Zone Management Centre, The Hague.

Aerts, J.C.J.H., Kriek, M. & Schepel, M. (1999) STREAM (Spatial Tools for River basins and Environment and Analysis of Management options): 'Set up and requirements'. *Physics and Chemistry of the Earth, Part B: Hydrology, Oceans and Atmosphere*, **24**, 591-595.

Alibert, C., Kinsley, L., Fallon, S.J., McCulloch, M.T., Berkelmans, R. & McAllister, F. (2003) Source of trace element variability in Great Barrier Reef corals affected by the Burdekin flood plumes. *Geochimica et Cosmochimica Acta*, **67**, 231-246.

Alory, G., Wijffels, S. & Meyers, G. (2007) Observed temperature trends in the Indian Ocean over 1960-1999 and associated mechanisms. *Geophysical Research Letters*, **34**

Anyamba, A., Tucker, C.J. & Eastman, J.R. (2001) NDVI anomaly patterns over Africa during the 1997/98 ENSO warm event. *International Journal of Remote Sensing*, **22**, 1847-1859.

Barnes, D.J. (1993) On the nature and causes of density banding in massive coral skeletons. *Journal of Experimental Marine Biology and Ecology*, **167**, 91-108.

Bouwer, L.M., Aerts, J.C.J.H., Droogers, P. & Dolman, A.J. (2006) Detecting the long-term impacts from climate variability and increasing water consumption on runoff in the Krishna river basin (India). *Hydrology and Earth System Sciences*, **10**, 703-713.

Box, G.E. & Jenkins, G.M. (1976) Time series analysis, control, and forecasting. In. San Francisco, CA: Holden Day

Bruggemann, J.H., Rodier, M., Guillaume, M.M.M., Andrefouet, S., Arfi, R., Cinner, J., Pichon, M., Ramahatratra, F., Rasoamanendrika, F., Zinke, J. & McClanahan, T.R. (2012) Wicked Social–Ecological Problems Forcing Unprecedented Change on the Latitudinal Margins of Coral Reefs: the Case of Southwest Madagascar. *Ecology and Society*, **17**, 47.

Carpenter, S.R., Cole, J.J., Pace, M.L., Batt, R., Brock, W.A., Cline, T., Coloso, J., Hodgson, J.R., Kitchell, J.F., Seekell, D.A., Smith, L. & Weidel, B. (2011) Early warnings of regime shifts: A whole-ecosystem experiment. *Science*, **332**, 1079-1082.

Chabanet, P., Adjeroud, M., Andréfouët, S., Bozec, Y.M., Ferraris, J., Garcìa-Charton, J.A. & Schrimm, M. (2005) Human-induced physical disturbances and their indicators on coral reef habitats: A multi-scale approach. *Aquatic Living Resources*, **18**, 215-230.

Chatfield, C. (2003) *The analysis of time series: an introduction*. CRC press.

Chen, D., Cane, M.A., Kaplan, A., Zebiak, S.E. & Huang, D. (2004) Predictability of El Niño over the past 148 years. *Nature*, **428**, 733-736.

Craney, T.A. & Surles, J.G. (2002) Model-dependent variance inflation factor cutoff values. *Quality Engineering*, **14**, 391-403.

Darling, E.S., McClanahan, T.R. & Côté, I.M. (2010) Combined effects of two stressors on Kenyan coral reefs are additive or antagonistic, not synergistic. *Conservation Letters*, **3**, 122-130.

Davis, J.C. (1986) *Statistics and Data Analysis in Geology*,

Dettinger, M.D., Cayan, D.R., McCabe, G.J. & Marengo, J.A. (2000) Multiscale streamflow variability associated with El Niño/Southern Oscillation. *El Niño and the Southern Oscillation: Multiscale Variability and Global and Regional Impacts*, 113-147.

Durbin, J. & Watson, G.S. (1971) Testing for serial correlation in least squares regression.III. *Biometrika*, **58**, 1-19.

Eakin, C.M., Lough, J.M. & Heron, S.F. (2009) Climate variability and change: Monitoring data and evidence for increased coral bleaching stress. *Coral Bleaching: Patterns, Processes, Causes and Consequences*, 41-67.

Eslinger, D., VanderWilt, M., Dempsey, E., Carter, J. & Wilson, B. (2005) The nonpoint-source pollution and erosion Comparison Tool. *Coastal GeoTools'05.*, 32.

Fabricius, K.E., Langdon, C., Uthicke, S., Humphrey, C., Noonan, S., De'ath, G., Okazaki, R., Muehllehner, N., Glas, M.S. & Lough, J.M. (2011) Losers and winners in coral reefs acclimatized to elevated carbon dioxide concentrations. *Nature Climate Change*, **1**, 165-169.

Fallon, S.J., White, J.C. & McCulloch, M.T. (2002) Porites corals as recorders of mining and environmental impacts: Misima Island, Papua New Guinea. *Geochimica et Cosmochimica Acta*, **66**, 45-62.

Fallon, S.J., McCulloch, M.T., Van Woesik, R. & Sinclair, D.J. (1999) Corals at their latitudinal limits: Laser ablation trace element systematics in Porites from Shirigai Bay, Japan. *Earth and Planetary Science Letters*, **172**, 221-238.

Felis, T. & Pätzold, J. (2003) Climate records from corals. *Marine Science Frontiers for Europe*, 11-27.

Gardner, T.A., Côté, I.M., Gill, J.A., Grant, A. & Watkinson, A.R. (2003) Long-term region-wide declines in Caribbean corals. *Science*, **301**, 958-960.

Goddard, L. & Graham, N.E. (1999) Importance of the Indian Ocean for simulating rainfall anomalies over eastern and southern Africa. *Journal of Geophysical Research D: Atmospheres*, **104**, 19099-19116.

Grottoli, A.G. & Eakin, C.M. (2007) A review of modern coral δ18O and Δ14C proxy records. *Earth-Science Reviews*, **81**, 67-91.

Grove, C.A., Zinke, J., Scheufen, T., Maina, J., Epping, E., Boer, W., Randriamanantsoa, B. & Brummer, G.J.A. (2012) Spatial linkages between coral proxies of terrestrial runoff across a large embayment in Madagascar. *Biogeosciences Discussion*, **9**, 3099-3144.

Grove, C.A., Nagtegaal, R., Zinke, J., Scheufen, T., Koster, B., Kasper, S., McCulloch, M.T., van den Bergh, G. & Brummer, G.J.A. (2010) River runoff reconstructions from novel spectral luminescence scanning of massive coral skeletons. *Coral Reefs*, **29**, 579-591.

Habeeb, R.L., Trebilco, J., Wotherspoon, S. & Johnson, C.R. (2005) Determining natural scales of ecological systems. *Ecological Monographs*, **75**, 467-487.

Hannah, L., Dave, R., Lowry Ii, P.P., Andelman, S., Andrianarisata, M., Andriamaro, L., Cameron, A., Hijmans, R., Kremen, C., MacKinnon, J., Randrianasolo, H.H., Andriambololonera, S., Razafimpahanana, A., Randriamahazo, H., Randrianarisoa, J., Razafinjatovo, P., Raxworthy, C., Schatz, G.E., Tadross, M. & Wilmé, L. (2008) Climate change adaptation for conservation in Madagascar. *Biology Letters*, **4**, 590-594.

Harper, G.J., Steininger, M.K., Tucker, C.J., Juhn, D. & Hawkins, F. (2007) Fifty years of deforestation and forest fragmentation in Madagascar. *Environmental Conservation*, **34**, 325-333.

Harris, A., Manahira, G., Sheppard, A., Gough, C. & Sheppard, C. (2010) Demise of Madagascar's once great barrier reef-change in coral reef condition over 40 years. *Atoll Research Bulletin*, 1-16.

Hoegh-Guldberg, O., Mumby, P.J., Hooten, A.J., Steneck, R.S., Greenfield, P., Gomez, E., Harvell, C.D., Sale, P.F., Edwards, A.J., Caldeira, K., Knowlton, N., Eakin, C.M., Iglesias-Prieto,

R., Muthiga, N., Bradbury, R.H., Dubi, A. & Hatziolos, M.E. (2007) Coral reefs under rapid climate change and ocean acidification. *Science (New York, N.Y.)*, **318**, 1737-1742.

Hofmann, J., Behrendt, H., Gilbert, A., Janssen, R., Kannen, A., Kappenberg, J., Lenhart, H., Lise, W., Nunneri, C. & Windhorst, W. (2005) Catchment-coastal zone interaction based upon scenario and model analysis: Elbe and the German Bight case study. *Regional Environmental Change*, **5**, 54-81.

Ingram, J.C. & Dawson, T.P. (2005) Climate change impacts and vegetation response on the island of madagascar. *Philosophical Transactions of the Royal Society A: Mathematical, Physical and Engineering Sciences*, **363**, 55-59.

Isdale, P.J., Stewart, B.J., Tickle, K.S. & Lough, J.M. (1998) Palaeohydrological variation in a tropical river catchment: A reconstruction using fluorescent bands in corals of the Great Barrier Reef, Australia. *Holocene*, **8**, 1-8.

Jackson, J.E. (1991) Other Competitors. *A User's Guide to Principal Components*, pp. 424-434. John Wiley & Sons, Inc.

Jupiter, S., Roff, G., Marion, G., Henderson, M., Schrameyer, V., McCulloch, M. & Hoegh-Guldberg, O. (2008) Linkages between coral assemblages and coral proxies of terrestrial exposure along a cross-shelf gradient on the southern Great Barrier Reef. *Coral Reefs*, **27**, 887-903.

Jupiter, S.D. (2006) *From cane to coral reefs: ecosystem connectivity and downstream response to land use intensification*. PhD, University of California, Santa Cruz.

Jury, M.R. & Pathack, B. (1991) A study of climate and weather variability over the tropical southwest Indian Ocean. *Meteorology and Atmospheric Physics*, **47**, 37-48.

Kuleshov, Y., Qi, L., Fawcett, R. & Jones, D. (2008) On tropical cyclone activity in the Southern Hemisphere: Trends and the ENSO connection. *Geophysical Research Letters*, **35**

Lea, D.W., Shen, G.T. & Boyle, E.A. (1989) Coralline barium records temporal variability in equatorial Pacific upwelling. *Nature*, **340**, 373-376.

Lehner, B., Verdin, K. & Jarvis, A. (2008) New global hydrography derived from spaceborne elevation data. *Eos*, **89**, 93-94.

Lewis, S., Brodie, J., McCulloch, M., Mallela, J., Jupiter, S., Stuart Williams, H., Lough, J. & Matson, E. (2012) An assessment of an environmental gradient using coral geochemical records, Whitsunday Islands, Great Barrier Reef, Australia. *Marine Pollution Bulletin*, **65**, 306-319.

Lewis, S.E., Brodie, J.E., McCulloch, M.T., Mallela, J., Jupiter, S.D., Williams, H.S., Lough, J.M. & Matson, E.G. (2011) An assessment of an environmental gradient using coral geochemical records, Whitsunday Islands, Great Barrier Reef, Australia. *Marine Pollution Bulletin*,

Lindenmayer, D.B., Hobbs, R.J., Likens, G.E., Krebs, C.J. & Banks, S.C. (2011) Newly discovered landscape traps produce regime shifts in wet forests. *Proceedings of the National Academy of Sciences of the United States of America*, **108**, 15887-15891.

Lough, J.M. (2011) Great Barrier Reef coral luminescence reveals rainfall variability over northeastern Australia since the 17th century. *Paleoceanography*, **26**

Lough, J.M., Barnes, D.J. & McAllister, F.A. (2002) Luminescent lines in corals from the Great Barrier Reef provide spatial and temporal records of reefs affected by land runoff. *Coral Reefs*, **21**, 333-343.

Lu, H., Moran, C.J. & Prosser, I.P. (2006) Modelling sediment delivery ratio over the Murray Darling Basin. *Environmental Modelling and Software*, **21**, 1297-1308.

Lui, G.C.S., Li, W.K., Leung, K.M.Y., Lee, J.H.W. & Jayawardena, A.W. (2007) Modelling algal blooms using vector

autoregressive model with exogenous variables and long memory filter. *Ecological Modelling*, **200**, 130-138.

Mansfield, E.R. & Helms, B.P. (1982) Detecting multicollinearity. *The American Statistician*, **36**, 158-160.

Mavume, A.F., Rydberg, L., Rouault, M. & Lutjeharms, J.R.E. (2009) Climatology and landfall of tropical cyclones in the south-west Indian Ocean. *Western Indian Ocean Journal of Marine Science*, **8**, 15-36.

McCulloch, M., Fallon, S., Wyndham, T., Hendy, E., Lough, J. & Barnes, D. (2003) Coral record of increased sediment flux to the inner Great Barrier Reef since European settlement. *Nature*, **421**, 727-730.

Mertz-Kraus, R., Brachert, T.C., Jochum, K.P., Reuter, M. & Stoll, B. (2009) LA-ICP-MS analyses on coral growth increments reveal heavy winter rain in the Eastern Mediterranean at 9 Ma. *Palaeogeography, Palaeoclimatology, Palaeoecology*, **273**, 25-40.

Mitchell, T.D. & Jones, P.D. (2005) An improved method of constructing a database of monthly climate observations and associated high-resolution grids. *International Journal of Climatology*, **25**, 693-712.

Mora, C. (2010) A clear human footprint in the coral reefs of the Caribbean. *Proceedings of Royal Society*, **275**, 767-773.

Moriasi, D.N., Arnold, J.G., Van Liew, M.W., Bingner, R.L., Harmel, R.D. & Veith, T.L. (2007) Model evaluation guidelines for systematic quantification of accuracy in watershed simulations. *Transactions of the ASABE*, **50**, 885-900.

Mumby, P.J., Dahlgren, C.P., Harborne, A.R., Kappel, C.V., Micheli, F., Brumbaugh, D.R., Holmes, K.E., Mendes, J.M., Broad, K., Sanchirico, J.N., Buch, K., Box, S., Stoffle, R.W. & Gill, A.B. (2006) Fishing, trophic cascades, and the process of grazing on coral reefs. *Science*, **311**, 98-101.

Nam, P.T., Yang, D., Kanae, S., Oki, T. & Musiake, K. (2003) Global soil loss estimate using rusle model: the use of Global spatial datasets on estimating erosive parameters. *Geoinformatics*, **14**, 49-53.

Nash, J.E. & Sutcliffe, J.V. (1970) River flow forecasting through conceptual models part I - A discussion of principles. *Journal of Hydrology*, **10**, 282-290.

Nassor, A. & Jury, M.R. (1998) Intra-seasonal climate variability of Madagascar. Part 1: Mean summer conditions. *Meteorology and Atmospheric Physics*, **65**, 31-41.

Nicholls, N. (1988) El Niño-Southern Oscillation and rainfall variability. *Journal of Climate*, **1**, 418-421.

Nicholoson, S.E. (1997) An analysis of the ENSO signal in the tropical Atlantic and western Indian Oceans. *International Journal of Climatology*, **17**, 345-375.

Nicholson, S.E. & Selato, J.C. (2000) The influence of La Nina on African rainfall. *International Journal of Climatology*, **20**, 1761-1776.

Nicholson, S.E., Leposo, D. & Grist, J. (2001) The relationship between El Niño and drought over Botswana. *Journal of Climate*, **14**, 323-335.

Paillard, D., Labeyrie, L. & Yiou, P. (1996) Macintosh program performs time-series analysis. *Eos Trans. AGU*, **77**, 379.

Pandolfi, J.M., Connolly, S.R., Marshall, D.J. & Cohen, A.L. (2011) Projecting coral reef futures under global warming and ocean acidification. *Science*, **333**, 418-422.

Prouty, N.G., Field, M.E., Stock, J.D., Jupiter, S.D. & McCulloch, M. (2010) Coral Ba/Ca records of sediment input to the fringing reef of the southshore of Moloka'i, Hawai'i over the last several decades. *Marine Pollution Bulletin*, **60**, 1822-1835.

Richmond, R.H., Rongo, T., Golbuu, Y., Victor, S., Idechong, N., Davis, G., Kostka, W., Neth, L., Hamnett, M. & Wolanski, E. (2007) Watersheds and coral reefs: Conservation science, policy, and implementation. *BioScience*, **57**, 598-607.

Rodionov, S.N. (2004) A sequential algorithm for testing climate regime shifts. *Geophysical Research Letters*, **31**, L09204 1-4.

Shen, G.T., Cole, J.E., Lea, D.W., Linn, L.J., McConnaughey, T.A. & Fairbanks, R.G. (1992), 563-588.

Sinclair, D.J. & McCulloch, M.T. (2004) Corals record low mobile barium concentrations in the Burdekin River during the 1974 flood: Evidence for limited Ba supply to rivers? *Palaeogeography, Palaeoclimatology, Palaeoecology*, **214**, 155-174.

Sussman, R.W., Green, G.M. & Sussman, L.K. (1994) Satellite imagery, human ecology, anthropology, and deforestation in Madagascar. *Human Ecology*, **22**, 333-354.

Tudhope, A.W., Lea, D.W., Shimmield, G.B., Chilcott, C.P. & Head, S. (1996) Monsoon climate and Arabian Sea coastal upwelling recorded in massive corals from southern Oman. *Palaios*, **11**, 347-361.

Vorosmarty, C., Fekete, B. & Tucker, B. (1998) Global river discharge database (RivDis), v. 1.1. *Institute for the Study of Earth, Oceans, and Space, University of New Hampshire. Retrieved from* http://www. *rivdis. sr. unh. edu*,

Vrieling, A., Sterk, G. & de Jong, S.M. (2010) Satellite-based estimation of rainfall erosivity for Africa. *Journal of Hydrology*, **395**, 235-241.

Ward, P.J., Beets, W., Bouwer, L.M., Aerts, J.C.J.H. & Renssen, H. (2010) Sensitivity of river discharge to ENSO. *Geophysical Research Letters*, **37**

Wilkinson, C.R. (2004) Status of the Coral Reefs of the World: 2004. In. Australian Institute of Marine Science, Townsville.

Zhang, X., Zwiers, F.W., Hegerl, G.C., Lambert, F.H., Gillett, N.P., Solomon, S., Stott, P.A. & Nozawa, T. (2007) Detection of human influence on twentieth-century precipitation trends. *Nature*, **448**, 461-465.

Zhong, A., Hendon, H.H. & Alves, O. (2005) Indian Ocean variability and its association with ENSO in a global coupled model. *Journal of Climate*, **18**, 3634-3649.

Zinke, J., Dullo, W.C., Heiss, G.A. & Eisenhauer, A. (2004) ENSO and Indian Ocean subtropical dipole variability is recorded in a coral record off southwest Madagascar for the period 1659 to 1995. *Earth and Planetary Science Letters*, **228**, 177-194.

Zinke, J., Pfeiffer, M., Timm, O., Dullo, W.C. & Davies, G.R. (2005) Atmosphere-ocean dynamics in the western Indian Ocean recorded in corals. *Philosophical Transactions of the Royal Society A*, **1826**

Zuur, A.F., Tuck, I.D. & Bailey, N. (2003) Dynamic factor analysis to estimate common trends in fisheries time series. *Canadian Journal of Fisheries and Aquatic Sciences*, **60**, 542-552.

Zuur, A.F., Ieno, E.N., Walker, N.J., Saveliev, A.A. & Smith, G.M. (2009) *Mixed Effects Models and Extensions in Ecology with R*. Springer

5. HUMAN DEFORESTATION OUTWEIGHS FUTURE CLIMATE CHANGE IMPACTS OF SEDIMENTATION ON CORAL REEFS

ABSTRACT

Near-shore coral reef systems are experiencing increased sediment supply due to conversion of forests to other land uses. Meanwhile, future changes in land use, precipitation and temperature associated with human resource use and climate change are expected to alter hydrological and sedimentation dynamics. Counteracting increasing sediment supply requires an understanding about the relationship between forest cover and sediments supply, and how this relationship might change in the future. We establish this understanding by simulating river flow and sediment supply in four watersheds that are adjacent to Madagascar's major coral reef ecosystems for a range of future climate change projections and land use land cover change scenarios. By 2090, all four watersheds are predicted to experience temperature increases and/or precipitation declines that, when combined, result in decreases in river flow and sediment supply. However, these climate change-driven declines are far outweighed by the impact of deforestation. To date, removal of natural forest has increased sediment supply up to five-fold since human settlement. Sediment supply is projected to increase further by 54-64% if 10-50% of natural forest is removed, but could be reduced by 19-68% if 10-50% of natural forest is restored. Consequently, our analyses suggest that regional land use management is far more important than mediating climate change for influencing sedimentation rates in Madagascar. Moreover, the four watersheds captured in our analysis are representative of tropical near-shore reef systems worldwide. All in all, we demonstrate an integrated terrestrial-marine framework for informing decisions concerning sediment supply to coral reefs.

5.1. INTRODUCTION

Madagascar is one of the highest biodiversity hotspots and conservation priorities in the world (Hannah *et al.*, 1998; Myers *et al.*, 2000). Biologically rich forests have experienced landscape-level conversion and deforestation primarily from anthropogenic agents, with approximately 90% loss of original forest cover over the last approximately 2000 years since human arrival (Green & Sussman, 1990; Harper *et al.*, 2007). Despite the attempts at protection that date back two centuries and investment of hundreds of millions of dollars, forest destruction continues (Hannah *et al.*, 1998; Hannah *et al.*, 2008). Changes in vegetation cover have caused disruption of water flow and soils in drainage basins' hydrological cycles, potentially undermining the resilience of physically and biologically linked ecosystems, including the near-shore coral reefs (Hannah *et al.*, 2008; Maina *et al.*, 2012). Meanwhile, the conservation of coral reefs in a high-carbon dioxide world in Madagascar and in other tropical countries requires as one of the key strategies: a reduction of terrestrial run-off of sediments, nutrients and other pollutants, by urgent formulation and implementation of conservation plans that incorporate land use management of coastal catchments and regional climate change (Game *et al.*, 2011; Klein *et al.*, 2012; Rau *et al.*, 2012). Therefore, quantifying hydrological changes of these coastal catchments under different climate and land use land cover change (LULCC) scenarios will provide a basis for understanding and predicting the influence of land-use on sedimentation of near shore marine areas, and subsequently help to identify land-use practices that will reduce the impacts (Richmond *et al.*, 2007).

Pronounced climate change and LULCC represent the two primary challenges that ecosystems will face this century (Brook, 2008). These changes will directly affect the hydrology of the land surface through changes in evapotranspiration and ground water (Ferguson & Gleeson, 2012; Douville *et al.*, 2013) and the amount of sediment and fresh

water discharged into marine coastal zones (Maina *et al.*, 2012). Predicting the impact of climate change and LULCC on the fluvial spatial and temporal dynamics in the tropics is complicated because of poor data availability, strong seasonality, and climate variability events such as El Niño-Southern Oscillation (ENSO) (Krishnaswamy *et al.*, 2001; Wohl *et al.*, 2012). Therefore, identifying and separating the human impacts on fluvial dynamics relative to background processes and natural variability is challenging. We compare both the effects of land use and projected climate change on river discharge and sediment yield from four Malagasy catchments (the southwest, west, northwest and northeast). Malagasy watersheds represent ecologically sensitive coastal catchments and, because latitudinal range and island aspect explain a large amount of environmental variability, they capture characteristically different climatic zones in Madagascar and represent a range of environments found throughout the global tropics (McClanahan *et al.*, 2009). The catchments are adjacent to four main regions supporting Malagasy coral reefs, and the resource use in these watersheds along with fishing are key components of the coral reef *social-ecological system* dynamics in Madagascar and throughout the tropics (Cinner *et al.*, 2012) (Fig.5.1).

5.2. MATERIALS AND METHODS

We used two existing models [STREAM*(Aerts et al., 1999)*] and N-SPECT*(Eslinger et al., 2005)* that have been developed for Madagascar (Maina et al., 2012) that utilize present day climate and land use data (1950-2006) to estimate 57 years' time series of river discharge (m^3sec^{-1}) and sediment yield (tonnes $year^{-1}$)(Maina et al., 2012). In these calibrated and validated models we substituted present day climate and land-use data with future climate projections and LULCC scenarios, in order to simulate river discharge and sediment yield with new climate and land-use data forcing.

These models are calibrated using temperature and precipitation monthly time series 55-km spatial resolution data (CRU version 3.1) (Mitchell & Jones, 2005). To process the future climate data for the hydrological model's input, first we extracted 31-year baseline period (1975-2005) from the present day climate data and computed averages for each month (i.e. monthly climatology) (Maina et al., 2012). Second, future precipitation and temperature data based on six GCM's with three SRES scenarios represented (i.e. A1b, A2 and B1, corresponding to 550, 700, and 850ppm atmospheric carbon dioxide in 2100 respectively) were obtained from world climate research programme (WCRP) Coupled Model Inter-comparison Project (CMIP3) multi-model dataset's archives (http://www-pcmdi.llnl.gov/projects/cmip/index.php). Finally, we applied a change over or time or delta-method to downscale the GCM projections to the present day spatial resolution (see (Diaz-Nieto & Wilby, 2005)). In this method, from each of the individual time series (2000-2100), we selected a future 31-year period (2065-2095) from which we calculated 31-year running averages for each month, for grid cells intersecting the four Malagasy watersheds adjacent important coral reef areas (i.e. north east, north west, west and south west) (Fig.5.1). Using the temperature baseline and future monthly climatologies, we computed anomalies or change maps for each month in the time series, as the absolute difference between future and present day values. Similarly, we expressed precipitation as fractional changes in monthly mean precipitation, by dividing the future monthly climatology by the baseline monthly climatology. These changes in climate and precipitation were then applied to the present day climate time series, to represent future climate at a relatively higher resolution.

To investigate the relative influence of forest cover on hydrology, we constructed nine LULCC scenarios as follows: (i) present day land use, based on the land-use map for year 2000, which was developed from multi-temporal 1998-2001 satellite data (Harper et al., 2007); (ii)

completely forested or undisturbed, represented by the vegetation bio-climate map (Schatz et al., 1996); (iii - viii) incremental deforestation and afforestation targets (i.e. 10, 25, and 50%), based on land use change simulation; and (ix) completely deforested. To simulate land use change, we defined spatially explicit alternative futures that may result from future land management policies and socio-economic drivers. Using present day land-use as the baseline, land-use changes for deforestation and afforestation targets at country level were simulated for each cell, based on distance to roads and slope. To develop afforestation and deforestation scenario maps, suitability maps were developed based on the slope and the distance to roads. For the deforestation scenarios, percentages (10%, 25%, 50%) of the forested cells with the highest susceptibility to deforestation (relatively flat areas in close proximity to roads) were deforested. Similarly, for the afforestation scenarios, non-forest cells were allocated to forest class based on their relative distances to roads and the local topography. These were carried out at the Island scale, such that the % of the cells eligible for change in either scenario differs among the watersheds. STREAM utilizes the crop factors maps, for determining potential and actual evapotranspiration (Aerts et al., 1999). Crop factors based on land-cover characteristics are therefore derived using land cover information. The land cover maps were re-classified to the crop factor maps for use in STREAM, using the crop factor values adapted from (Aerts et al., 1999).

To simulate river discharge under present day and future climate, and under the LULCC scenarios, the respective climate and land use data were substituted in the calibrated STREAM model (Maina et al., 2012) (S4.1). Hydrological models for simulating sediment yield (i.e. N-SPECT) were constructed using the present day climate and the nine LULCC scenarios. To estimate sediment yield using future climate, relationships between time series for present day river discharge (i.e. annual maximum) and the corresponding data for sediment yield, for

each region and LULCC scenario were established using bivariate regressions. These relationships were then applied to estimate corresponding future sediment. These were summarized to derive mean monthly river discharge and mean annual sediment yield for paired climate and a LULCC scenario.

5.3. RESULTS AND DISCUSSION

To determine the relative influence of climate change on sedimentation, we derived projected multi-model ensemble mean changes in precipitation and temperature from six GCMs, in which three Intergovernmental Panel on Climate Change (IPPC) emission scenarios (Special report on Emission Scenarios, B1, A1b, A2) (Nakicenovic, 2000) were represented. Temperature is projected to increase by about 1- 4^oC in all seasons and in the four regions depending on different projections of three climate scenarios - by the end of the 21st century, with SRES B1, A1b, and A2 showing small, moderate and large increases, respectively (Fig.5.2). The multi-model ensemble predictions indicate a slight increase in precipitation (5 to 10%) for the wet season and a drying across the four regions during the dry season (5-10% in the NE and NW) that is especially robust in the subtropical west and southwest (up to 20%) (Fig.5.2). These patterns are qualitatively in agreement with previous analyses for the south-western mainland of Africa   e.g.(Tadross *et al.*, 2005; Christensen & Hewitson, 2007).

Climate-mediated changes in precipitation and temperature have variable effects on river flow between regions and scenarios (Fig.5.2). The south-western catchment has reduced water balance and the greatest decline in river flow in all emission scenarios (ensemble median 39-56%); NE and NW have moderate decline at 15-30%; while the western catchment had the lowest decline of ~10%. The projected dry and hot climatic conditions will have substantial impacts on

ground water resources (Ferguson & Gleeson, 2012) and soil moisture (Dai, 2013) especially for the drier southwest, factors that contribute to the simulated declines in river discharge and sediment yield. This also highlights the vulnerability of water resources in this region, even as sedimentation pressure on coastal ecosystems eases marginally (~10%) by the end of the 21st century with the unlikely no-change in LULCC scenario.

To determine the influence of LULCC on sedimentation, we constructed different possible land use inputs for the hydrological models (see methods). These configurations were based on present day land-use (2000), undisturbed natural forest based on bio-climate zones (Schatz *et al.*, 1996; Harper *et al.*, 2007), and spatially explicit island-wide deforestation and afforestation targets of 10, 25, 50, and 100%. The afforestation management regimes assume a sustained environmental campaigns and a heightened role for conservation than currently exists while deforestation would be associated with continued loss of forest cover or other changes in policy and action that promote the removal of forests.
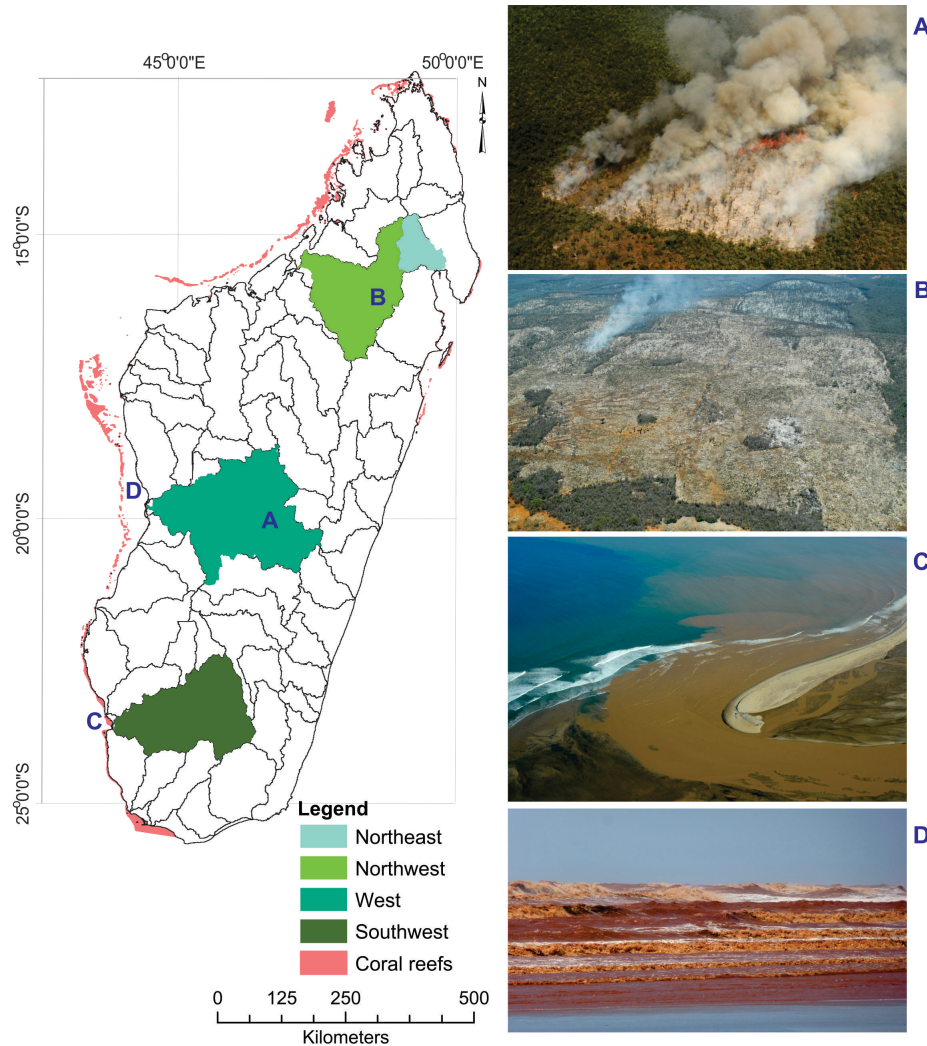
*Figure 5.1: Map of Madagascar showing coral reef areas and the four studied watersheds. Images of deforestation (A & B) and reef sedimentation (C & D) are shown with corresponding letters on the map showing approximate location of the image capture. Photo credit **Xavier Vincke** (A,B,C,) and **Olivier Raynaud** (D).*

LULCC impacts on sediment yields demonstrate the profound influence of human actions on tropical hydrology (Wohl *et al.*, 2012);

and the potential of management measures to curb deforestation and to increase forest coverage. On one extreme, afforestation of all areas to natural conditions would decrease sediment yield in all the four regions by 75% - 80% (Fig.5.3; Table 5.1); while on the other extreme, forest conversion in all areas would increase sediment yield by up to five-fold in the NE and two-fold in the other regions (Fig.5.3; Table 5.1).

Simulated changes in sediment yield when plotted against change in forest cover for each region indicates regionally specific trajectories owing to the bio-climatic differences and the disproportionate effects of forest manipulation policies on forest cover (Fig.5.3). Sediment changes are not dependent on the different predictions of the three climate scenarios. In the NE and NW regions, 25% island-wide afforestation scenario is estimated to restore 11% and 25% forest cover respectively, while a 50% scenario would restore 41 and 56 % respectively. These afforestation targets for NE and NW would lead to substantial declines (~ 60-80%) in the mean annual sediment yield.

The NE region is one of the most hydrologicaly sensitive watersheds, where small changes in forest cover are projected to produce large sediment yield. The region is still covered by relatively large areas of low lying tropical forests, albeit fragmented, as a result of complex terrain, relatively low population density and infrastructural development (Harper *et al.*, 2007). The relatively high forest coverage in this region relative to other regions is also consistent with our forest manipulation models (Fig.5.3), which predict low susceptibility to deforestation due to the steep terrain and less developed infrastructure. Sediment yield changes along the forest cover gradient for the SW and W regions depict nearly identical response behaviour patterns, perhaps owing to relatively similar climate and natural vegetation of mostly dry forest areas with less soil binding vegetation (Myers, 1988). In this region, 25% island-scale forest conversion (removes ~44% and 46% of

forest cover in SW and W respectively) leads to up to two-fold increase in sediment yield. It appears that at this level of deforestation, topsoils are completely depleted with sediment yield reaching a saturation point, which does not change with further decreases in forest cover. For the SW, 10 and 25% island-scale afforestation targets would not have much impact on sediment yield, as this increases the forest cover in the watershed by only 4 and 12%. Significant sediment declines in the SW would be achieved with implementation of 50% island-scale afforestation target, which would add 29% of forested area and consequently reduce sediment yield by approximately 50%. Similarly in the west, an estimated 60% decline in sediment yield is achieved with an island-scale afforestation target of 50%.
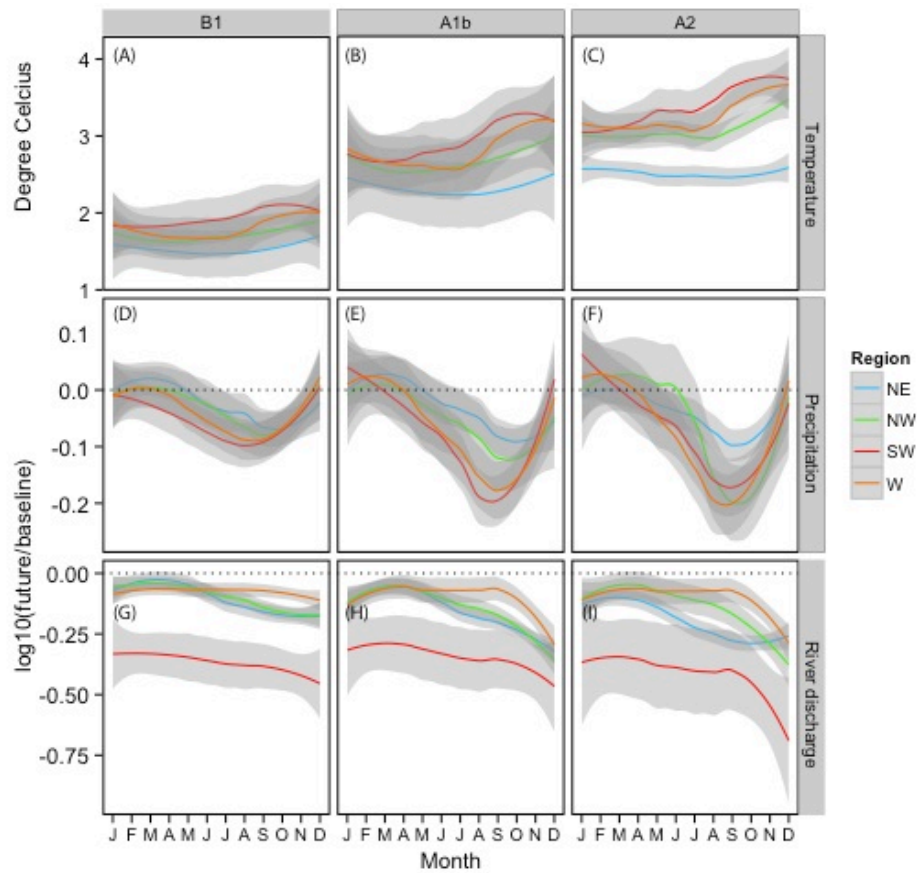
Figure 5.2: Predicted seasonal changes in temperature (a-c) and proportional changes in precipitation (c-e) and simulated watershed discharge (e-g) for the period 2070-2090 relative to the present day (1975-2005). A smooth line with 95% confidence interval (grey bands) representing variability in projections from different GCMs is fitted using Locally Weighted Scatterplot Smoothing (LOESS). Projections are presented by SRES scenarios (columns) and by region (colours).
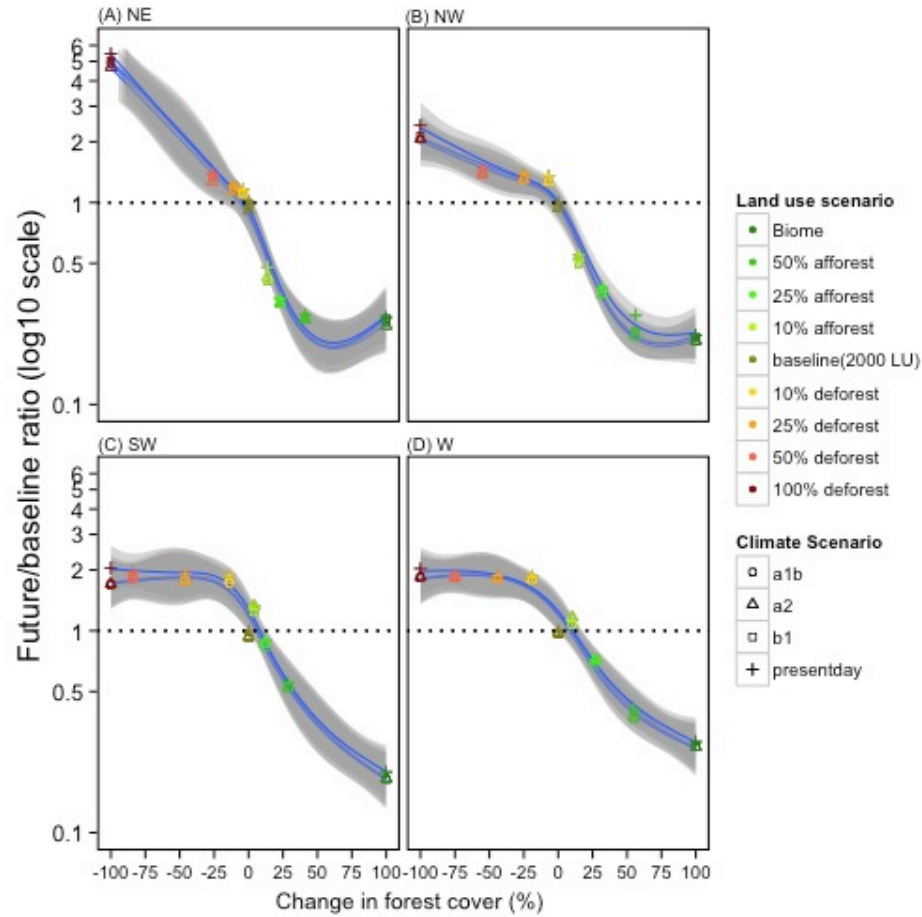
Figure 5.3: Mean predicted changes in sediment yields for each climate scenario (shapes) by region (panels) for 2090 for the period 2070-2090 relative to the present day (1975-2005), against change in forest cover changes based on the different LULCC scenarios (colour scale). A generalized linear model (GLM) smoother line for each climate scenario and the associated 95% confidence bands are displayed as blue lines and grey shades respectively

Model results provide insights into the effects of land conversion in the face of rising temperatures under climate change as well as afforestation policies and goals appropriate for the respective regions. Although climate change may be expected to exacerbate these challenges through forest diebacks (Choat *et al.*, 2012; Dai, 2013), forest conversion remains the principal contributor to increased sedimentation of the near shore marine environments. It is likely that the stabilization of atmospheric CO_2 at safe levels will not be achieved (UNFCC, 2011; Frieler *et al.*, 2013) (i.e. likely chance of holding the increase in global average temperature below 2^oC), while there are uncertainties around adaptation and acclimation of coral reefs to rising sea temperatures and ocean acidification (Rau *et al.*, 2012). Therefore local-scale mitigation through among other strategies, curbing sediment pollution has been promoted as particularly relevant for many tropical coastal communities who depend directly on marine resources for their livelihood. It is an important realization that the management of land-use offers a practical solution to reducing sedimentation and contributing to the resilience and adaptability of coral reefs facing both direct and indirect threats of rising CO_2 (Nakicenovic, 2000).

The Malagasy and other governments are experiencing increased interests from the broader donor, environmental, and conservation communities to reverse deforestation and maintain the hydrological and biological functions of forests (Hannah *et al.*, 2008). However, forest conservation in Madagascar faces several challenges and competing interests that create a tension between resource allocation and conservation, such as increasing population, demand for agricultural land, and mineral exploration and mining (Watson et al., 2010). Furthermore, there are technical challenges that include monitoring forests dynamics and predicting how forests will respond to future climate change (Wohl et al., 2012) in order to assess the sustainability and social equity of different management regimes (McConnell & Sweeney, 2005). For instance, forest die backs due to

drought are likely to hamper reforestation and lead to further losses of agricultural productivity and forest cover (Anderegg *et al.*, 2012; Choat *et al.*, 2012; Dai, 2013). These challenges are monumental but are achievable with broader international support along with the government and community's good will and engagement. Finally, if afforestation were adopted and applied comprehensively and consistently within a broader management policy and actions framework, it offers promise for sustainable environmental outcomes in the face of climate change in one of the world's most important biodiversity hotspots.

Table 5.1: Sediment change expressed as fractional change relative to the current estimates based on the 2000 land use and present day climate. Sediment yield fractional changes for the current estimates (i.e. 2000 land use and present day climate) are relative to the natural conditions, i.e. the bio-climate map

LULCC	Climate scenario	NE	NW	SW	W
Bio-climate map	b1	0.27 ± 0.00	0.21 ± 0.00	0.18 ± 0.00	0.27 ± 0.00
	a1b	0.26 ± 0.00	0.21 ± 0.00	0.19 ± 0.00	0.27 ± 0.00
	a2	0.25 ± 0.00	0.21 ± 0.00	0.19 ± 0.00	0.27 ± 0.00
	presentday	0.27 ± 0.00	0.22 ± 0.00	0.20 ± 0.00	0.28 ± 0.00
50% afforest	b1	0.26 ± 0.00	0.23 ± 0.00	0.51 ± 0.01	0.36 ± 0.00
	a1b	0.27 ± 0.00	0.23 ± 0.00	0.53 ± 0.00	0.39 ± 0.00
	a2	0.26 ± 0.00	0.22 ± 0.00	0.53 ± 0.01	0.37 ± 0.00
	presentday	0.28 ± 0.00	0.28 ± 0.01	0.55 ± 0.01	0.41 ± 0.01
25% afforest	b1	0.32 ± 0.00	0.36 ± 0.00	0.83 ± 0.01	0.68 ± 0.01
	a1b	0.33 ± 0.00	0.37 ± 0.00	0.86 ± 0.01	0.73 ± 0.01
	a2	0.32 ± 0.00	0.35 ± 0.01	0.87 ± 0.01	0.71 ± 0.01
	presentday	0.34 ± 0.00	0.38± 0.01	0.90 ± 0.01	0.72 ± 0.01
10% afforest	b1	0.41± 0.00	0.51± 0.00	1.25 ± 0.01	1.08 ± 0.01
	a1b	0.41± 0.00	0.49± 0.01	1.23 ± 0.01	1.07 ± 0.01
	a2	0.43 ± 0.01	0.54 ± 0.02	1.32 ± 0.02	1.17 ± 0.01
	presentday	0.48 ± 0.05	0.55 ± 0.01	1.32 ± 0.03	1.13 ± 0.03
Baseline (2000 land use)	b1	0.98 ± 0.01	0.97 ± 0.01	0.92 ± 0.01	0.96 ± 0.01
	a1b	0.95± 0.01	0.93± 0.01	0.93 ± 0.01	0.97 ± 0.01
	a2	0.91± 0.01	0.94± 0.01	0.93 ± 0.01	0.97 ± 0.01
	presentday	3.69± 0.01	4.49± 0.00	5.09 ± 0.00	3.53 ± 0.01
10% deforest	b1	1.10± 0.01	1.30± 0.01	1.73 ± 0.02	1.77 ± 0.01
	a1b	1.12± 0.01	1.26± 0.01	1.72 ± 0.01	1.77 ± 0.01
	a2	1.10± 0.01	1.26± 0.01	1.78 ± 0.02	1.81 ± 0.02
	presentday	1.16± 0.00	1.36± 0.00	1.89 ± 0.00	1.86 ± 0.00
25% deforest	b1	1.22± 0.01	1.35± 0.01	1.76 ± 0.01	1.80 ± 0.01
	a1b	1.17± 0.01	1.30± 0.01	1.79 ± 0.02	1.81 ± 0.02
	a2	1.14± 0.01	1.31± 0.01	1.79 ± 0.02	1.82 ± 0.02
	presentday	1.21± 0.00	1.39± 0.00	1.91 ± 0.00	1.87 ± 0.00
50% deforest	b1	1.36± 0.01	1.42± 0.01	1.81 ± 0.02	1.83 ± 0.01
	a1b	1.32± 0.01	1.37± 0.01	1.84 ± 0.02	1.84 ± 0.02
	a2	1.27± 0.01	1.38± 0.02	1.83 ± 0.02	1.84 ± 0.02
	presentday	1.38± 0.02	1.47± 0.03	1.95 ± 0.02	1.88 ± 0.03
100% deforest	b1	5.04± 0.04	2.14± 0.02	1.69 ± 0.01	1.83 ± 0.01
	a1b	4.91± 0.04	2.05± 0.02	1.71 ± 0.02	1.84 ± 0.02
	a2	4.68± 0.04	2.07± 0.03	1.71 ± 0.02	1.85 ± 0.02
	presentday	5.45± 0.07	2.41± 0.04	2.05 ± 0.02	2.03 ± 0.04

5.4. ACKNOWLEDGEMENTS

References

Aerts, J.C.J.H., Kriek, M. & Schepel, M. (1999) STREAM (Spatial Tools for River Basins and Environment and Analysis of Management Options): 'Set up and requirements'. *Physics and Chemistry of the Earth Part B-Hydrology Oceans and Atmosphere*, **24**, 591-595.

Anderegg, W.R.L., Anderegg, L.D.L., Sherman, C. & Karp, D.S. (2012) Effects of Widespread Drought-Induced Aspen Mortality on Understory Plants. *Conservation Biology*, **26**, 1082-1090.

Brook, B.W. (2008) Synergies between climate change, extinctions and invasive vertebrates. *Wildlife Research*, **35**, 249-252.

Choat, B., Jansen, S., Brodribb, T.J., Cochard, H., Delzon, S., Bhaskar, R., Bucci, S.J., Feild, T.S., Gleason, S.M., Hacke, U.G., Jacobsen, A.L., Lens, F., Maherali, H., Martinez-Vilalta, J., Mayr, S., Mencuccini, M., Mitchell, P.J., Nardini, A., Pittermann, J., Pratt, R.B., Sperry, J.S., Westoby, M., Wright, I.J. & Zanne, A.E. (2012) Global convergence in the vulnerability of forests to drought. *Nature*, **491**, 752–755.

Christensen, J.H. & Hewitson, B. (2007) Regional Climate Projections. *Climate Change 2007: The Physical Science Basis*, 847-940.

Cinner, J.E., McClanahan, T.R., Graham, N.A.J., Daw, T.M., Maina, J., Stead, S.M., Wamukota, A., Brown, K. & Bodin, O. (2012) Vulnerability of coastal communities to key impacts of climate change on coral reef fisheries. *Global Environmental Change-Human and Policy Dimensions*, **22**, 12-20.

Dai, A. (2013) Increasing drought under global warming in observations and models. *Nature Clim. Change*, **3**, 52-58.

Diaz-Nieto, J. & Wilby, R.L. (2005) A comparison of statistical downscaling and climate change factor methods: Impacts on low flows in the River Thames, United Kingdom. *Climatic Change*, **69**, 245-268.

Douville, H., Ribes, A., Decharme, B., Alkama, R. & Sheffield, J. (2013) Anthropogenic influence on multidecadal changes in reconstructed global evapotranspiration. *Nature Clim. Change*, **3**, 59-62.

Eslinger, D., VanderWilt, M., Dempsey, E., Carter, J. & Wilson, B. (2005) The nonpoint-source pollution and erosion Comparison Tool. *Coastal GeoTools'05.*, 32.

Ferguson, G. & Gleeson, T. (2012) Vulnerability of coastal aquifers to groundwater use and climate change. *Nature Climate Change*, **2**, 342-345.

Frieler, K., Meinshausen, M., Golly, A., Mengel, M., Lebek, K., Donner, S.D. & Hoegh-Guldberg, O. (2013) Limiting global warming to 2[thinsp][deg]C is unlikely to save most coral reefs. *Nature Clim. Change*, **3**, 165-170.

Game, E.T., Lipsett-Moore, G., Saxon, E., Peterson, N. & Sheppard, S. (2011) Incorporating climate change adaptation into national conservation assessments. *Global Change Biology*, **17**, 3150-3160.

Green, G.M. & Sussman, R.W. (1990) Deforestation history of the eastern rain forests of madagascar from satellite images. *Science*, **248**, 212-5.

Hannah, L., Rakotosamimanana, B., Ganzhorn, J., Mittermeier, R.A., Olivieri, S., Iyer, L., Rajaobelina, S., Hough, J., Andriamialisoa, F., Bowles, I. & Tilkin, G. (1998) Participatory planning, scientific priorities, and landscape conservation in Madagascar. *Environmental Conservation*, **25**, 30-36.

Hannah, L., Dave, R., Lowry, P.P., Andelman, S., Andrianarisata, M., Andriamaro, L., Cameron, A., Hijmans, R., Kremen, C., MacKinnon, J., Randrianasolo, H.H., Andriambololonera, S., Razafimpahanana, A., Randriamahazo, H., Randrianarisoa, J., Razafinjatovo, P., Raxworthy, C., Schatz, G.E., Tadross, M. & Wilmee, L. (2008) Climate change adaptation for conservation in Madagascar. *Biology Letters*, **4**, 590-594.

Harper, G.J., Steininger, M.K., Tucker, C.J., Juhn, D. & Hawkins, F. (2007) Fifty years of deforestation and forest fragmentation in Madagascar. *Environmental Conservation*, **34**, 325-333.

Klein, C.J., Jupiter, S.D., Selig, E.R., Watts, M.E., Halpern, B.S., Kamal, M., Roelfsema, C. & Possingham, H.P. (2012) Forest conservation delivers highly variable coral reef conservation outcomes. *Ecological Applications*, **22**, 1246-1256.

Krishnaswamy, J., Halpin, P.N. & Richter, D.D. (2001) Dynamics of sediment discharge in relation to land-use and hydro-climatology in a humid tropical watershed in Costa Rica. *Journal of Hydrology*, **253**, 91-109.

Maina, J., de Moel, H., Vermaat, J.E., Bruggemann, J.H., Guillaume, M.M.M., Grove, C.A., Madin, J.S., Mertz-Kraus, R. & Zinke, J. (2012) Linking coral river runoff proxies with climate variability, hydrology and land-use in Madagascar catchments. *Marine Pollution Bulletin*, **64**, 2047-2059.

McClanahan, T.R., Ateweberhan, M., Omukoto, J. & Pearson, L. (2009) Recent seawater temperature histories, status, and predictions for Madagascar's coral reefs. *Marine Ecology-Progress Series*, **380**, 117-128.

McConnell, W.J. & Sweeney, S.P. (2005) Challenges of forest governance in Madagascar. *Geographical Journal*, **171**, 223-238.

Mitchell, T.D. & Jones, P.D. (2005) An improved method of constructing a database of monthly climate observations and associated high-resolution grids. *International Journal of Climatology*, **25**, 693-712.

Myers, N. (1988) Threatened biotas: "hot spots" in tropical forests. *Environmentalist*, **8**, 187-208.

Myers, N., Mittermeier, R.A., Mittermeier, C.G., da Fonseca, G.A. & Kent, J. (2000) Biodiversity hotspots for conservation priorities. *Nature*, **403**, 853-8.

Nakicenovic, N. (2000) Greenhouse gas emissions scenarios. *Technological Forecasting and Social Change*, **65**, 149-166.

Rau, G.H., McLeod, E.L. & Hoegh-Guldberg, O. (2012) The need for new ocean conservation strategies in a high-carbon dioxide world. *Nature Climate Change*, **2**, 720-724.

Richmond, R.H., Rongo, T., Golbuu, Y., Victor, S., Idechong, N., Davis, G., Kostka, W., Neth, L., Hamnett, M. & Wolanski, E. (2007) Watersheds and coral reefs: Conservation science, policy, and implementation. *BioScience*, **57**, 598-607.

Schatz, G.E., Lowry, P.P., LEscot, M., Wolf, A.E., Andriambololonera, S., Raharimalala, V. & Rahamampionona, J. (1996) Conspectus of the vascular plants of Madagascar: A taxonomic and conservation electronic database. *Biodiversity of African Plants*, 10-17.

Tadross, M., Jack, C. & Hewitson, B. (2005) On RCM-based projections of change in southern African summer climate. *Geophysical Research Letters*, **32**

UNFCC (2011) EStablishment of an Ad Hoc Working group on the Durban Platform for Enhanced Action. In. UNFCC

Watson, J.E.M., Joseph, L.N. & Fuller, R.A. (2010) Mining and conservation: implications for Madagascar's littoral forests. *Conservation Letters*, **3**, 286-287.

Wohl, E., Barros, A., Brunsell, N., Chappell, N.A., Coe, M., Giambelluca, T., Goldsmith, S., Harmon, R., Hendrickx, J.M.H., Juvik, J., McDonnell, J. & Ogden, F. (2012) The hydrology of the humid tropics. *Nature Climate Change*, **2**, 655-662.

II. Synthesis

In this thesis, I explored the dynamics of environmental stressors on coral reefs in terms of their spatial distribution, interactions with one another, and their relative importance. I also explored the potential for conservation to exploit the differences in sensitivity of *Symbiodinium* clades (A-D), which associate with scleractinian corals, to temperature as an adaptation mechanism of corals to thermal stress. Further, I examined the drivers of local stressors—i.e., sedimentation in Madagascar—and developed a sorely needed integrated land-sea framework for assisting conservation goals concerning reef sedimentation. Furthermore, in this later study, I evaluated the relative importance of land-use and climate change on coastal sedimentation of coral reefs in Madagascar, one of the world's biodiversity hotspots.

The multivariate model of global exposure indicates relative exposure of reefs worldwide to thermal, sedimentation and eutrophication stress. The key finding from this study is that coral reefs vary in exposure, on a global scale, to climate change induced thermal stress, and sedimentation and eutrophication related stress. Therefore, the management decisions for specific reefs are expected to be influenced by the relative position of the respective reefs along the thermal stress and sedimentation and eutrophication stress axes. There are different schools of thought on how exposure and vulnerability information should be used in management decisions for applied conservation of corals. These proposed strategies are to protect the least vulnerable reefs, the most vulnerable, or all reefs regardless of their vulnerability status (Game *et al.*, 2008). Despite the ongoing debate surrounding reef protection scenarios (Roberts *et al.*, 2003; Game *et al.*, 2008), our map of reef coral exposure provides a means for discerning protection strategies independent of protection scenarios. Notwithstanding the various model and data limitations, as described in the Chapters 1 and 3, the relative significance of the multiple stressors are spatially

provided for all reefs globally, as simple indices that can be understood and applied easily by managers.

Moreover, the coral exposure metric can be coupled with outputs from the following study on geographical distribution estimates of *Symbiodinium* clades, to elucidate spatially explicit exposure and potential adaptation gradients. Moreover, the *Symbiodinium* clade distribution study finds that Clade A and Clade D have a higher thermal and photo-radiation tolerance, relative to clades B and C.

Reinforcing stressors, as showcased by the case study in Madagascar, could be reduced more effectively by spatially adaptive land-use management strategies aimed at reducing the amount of sediment reaching coral reefs. Further, this strategy is more effective at reducing sediment supply to coral reefs than climate change mitigation. These results can inform conservation decisions around the globe by tackling the complex issues concerning integrated land-sea management and the reduction of sediment supply to coral reefs.

Together, the results presented in my thesis will help support decisions aimed at the reduction of local threats on coral reefs and to promote their adaptation and resilience in the face of climate change impacts. Because the findings have global significance, I hope that they will catalyse efforts to collect key information on specific reefs, to protect forests and for improved management of tropical reefs worldwide.

References

Game, E.T., McDonald-Madden, E., Puotinen, M.L. & Possingham, H.P. (2008) Should we protect the strong or the weak? Risk, resilience, and the selection of marine protected areas. *Conservation Biology*, **22**, 1619-1629.

Roberts, C.M., Branch, G., Bustamante, R.H., Castilla, J.C., Dugan, J., Halpern, B.S., Lafferty, K.D., Leslie, H., Lubchenco, J. & McArdle, D. (2003) Application of ecological criteria in selecting marine reserves and developing reserve networks. *Ecological Applications*, **13**, 215-228.